UNIVERSITY OF NAVARRA
SCHOOL OF ENGINEERING
DONOSTIA-SAN SEBASTIÁN

Designing deformable models of soft tissue for virtual surgery planning and simulation using the Mass-Spring Model

DISSERTATION
submitted for the
Degree of Doctor of Philosophy
of the University of Navarra by

Gaizka San Vicente Otamendi

January, 2011

Servicio de Publicaciones de la Universidad de Navarra

ISBN 84-8081-144-7

A mi familia

"Think how hard physics would be if particles could think."
Murray Gell-Mann (Nobel Prize in Physics, 1969)

"At the end of the year 1820 the fruit of all the ingenuity expended on elastic problems might be summed up as an inadequate theory of flexure, an erroneous theory of torsion, an unproved theory of vibrations of bars and plates, and the definition of Young's modulus."
A Treatise on the Mathematical Theory of Elasticity.
A.E.H. Love, 1927.

AGRADECIMIENTOS

En primer lugar quería agradecer a todos aquellos compañeros que me han ayudado técnica y anímicamente en la difícil labor de intentar decir algo nuevo. Entre otros, quiero agradecer a mis directores de tesis, compañeros de despacho, colegas colindantes y resto de camaradas, tanto cercanos como lejanos. Gracias por escuchar con inexplicable atención mis ininteligibles razonamientos, intentar (a veces con éxito) que mi comunicación con el ordenador sea posible, alimentar mis ilusiones aunque fuera incierto que se pudieran llevar a cabo, hacer realidad mis sueños y, como no, aguantar mi excesiva energía.

También quería hacer una mención especial a las instituciones y trabajadores que hacen que nuestra tarea sea posible. No me puedo olvidar de las personas que siempre me conceden una agradable sonrisa, las que se ríen cuando me ven llegar al Ceit los fines de semana para trabajar un poco más o las que diariamente me dan un café cargado de bromas y risas.

Por último, aunque creo que debería ir en primer lugar, me gustaría agradecer profundamente a mi familia por haberme apoyado incondicionalmente durante todos estos años. Tanto cuando llegaba a casa entusiasmado y con ganas de explicar en detalle todo lo poco que estaba descubriendo, como cuando entrada en el salón pensativo, envuelto en un ambiente silencioso y cargado de dudas.

Gracias a todos y tranquilos, esta vez no os voy a liar.

CONTENTS

LIST OF FIGURES

LIST OF TABLES

RESUMEN

Los simuladores quirúrgicos, estudios biomecánicos y algunas aplicaciones de realidad virtual requieren emplear el comportamiento mecánico de diferentes tipos de tejidos biológicos. Cada tipo de tejido reacciona de diferente manera ante la acción de las fuerzas externas aplicadas. En particular, el diseño de modelos mecánicos que representen fielmente el comportamiento de los tejidos blandos supone un reto.

Se han propuesto numerosos modelos de sólidos deformables para aproximar la respuesta de tejidos vivos blandos. Sin embargo, es difícil cumplir con dos requerimientos simultáneamente: cálculo rápido de las deformaciones y resultados precisos. Este reto es aun mayor cuando el entorno de trabajo requiere resultados en tiempo real como es el caso de los simuladores interactivos de cirugía.

En esta tesis se proponen dos nuevos métodos para diseñar Modelos Masa-Muelle (MMM) rápidos y precisos, especialmente concebidos para la simulación de tejidos deformables. El primero de ellos permite modelar el comportamiento lineal elástico en régimen de pequeñas deformaciones. En concreto, se basa en un análisis comparativo entre el sistema de ecuaciones linealizado de un MMM y un Modelo de Elementos Finitos (MEF) elástico lineal. Para ello se emplea el estudio de vectores y valores propios de los modelos correspondientes.

El segundo método permite diseñar modelos de tejidos blandos en el rango de las grandes deformaciones. El método se basa en el hecho de que los MMMs responden intrínsecamente de manera no lineal ante grandes deformaciones. En particular, se realiza un ensayo de tracción uniaxial para obtener los parámetros del MMM a partir de modelos de material o ensayos reales.

Finalmente, los modelos desarrollados en esta tesis se han implementado en prototipos de simuladores médicos. Los resultados indican que los MMM pueden ser una alternativa interesante a otros modelos como los MEF cuando el requerimiento de eficiencia computacional es superior al de la precisión.

ABSTRACT

Surgery simulators, biomechanical studies and some virtual reality applications require the handling of the mechanical behaviour of different biological tissue types. Each tissue type reacts in different ways to the action of the external loads applied onto the object. In particular, designing suitable mechanical models to represent the behaviour of soft tissue is a challenging task.

Many models for deformable bodies have been proposed to approximate the behaviour of living deformable tissues. However, it is difficult to fulfil simultaneously two basic requirements: fast computation of the deformations and accuracy in the results. This challenge is even greater when the working environment requires real-time results, like in the case of interactive surgical simulators.

In this thesis two new methods to design fast and accurate Mass-Spring Model (MSM) are proposed. The methods are specifically focused on the simulation of deformable tissues. The first method allows modelling the linear elastic behaviour under small deformations. In particular, it is based on the comparative analysis of the linearized system of equations of the MSM and a linear elastic Finite Element Method (FEM). This is performed by studying the eigenvalues and eigenvectors of the corresponding models.

The second method allows designing soft-tissue models valid in the range of large deformations. This method is based on the fact that MSMs intrinsically behave nonlinearly under loads that lead to large deformations. In particular, a uniaxial tensile test is made to obtain the parameters of the MSM from material models or experimental data.

Finally, the models proposed in this thesis have been implemented in medical simulators prototypes. The results suggest that MSMs can be an interesting alternative to other models such as FEM when the requirement on the computation efficiency is more important than model accuracy.

CHAPTER 1

INTRODUCTION

1.1 MOTIVATION

Medicine is an extremely challenging field of research since it is of fundamental importance in human existence. The variety and inherent complexity of unsolved medical problems has made it a major driving force for many natural and engineering sciences.

One of the most exciting specialities in the medical field is surgery. Its relevance is increasing as life expectancy increases. According to the estimations made by Weiser et al. (Weiser2008) analyzing information provided by the World Health Organization, more than 230 million major surgical procedures are undertaken every year worldwide.

Surgery is concerned with the treatment of injuries, diseases, and disorders to help improve bodily function or appearance by changing the body with an operative procedure. Each of the existing operation methods combined with the different areas of the human body where the treatment is provided has resulted in many surgical specialties.

The progress in these procedures has been characterized by a continuous cycle of innovation thanks to the convergence of technical advances and creative surgeons whose major goal has been fighting against sickness. Indeed, the exhaustive study of the variety of procedures has turned the artisanal first operations with bone needles performed 30,000 years ago into the complex robotic-based surgeries of today (see figures 1.1 and 1.2).

Figure 1.1. (a) Trepanation made by Inca surgeons in ancient Peru. (b) Illustration of a trepanation in France in the XVIII century.

Thus, modern surgery has nothing to do with prehistoric operations. Gone are the days when Lord Thurlow in 1811 in a Parliamentary debate on the establishment of a Royal College of Surgeons stated that "*There is no more science in surgery than in butchering*."

Figure 1.2. Modern surgery room (DaVinci).

The modern concept of surgery, on the contrary, is more clearly reflected in the words of Mark M. Ravitch "*Surgery is not a place, not an event- rather it is fundamentally an intellectual discipline, frequently involving a surgical procedure, but most importantly characterized by an attitude of responsibility toward the care of the sick. The closed reduction of a fracture is part of orthopaedic surgery, the nonoperative management of a splenic injury or of gallstone pancreatitis is still clearly within the purview of the field of surgery and the surgeon's care*" (Krummel2006). These words capture concisely the modern concept of surgery where the idea of a careless surgical procedure has moved to an integral medical service given by highly qualified professionals to the patient, the focus of the surgical activity.

Until the end of the 20th century the thrust of surgeon was how they could do more and more, safely and effectively, to extend the quantity and quality of life. However, in the past two decades the emphasis has shifted to how much less can surgeons do to achieve their goal of treatment (Johnson2005). In consequence, any technological tool that helps obtaining the same result but simplifying the surgical procedure is very welcome.

In modern surgery, the procedure itself is enclosed by some essential processes. In the first place, certain questionnaires, explorations and probes are made to give the doctor enough information about the patient. The medical data can be manifold, from simple blood analysis to complex medical images. Then, the doctor analyses the available information and makes a diagnosis. The following step corresponds to the selection of the specific treatment that better overcomes that specific medical problem.

At this stage, if the treatment includes surgical procedures, a surgical treatment planning is designed to better accomplish the operation and the actual surgery is performed.

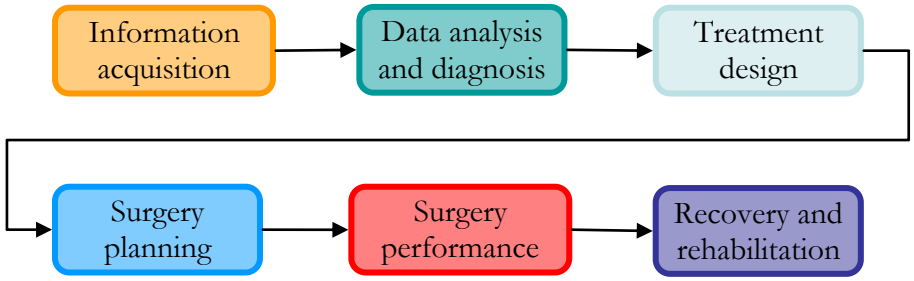

Figure 1.3. The standard tasks involved in an integral surgical service.

Finally, a recovery and rehabilitation phase comes where the patient is monitored, in order to follow the evolution, and check the effectiveness of the treatment. Obviously, all these steps depend totally on the type of intervention, since the range of operations goes from minor outpatient procedures as biopsies to major procedures such as a heart transplant. The sequence of the whole process can be seen summarized in figure 1.3.

The ideal surgery consists on a detailed plan of the intervention, an execution exempt of complications and a short recovery time of the patient. However, the everyday practice of surgeons is very different. Usually, the quality of the medical images is not as high as they wish to be, and the surgery cannot be optimally planed since the simulator does not have enough information. Furthermore, during the surgery it is inevitable to come up against unexpected situations as lesions that do not appear in the medical images, worse conditions of a tear than the expected one, poor tissue quality, bleeding, etc. These issues make the work of surgeons to be full of risk situations where their skills are put to test.

Consequently, the professionals involved in surgical procedures require the last technology to overcome these difficulties and practice with safe tools. For this reason, their demands can be brought together into three groups: learning process, surgery planning tools and instrumentation for the surgery room.

The outcome of surgical procedures is closely related to the skills that are being developed over years of surgical training. Therefore, surgeons demand typically training to get used to the organization of an operating room before facing up a real surgery, reduce the learning curve, learn surgical procedures and physical ergonomics, and simulate with a model as close to the patient as possible.

In the pre-surgery stage, physicians demand from technology developers an increase and improvement of the information acquiring methods, and the development of new tools to better plan and simulate surgical procedures. On the other hand, during the surgery, they request advanced passive and active instrumental to reduce patient invasion, complication rate, intervention cost and hospital stay. Additionally, virtual reality and robotics are also welcome to the surgery practice, since they increase or improve the capabilities of the surgeons. Usually, this kind of technology provides additional information channels and new data manipulation tools.

Therefore, engineering specialities related to surgery have a wide range of challenges where the cooperation between different disciplines is mandatory. Figure 1.4 displays some of the typical elements present in the above mentioned three groups, namely, learning process, pre-surgery phase, and actual surgery. Some of these elements can also be shared with other groups however, they are only included in the most common stage.

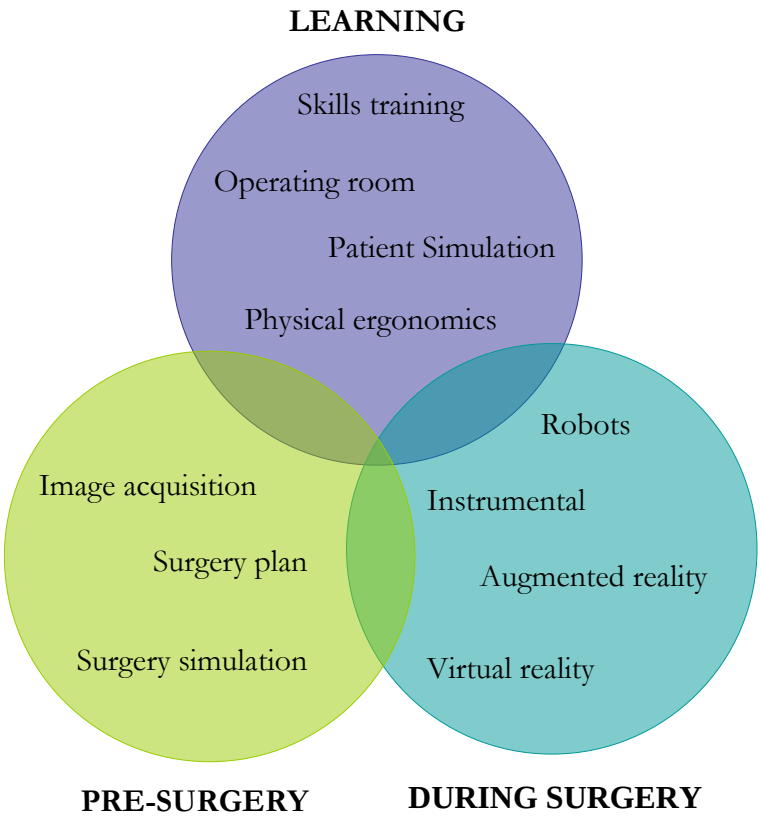

Figure 1.4. The different elements present in the learning, pre-surgery and during surgery stages.

1.2 SURGERY LEARNING, PLANNING AND SIMULATION

In the learning process of any surgical skill, even a task as simple as tying a knot, goes through different stages. First, the learner must understand the mechanics of the skill; that is, how to hold the tie, how to place the throws, and how to move the hands. With practice and feedback, knowledge is

translated into appropriate motor behaviour and the learner is able to execute the task more fluidly and with fewer interruptions. However, the trainee is still thinking about how to move the hands and hold the tie. In the final stage, practice gradually results in smooth performance and the learner no longer needs to think about how to execute this particular task and can concentrate on other aspects of the procedure.

Other fundamental issues cannot be forgotten in the teaching program like organ identification, distinction of different healthy tissue types, or tumour tissue localization. Usually, the images shown in academic books are properly enhanced in order to better explain certain aspects of the subject. However, during an actual surgery the information is not so clear. For this reason, the teaching programs should include specific visualization tools that allow the trainee the *immersion* in a real surgery context.

This knowledge acquisition process can be hard and the learner needs to be relaxed and concentrated into the task. However, real-life operations are complex and it is difficult to focus on one single task of the procedure. Thus, in the early stages of the learning process, it is better to learn and practice some basic skill in controlled environments before getting into the operating room experience. The solution to study these technical procedures until automaticity is achieved can be to practice with physical models or to train with virtual surgery simulators.

Most surgical training programs make use of a variety of models, including inanimate models, virtual reality, live animals, and human cadavers, to simulate living human tissue and anatomy, as well as high-performance patient simulators for critical-incident and team training. Although human cadavers most closely approximate reality, their cost and limited availability, and the poor compliance of cadaveric tissue limit their use. Working with live animals is also problematic because of ethical concerns and high costs.

In contrast, inanimate models are generally safe, reproducible, portable, readily available and more cost-effective than animals or cadavers. Additionally, virtual reality based teaching provides better measurements of trainee performance than it is possible in the real world (Darzi2001). However, the main drawback relies on the difficulty of this technique to represent realistically both, visual elements and mechanical responses.

Even though the previous techniques have their own advantage and disadvantages, all of them can be useful during the process of learning certain procedures. For instance, learning how to make knot can be performed using a piece of a dead animal, a mattress or a virtual reality based simulator (see figure 1.5).

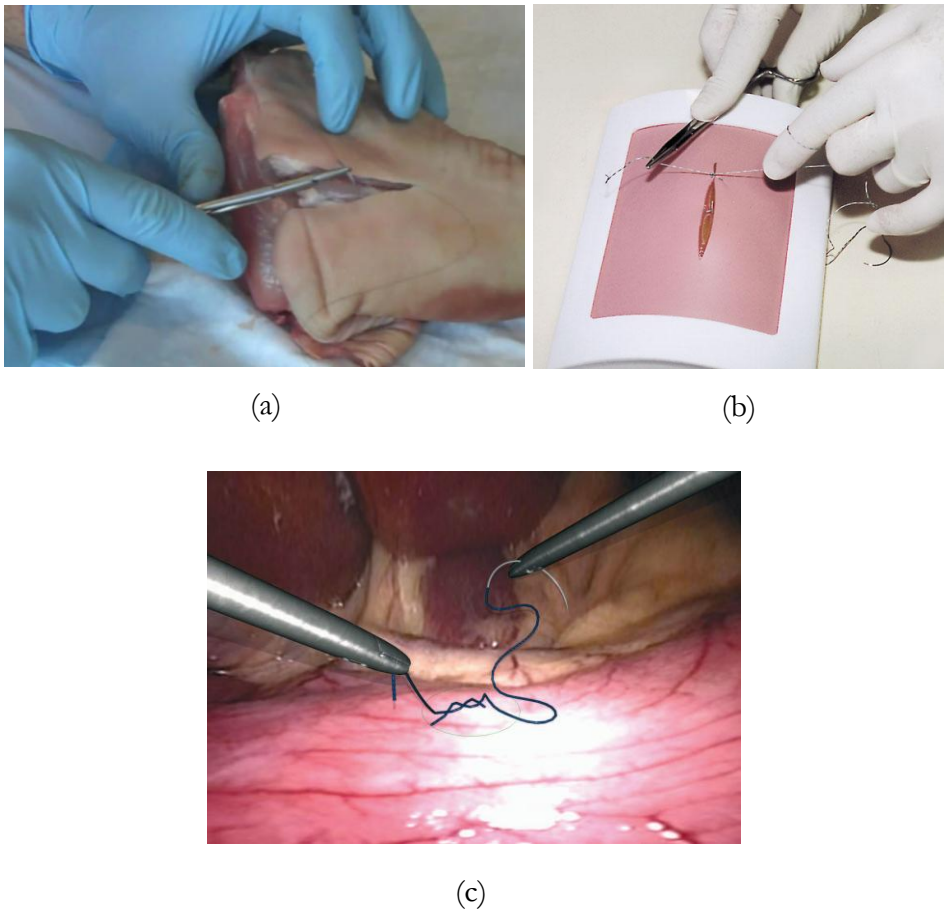

Figure 1.5. Three different techniques to learn suturing: (a) a leg of a dead animal, (b) horizontal mattress and (d) virtual reality based simulator (LapSim®, Surgical Science).

Some of the advantages and disadvantages of various models used in surgery learning, planning and simulation are summarized in the following table 1.1 (table taken from Reznick2006).

Simulation	Advantages	Disadvantages	Best use
Bench models	Cheap, portable, reusable, minimal risks	Acceptance by trainees, low fidelity, basic tasks not operations	Basic skills for novice learners, discrete skills
Live animals	High fidelity, availability, can practice haemostasis and entire operations	Cost, special facilities and personnel required, ethical concerns, single use, anatomical differences	Advanced procedural knowledge, procedures in which blood flow is important, dissection skills
Cadavers	High fidelity, only "true" anatomy simulator currently, can practice entire operations	Cost, availability, single use, compliance of tissue, infection risk	Advanced procedural knowledge, dissection, continuing medical education
Human performance simulators	Reusable, data capture, minimal setup time	Cost, maintenance, and downtime; limited "technical" applications	Team training, crisis management
Virtual reality surgical simulators	Reusable, data capture, minimal setup time	Cost, maintenance, and downtime, acceptance by trainees, 3D not well simulated	Basic laparoscopic skills, endoscopic and transcutaneous procedural skills

Table 1.1. Some of the advantages and disadvantages of various models used in surgery learning, planning and simulation.

Surgery planning and simulation require very different strategies to training. Training does not need a patient specific model; thus, animal and dead bodies are valid to practice. However, in the case of rehearsal it is necessary to use a realistic model of the patient. The main difference between virtual models designed for planning and training purposes is that the objective of the first one is to be as accurate and realistic as possible while the second one has to be appropriate to transfer certain skills. When designing a brain intervention for instance, it can be more important to define the path for reaching a tumour than simulating accurately the needle suturing. However, in the early steps of surgery learning it can be more interesting to acquire precise skills of suturing a wound.

There are two possibilities for the creation of patient specific models: physical and computer-based models. Physical models are time consuming and costly, since they need to be manufactured with the required precision and fidelity. Additionally, in most of the cases, they are valid for one unique trial. On the contrary, computer-based simulation models do not have those limitations. Furthermore, the information obtained in computer-based models can be used during the procedure. Some of their drawbacks, however, are the way of interacting with them and how close to reality is the perception of the procedure.

Virtual reality and three-dimensional representation of pathologies embedded in surgery simulators may facilitate screening, training, planning interventions or diagnosis, in addition to the practice and evaluation of clinicians in the performance of procedures for certification. Therefore, these tools are very appropriate for overcoming important problems and limitations commonly found in nowadays surgery.

Bringing forward some of the objectives that are going to be explained in the following sections, in this thesis the attention has been focused on overcoming some of the limitations of virtual reality based tools. Particularly, the main objective is to build realistic deformable virtual models to be used in learning engines, and in surgery planning and simulation tools.

1.3 GENERAL SURGERY SIMULATORS

Surgical simulators can be useful in training as well as in procedure planning and simulation. The main difference is that in the training phase the

simulation does not need to be patient specific and it can be focused in a certain task rather than in the whole surgery (see figure 1.6).

On the other hand, surgery simulation can be seen as a natural extension of the intervention planning process. In this case, it is mandatory to use patient specific data and usually requires simulators that are more complex than those used in learning programs. This kind of simulator allows the study of the effects of the planning, prevents unexpected situations, and prepares the surgeon to proceed in the most secure manner.

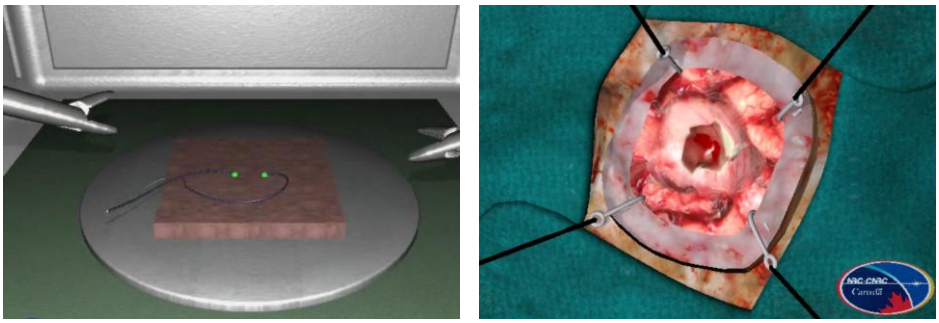

(a) (b)

Figure 1.6. (a) Learning simulator that uses synthetic data (LapSim®, Surgical Science) and (b) patient-specific virtual neurosurgery simulator (source: National Research Council[1]).

Every surgery simulation process can be divided, basically, into four steps: medical image acquisition and geometric model generation, virtual deformable model building, user interaction management, and deformation simulation (see figure 1.7).

1.3.1 DATA ACQUISITION AND GEOMETRICAL MODEL GENERATION

Depending on the objective of the simulator, the source data to build a virtual model is twofold: synthetic data and patient specific medical data. For basic skill learning purposes, such as suturing, it can be enough to use synthetic data. However, using a simulator for planning a real case of surgery requires specific data pertaining to the patient.

[1] http://www.nrc-cnrc.gc.ca/eng/projects/ghi/virtual-reality/video.html

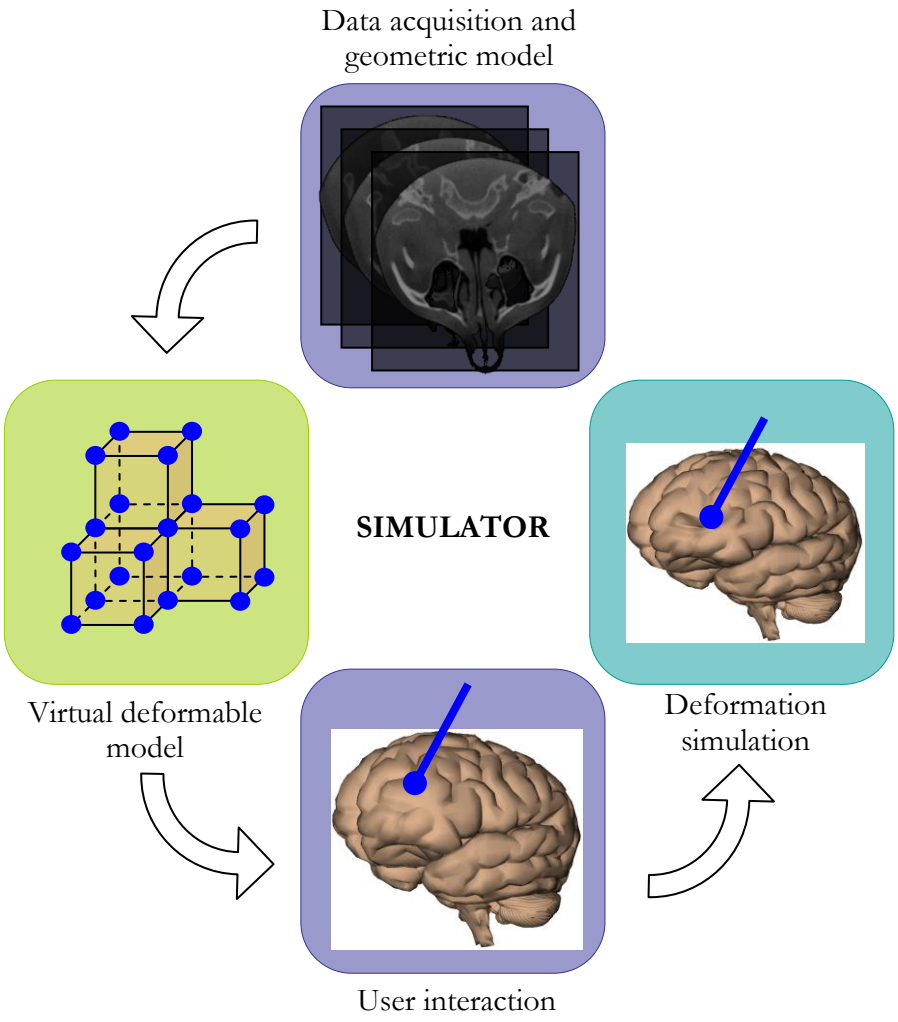

Figure 1.7. Modular structure of a generic surgical simulator.

In some cases both types of information are combined to develop suitable simulators. Some learning simulators, for instance, use synthetic data that comes from combining different medical information from different patients. In other words, they use *average patient models*. Alcañiz et al. (Alcaniz2003), for instance, developed a surgery simulator that allows the user to select the tools and the organs needed for the simulation of the operation. The organs loaded in the simulator can be real or synthetic and with or without pathologies.

Medical imaging is the principal source of information for creating this kind of model. New image acquisition devices, apart from offering enhanced representations of the reality, allow applying three-dimensional and virtual reality techniques to generate detailed models of biological tissues. These geometrical models are the visual objects that the surgery simulator will use. Therefore, high resolution acquisitions are desired.

The most common medical image acquiring techniques are Computer Tomography (CT) and Magnetic Resonance Imaging (MRI). Both are based on different physical principles and produce different image characteristics. CT provides images with sharp contours of bones since they have high contrast between bones and soft tissue. On the contrary, MRI is more suitable for obtaining images with greater contrast between the different soft tissues of the body. Neither imaging modality can produce clear contours of both the bone and the surrounding soft tissues, even though they provide complementary information.

In modern medicine there are many other medical imaging approaches apart from CT and MRI like photoacoustic, ultrasound, termography, and nuclear medicine based imaging.

After acquiring the medical images it is necessary to process them in order to transform those data into useful information. The objective of a simulator is to show and interact with different organs and tissues; thus, the image processing tools has to be able to extract the corresponding information. This information may include geometric data, structure of organs or identification of material type. To achieve this objective, the normal procedure is to use image segmentation, registration and reconstruction methods.

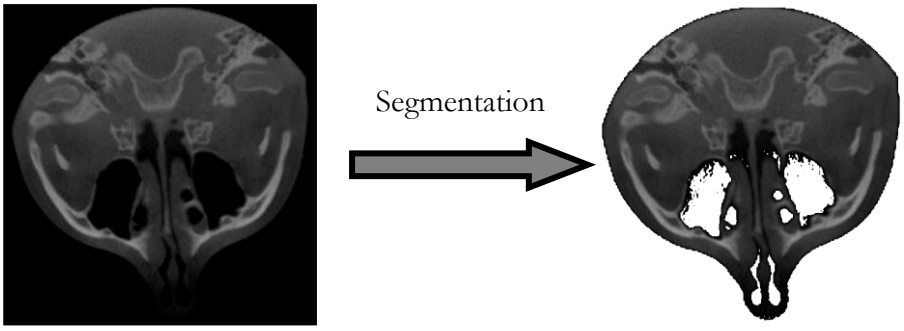

Figure 1.8. Example of a segmentation of CT scan of the head.

Segmentation is the process of identifying and classifying data found in a digitally sampled representation. It allows defining the limits of each type of tissue (see figure 1.8).

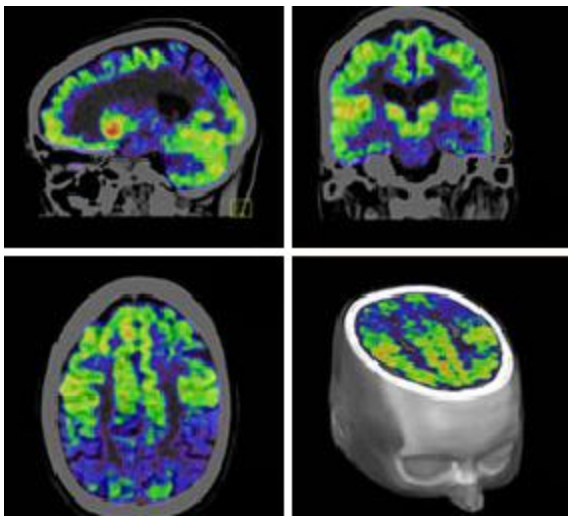

Figure 1.9. Example of the registration of different brain images.

Registration is the task of aligning or developing correspondences between data. For example, a CT scan may be aligned with a MRI scan in order to combine the information contained in both (see figure 1.9).

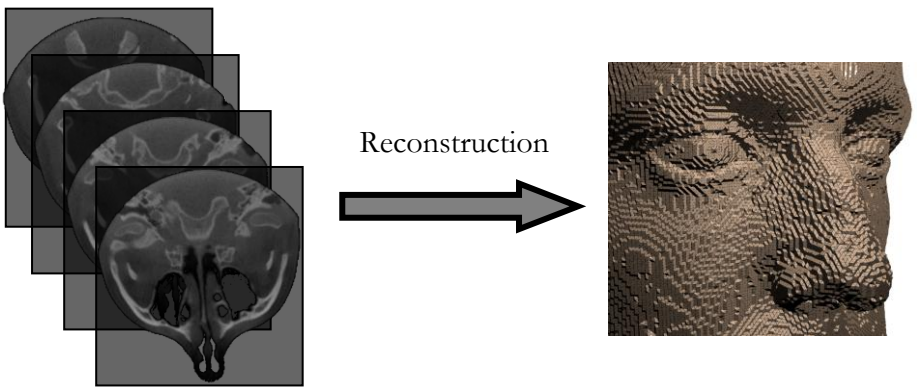

Figure 1.10. Example of the 3D reconstruction of a set of head images.

As the segmented and registered images usually are 2D slices, it is necessary to combine them in order to generate 3D geometries. There are many techniques to build these geometries; the easiest one is to assign to

each pixel of the slices a height and transform them into voxels (see figure 1.10). Afterwards, there are several ways to convert this cubical geometry into smooth triangular meshes, for instance, the marching cubes method (Lorensen1987). Both the triangle meshes and the voxel information can be used to represent the anatomy of the patient in a 3D interactive virtual model.

1.3.2 VIRTUAL DEFORMABLE MODEL BUILDING

Once the different regions captured with the medical imaging devices are identified, the 3D objects have to be translated into virtual mechanical objects so that the computer can simulate their physical behaviour when the user interacts with them in the virtual environment in a realistic way. In particular, it is important to represent realistically how the different soft tissues deform under the virtual forces applied in the interaction.

There are different techniques to create deformable models and each of them allows specific ways of simulation. Some models are based on geometric approaches while others are physically-based. In surgical applications geometrical approaches are hardly seen since they do not provide accurate results and do not allow computing mechanical measures such as forces. Physically-based approaches, in turn, are widely adopted in mechanical simulation field as they are much more versatile and accurate.

Those models that are simulated using geometrical constraints and keyframe interpolations belong to the group of geometric approaches. Although it is not mandatory, they typically define the deformable object as a surface and only look for a visually satisfactory result. The weakest point of this sort of models is that they provide very poor interaction experiences since they cannot calculate any feedback force to return to the user. Additionally, as they cannot simulate the physical behaviour of the body, it is impossible to apply them to make realistic procedure learning or simulation. Therefore, their use is mainly limited to the production of didactic videos (see figure 1.11).

On the other hand, deformable bodies based on physical laws are able to simulate closely the behaviour of living tissues since they evaluate also the mechanical response of the matter. In this context, there are two main approaches: the continuum and the discrete point of view. The Finite Element Method (FEM) is the most relevant continuum-based method while the gold method for the discrete approaches is the Mass-Spring Model (MSM).

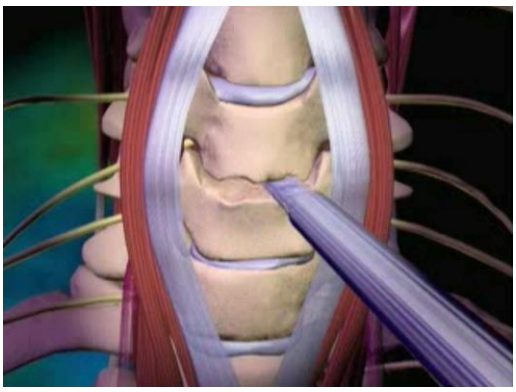

Figure 1.11. An image from a didactic video about cervical surgery (courtesy of SpineUniverse.com, a Vertical Health Web Property).

Physically-based deformable models have two important characteristics: mechanical behaviour and topologic configuration. As each region belongs to different types of tissue it can show different behaviour and has to be characterized using different parameters even material models. Since most simulation models are built up using simple geometrical figures, the 3D bodies are tessellated adopting, usually, cubes or tetrahedra.

The information contained in the medical images allows transforming the geometrical model into a deformable model by assigning some parameter values to each region (see figure 1.12).

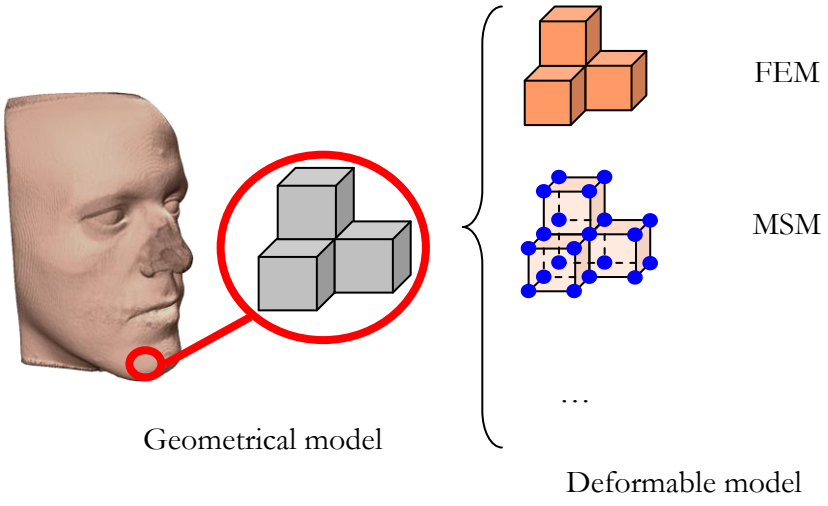

Figure 1.12. The geometrical model is transformed into a virtual deformable model.

Mechanical parameters depend on the tissue type, deformation velocity and the extent of the deformation. In general, biological soft tissues have very complex behaviour. However, they are usually taken as linear elastic in the case of small deformations and hyperelastic in the case of big deformations. In both cases, material properties can be either uniform or non-uniform.

Apart from using medical images of a certain patient to build up the virtual model it is also possible to use synthetic data. If the objective of the deformable model is to develop a simulator to learn suturing it can be enough to build a model in which the mechanical properties are essential but the geometry is not so important. In this case, the behaviour of the tissue can be obtained from mechanical tests such as indentation, compression, aspiration or shear testing (Mazza2007).

1.3.3 USER INTERACTION

There are different interaction modalities depending on the objective of the simulation. If the aim of the simulation is to design a surgery plan it may be interesting to show the outcome of the procedure. However, if the objective is the training of certain surgical techniques, it might be more interesting to develop a simulator that reacts interactively in real time and provides the user with feedback information of the deformations and forces.

In the practice of surgery, there are many mechanical instruments such as forceps, needles and scissors, and they produce numerous interactions types: palpation, punctuation, injection, suction, grasping, pulling, gripping, clamping, etc. All of them change the initial state of the subject generating geometrical and mechanical modifications. Thus, the surgery interaction module has to analyze the interaction type and its magnitude to transform it into mechanical parameters.

The deep analysis of some of the issues that arise during interaction is very complex but in most of the surgical applications they are simplified in order to make computationally efficient simulations. Typical interaction routines include collision detection algorithms and collision response computation, which usually involves collision reaction and friction force calculus (see figure 1.13).

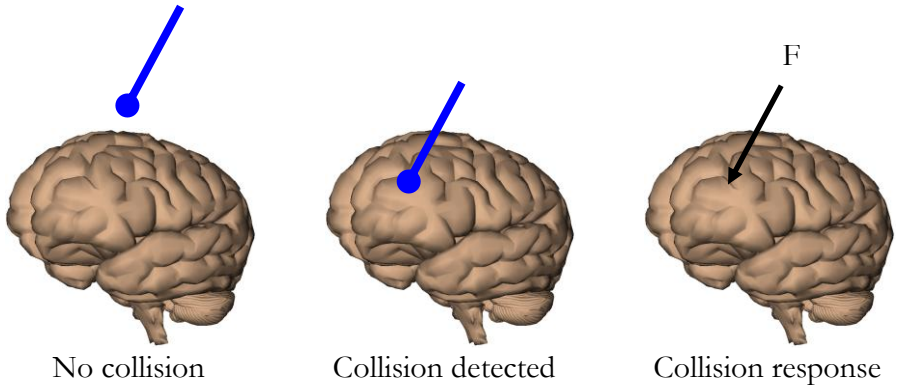

Figure 1.13. The interaction management involves detecting and computing collisions.

1.3.4 SIMULATION

The aim of the simulation consists in studying the effects of the user interactions over the deformable body. That is, the simulation routine has to evaluate the mechanical effects of the net forces applied on the body or specific parts of the body. As all the biological tissues have certain mass, those forces cause accelerations to each element of the body that lead to displacements, rotations and deformations (see figure 1.14).

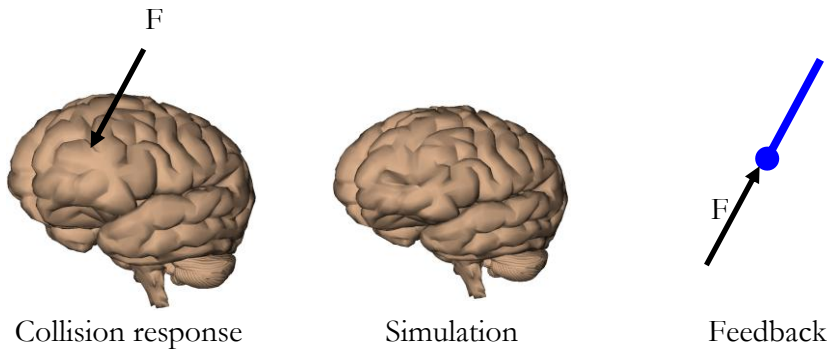

Figure 1.14. The simulation module computes the deformed state and may return force feedback due to the change of the conditions of the primary interaction.

The simulation module computes a new deformation state which can involve changing the conditions of the interactions. Therefore, in some simulators this module also returns some force information that may modify the force computed in the user interaction module.

To update the state of the model it is necessary to evaluate the deformation making kinetic and kinematic analysis. As these approaches usually require using time integration methods, the most common problems that accompany these procedures are mathematical convergence and stability issues.

1.4 OBJECTIVES AND SCOPE

Once the overall structure of a surgical simulator has been seen and taking into account the requirements and challenges suggested by the medical community involved in surgical treatments, three different main areas of research can be distinguished: development of innovative medical imaging techniques, development of realistic surgery planning and simulation modules, and design of new surgical instruments (including devices for robotised procedures).

In particular, this thesis is focused on the second category, that is, the interactive surgery planning and simulation stages. In this field, the designers of medical simulators have to tackle with two major challenges: reproducing with accuracy the deformations of real biological tissues and giving realistic feedback to the user of the surgical interactions.

This thesis will focus on the first of these challenges, and its main objective is the characterization of virtual deformable bodies for the realistic and accurate simulation of medical procedures.

1.4.1 SCOPE

As deformable models need a platform to be tested a generic interactive simulator is going to be developed whose purpose is to give a context to the proposed deformable model and evaluate its usability. In the previous sections it has been shown that in a simulator many processes are involved. However, the effort is going to be focused in the deformable model building process. The rest of the components of the simulator are out of the scope of this thesis. Therefore, those issues related to image acquisition and analysis, collision detection, and specific simulation problems like instabilities will not be addressed.

According to the input data, as it has been mentioned previously, there are two types of medical information used for generating medical models, namely, synthetic and patient-specific data. Thus, it is desirable to

design generic deformable models suitable for adapting their parameters to both kinds of data.

Additionally, the outcome of this research work has to fulfil some requirements that concern the description of the behaviour of the model, the characteristics of the interactions, and the feedback information with which the user is provided.

Although a high variety of elements are present in the human body, the studied models will be limited to solid deformable bodies. Fluids and gases will be excluded from the modelling process. Even though they suppose the highest percentage of the volume of the human body in many cases their mechanical effects can be simplified substantially. Assuming that nonsolid materials are confined in a closed space or their flow is fairly constant; then, their modelling can be similar to that of the solid bodies.

The non-homogeneous group of solid bodies includes, among others, muscles, ligaments and tendons. Although their properties are radically different it is usual to suppose that their behaviour is linear elastic under small deformations and nonlinear when high deformations are involved (Taylor2009). For this reason, following the generic view of this thesis it is necessary to consider both material models.

Another well-known complexity of the human body is that it is continuously changing and adapting itself to the external conditions. Studying living processes like bone growth, platelet activity in a wound or the muscle elasticity variations due to temperature changes requires very specific virtual models. As this research work is focused on developing generic models for deformable tissues in virtual reality simulation this sort of processes will not be considered.

The user interactions that will handle the developed generic simulator are limited to palpation-like tasks since they are enough to test the model and study its usefulness. For this reason, the specific study of mechanical effects concerning the interactions with medical instruments such as scalpels, scissors and needles remain out of the scope of this work.

1.4.2 OBJECTIVES

The main objective of this thesis is to study and analyse deformable models specifically designed for the simulation of biological tissue manipulation. Specifically, the aim of this work is to characterize models suitable for realistic, accurate and fast simulations of the deformations of living tissues.

In particular, special attention will be paid to one of the most critical points of the deformable model design, namely, the process of deriving the parameters of these models.

The following points summarize the particular objectives of this research work and specify the characteristics that the simulation model has to fulfil:

- As stated in previous sections, surgery planning and simulation tools usually need to calculate the mechanical response in real time. Therefore, the deformable model has to allow fast computation of the mechanical behaviour in order to guarantee **real-time response in interactive simulations**.

- To guarantee a reliable performance during the simulation, the methods proposed to characterize the models have to **ensure their accurate behaviour**.

- The feedback of the simulation model cannot be limited to visual information of the model deformation. In turn, it has to **give mechanical feedback**. These results can be either deformation or force values.

- In many previous works, to achieve real-time performance, the living tissues have been modelled using simplified linear elastic and homogenous material models. In this research work, a more realistic and complex behaviour is sought. That is, the proposed model has to be able to **describe non-homogeneous and nonlinear behaviour**.

- In order to develop a simulation model as flexible as possible, the algorithms proposed to generate the models have to be suitable to **build generic as well as patient-specific models**.

- The simulation model has to be capable of **dealing with user interactions such as palpation**. The considered mechanical interactions will be limited to palpation manoeuvres using stick-like medical instruments.

- The final software implementation of the proposed method is out of the scope of this work. Therefore, the **real-time performance capability of the proposed approach has to be tested using existing commercial or freely available simulation software**.

1.5 DOCUMENT ORGANIZATION

The contents of this memory are divided into 7 chapters. The first chapter has presented the motivations for this thesis. The second chapter outlines the most relevant methods proposed in literature for the simulation of deformable bodies, such as the FEM or the MSM. In this chapter it will be seen that MSMs provide a general framework that fulfils many of the requirements for this work.

The derivation of the parameters of a MSM is still an open research question. Chapter 3 shows an overview of the methods used for the derivation of the parameters of MSMs and proposes two new different methods that will be described in more detail in the following chapters:

- Chapter 4: a new method valid for small deformations that uses linear material models as input data. This method is based on the linearization of the nonlinear equations of MSMs; thus, its usability is limited to specific circumstances.

- Chapter 5: As the generic behaviour of biologic living tissues is hyperelastic, a new method is proposed to generate such models. This method takes advantage of the nonlinear nature of traditional MSMs and is valid for large deformations.

Chapter 6 shows two medical applications implemented using the proposed methods. Chapter 7 presents the conclusions derived from this work and proposes some future research lines.

CHAPTER 2

STATE OF THE ART IN SOFT-TISSUE DEFORMABILITY MODELLING

The development of deformable models for the simulation of living tissues gained great importance in the middle of the 1990's due to the emergence of the simulation of surgical procedures. This was part of the paradigm shift in the field of medicine that brought concepts such as telepresence surgery, virtual reality based surgical simulators, medical informatics and rehabilitation. The main precursor of these techniques was the American Department of Defence who considered surgery simulation a fundamental part of emergency medicine (Satava1994).

The need of virtual deformable models for these applications caused the study of many different approaches, which, consequently, lead to the development of many types of simulation algorithms, such as MSMs, or the adaptation of other approaches present in other fields of research, such as the FEM. All of these methods share the objective of finding a model that is capable of reproducing or predicting the outcome of the interaction with real soft tissues for a given set of start conditions using mathematical and computational modelling tools.

In contrast to the behaviour of other typical elements present in computer simulations such as rigid body simulation, the behaviour of soft tissue is usually more complex and requires different approaches. The direct

application of the classical laws of Continuum Mechanics mostly leads to mathematical formulations that cannot be solved analytically and whose numerical solutions are time-consuming and difficult or even impossible due to numerical instability. To overcome these problems, a variety of simplifications and other approaches have been proposed. Some of them are referred to as *physically-based*, such as MSMs, whereas others can clearly be associated with animation techniques, parametric surfaces for instance. On the other hand, the approximated simulations based on the constitutive laws used in soft-tissue modelling include linear and corotational FEM.

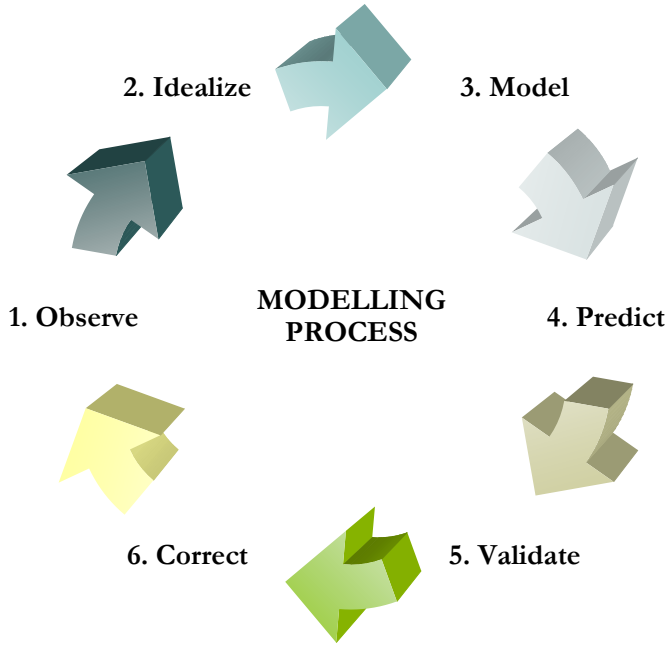

Figure 2.1. The different tasks that take place during the modelling process.

No matter which category a particular model might fall into, the process of finding a model always includes similar set of tasks. In general, modelling real biological tissues requires following the next sequence of steps (see figure 2.1):

1. Observe the domain of the problem and try to find regularities that can be used for a model.

2. Find an idealization for the problem that is capable to reproduce the observed regularities.

3. Construct a model that reflects the observed regularity, generally using a mathematical formulation.

4. Make some simulations to predict certain performance.

5. Validate the predictions with experiments.

6. Correct the model and start the process all over until the validation meets the acceptance conditions.

Frequently, the resulting mathematical formulation has the problem of being too complex. In those cases, it is a common procedure to make some simplifications that limit the framework of the model but making it more suitable to the everyday practice.

In this chapter, first, the different techniques applied to obtain the mechanical parameters of soft tissue are presented. Then, the main characteristics of biological soft tissues will be addressed and some of the typical simplifications adopted when describing their behaviour will be presented. Afterwards, the most common deformable models will be introduced. This review will not limit itself only to soft-tissue simulation but it will also deal with other related topics such as cloth simulation and character animation, because those fields suppose an interesting source of ideas, which, in some cases, can be directly applied to medical simulation.

2.1 MECHANICAL PROPERTIES OF SOFT TISSUE

There are different environments in which medical data is obtained. They can be roughly divided into three types: *in vivo*, *ex vivo* and *in vitro*. The experiments made using a whole, living organism are called *in vivo* experiments. *Ex vivo*, in turn, is related to the studies made in an artificial environment outside an organism. Finally, *in vitro* corresponds to those analyses performed in a test tube outside an organism.

There are many studies on the mechanical properties of biological soft tissues, however very limited data are available of the *in vivo* behaviour of soft tissues associated with human organs.

The main reason for this deficiency is the severe technical and ethical problems related to this kind of experiments. Usually, these techniques require direct access to the internal organs of a patient, leading to interference and disruption of the primary surgical procedure. Additionally,

the standard methods of material testing, such as tensile or bending experiments, are not appropriate for *in vivo* procedures.

Many different approaches have been proposed for *in vivo* analysis such as indentation (Samur2007, Kim2008) and aspiration (Nava2008, Schiavone2009) (see figure 2.2). The two main drawbacks of most of *in vivo* approaches are the difficulty to impose well-defined boundary conditions and the requirement of *opening* the patient for the characterization of inner organs.

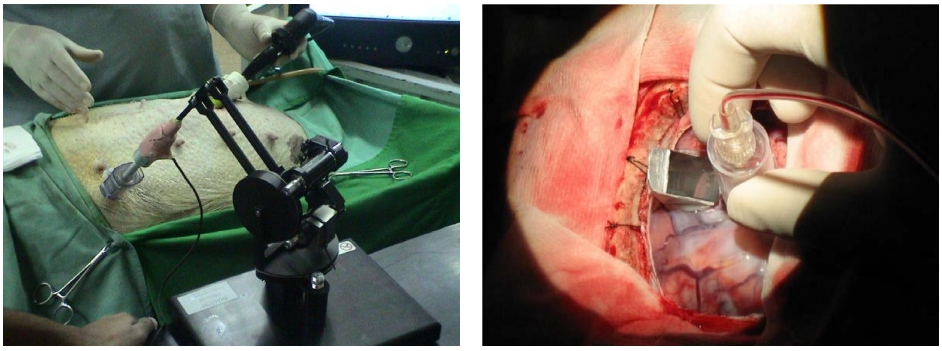

(a) (b)

Figure 2.2. Two different *in vivo* approaches for the characterization of soft tissues: (a) a robotic indenter for minimally invasive measurement (Samur2007) and (b) human brain elasticity measurement using a light aspiration device (Schiavone2009).

On the contrary, when analyzing inner organs, ultrasound and acoustic wave propagation based measurements are also *in vivo* but not invasive. For instance, acoustic radiation force imaging (ARFI) modalities are being studied to non-invasively characterize the liver without the need for liver biopsy (Palmeri2008). Another interesting approach is elastography, which is a non-invasive method that uses stiffness or strain images of soft tissue to detect or classify tumours (Iglesias-Garcia2009).

The most important limitation of non invasive *in vivo* approaches is that they can be used to obtain some behavioural information but in general they do not allow defining load-deformation curves. Moreover, as the measurements are taken from the exterior it is fairly impossible to obtain detailed data about the change of these properties along the different locations and directions.

On the other hand, *ex vivo* and *in vitro* experiments need extracting a tissue sample of the patient. In practice, these techniques are applied to derive general mechanical behaviour of some tissues, obtain information about the constitution of a sample or detect the presence of certain substance or disease. As these techniques are invasive and require extracting a sample, if there is not a justified reason, they are not applied to characterize the mechanical response of the tissue of a particular patient for patient-specific surgery.

Let us take as an example the study of the mechanical properties of the brain to show how difficult is to obtain mechanical parameters and their variability from one another experiment.

Most authors propose to simplify the modelling hypothesis by relying on a small deformation linear elastic constitutive equation to characterize the mechanical behaviour of the brain tissue. Even in this quite restrictive framework, parameter values selected to define the mechanical behaviour vary significantly, with a Young's modulus ($\boldsymbol{E}$) between 0.6 kPa (Clatz2005) and 180 kPa (Kyriacou1999), and Poisson's ratio ($\boldsymbol{\nu}$) between 0.4 (Skrinjar2002) and 0.499 (Miller2000).

The variety of the results found for the specific case of the mechanical properties of the brain cannot be generalized. In some cases, it is possible that obtaining those properties is easier because the region is very accessible, skin for example, and the results might be more similar. However, characterizing a whole organ which is not easily accessible is very hard because punctual measurements may not obtain directional information of tissues such as reinforced fibres of muscles, for instance.

The direct consequence of this issue is that surgical simulators have limited input data. Ideally, surgery planning and simulation tools require accurate information about the behaviour of the whole region of interest of a surgery, under different loading conditions and preoperatively. Generally speaking, with the current techniques it is difficult to have accurate data before the surgery and during the surgery there is not enough time to make useful simulations that may change the operation strategy.

2.2 CHARACTERIZING SOFT LIVING TISSUES

The mechanical properties measured using the previously presented techniques have to be analyzed and a mathematical formulation has to be developed to model them. The characterization of the behaviour of

deformable bodies is one of the most complex aspects in continuum mechanics because the existing mathematical theories are, in general, incomplete and are not able to characterize soft living tissues completely.

However, some approximated material models have been developed from experimental observations and are useful to predict their behaviour. These models must be viewed simply as idealizations of regimes of material response under specific types of loading and environmental conditions.

While studying the living tissue biomechanics, the common practice has typically been to use engineering methods and models, known from classic material science. However, living tissues have properties that make them very different from typical engineering materials. They permanently consume energy and exchange matter with their environment to maintain the essential metabolic processes. For example, living tissues have self-adapting and self-repairing abilities, which enable wound healing and stress relaxation of loaded tissue.

The diversity of mechanical properties encountered in soft biological tissues is huge. Numerous experimental and theoretical studies in the field of tissue biomechanics have been carried out in recent years (Fung1993, Maurel1998, Oezkaya1999). Summarizing the facts observed in different experiments with different tissue types, soft tissues generally exhibit quasi-incompressible, nonlinear plastic-viscoelastic material properties. Additionally, they often have a layered or an even more complicated structure and non-homogeneous distribution of the constituents. This causes the mechanical properties to be anisotropic and non-uniform.

The properties listed above are briefly described in order to help better understanding the characteristics of living tissues and posterior analysis of the techniques used to model them:

- **Non-uniformity, anisotropy:** Soft tissues are multi-composite materials containing cells, intracellular matrix, fibrous and other microscopical and macroscopical structures. This means that the mechanical properties of living tissues vary from point to point within the tissue. Essential for modelling are the spatial distribution of material stiffness and the organization of fibrous structures such as collagen and elastin fibres, which have frequently some preferential orientation. The dependence on coordinates along the same spatial direction makes the properties to be *non-uniform*. If a material property depends on the direction, such material is called *anisotropic*. Although

properties of most of the living tissues are non-uniform and anisotropic, there are few quantitative data about them.

- **Stress-strain:** *stress* (**σ**) is a measure of the average force per unit area of a surface within a deformable body on which internal forces act. *Strain* (**ε**), in turn, is the geometrical measure of deformation representing the relative displacement between particles in the material body. It measures how much a given displacement differs locally from a rigid-body displacement. In general, the mechanical behaviour of a tissue is given in terms of stress-strain diagrams or constitutive equations.

- **Elasticity:** it is the physical property that describes the tendency of an object to deform along an axis when opposing forces are applied along that axis. It is commonly characterized by the slope of the stress-strain curve.

- **Material nonlinearity:** The stress-strain relationship of general soft tissues is nonlinear. Usually, the nonlinear stress-strain curve (see figure 2.3) is divided into three phases (Fung1993). In the first part (phase I), the load increases exponentially with increasing elongation. In the second part (phase II), the relationship is fairly linear. In the third part (phase III) the relationship is nonlinear and ends with rupture. The *toe* region (phase I) is usually the physiological range in which the tissue normally functions.

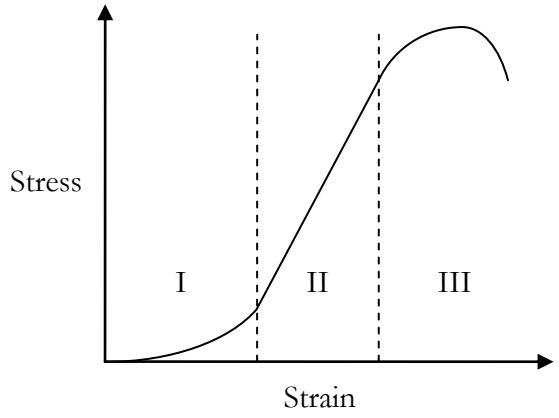

Figure 2.3. Typical nonlinear stress-strain curve of soft tissue (Fung1993).

- **Viscoelasticity and hysteresis:** viscoelastic materials are those for which the current deformation is a function of the entire history of loading, and conversely, the current stress is a function of the entire history of straining. After the stress is removed the material recovers the original state. However, the resulting loading and unloading stress-strain diagrams are different. This phenomenon is known as hysteresis.

- **Viscoplasticity:** it is the permanent, or plastic, deformation produced by a cyclic deformation process that does not return the material to its initial state, even after relaxation. This occurs when processes in the material that respond to a change in stress or strain result in irreversible changes. This prevents the material from assuming its initial state after restoration of the mechanical magnitudes to their original values.

- **Force-relaxation (or stress-relaxation):** it is a phenomenon that occurs in a tissue stretched and held at a fixed length. Over time the force present within the tissue continually declines.

- **Quasi-incompressibility:** a material is called incompressible if its volume remains unchanged by the deformation. Soft tissue is a composite material that consists of both incompressible and compressible ingredients. Tissues with high proportion of water, like brain for instance, are usually modelled as incompressible materials, while tissues with low water proportion are assumed quasi-incompressible.

Observing the complexity of the mechanical characteristics of living soft tissues, it results evident that it is mandatory to make some assumptions in other to simplify the observed behaviour and propose useful models. These idealizations depend on the working context; thus, some tissue may have different models in different situations.

Material models used in soft-tissue simulation do not describe materials themselves. Rather they describe the behaviour of materials under well-defined working conditions. A very common example of this idea is water since there is not a unique constitutive relation for it. There are a least three different material models for water in its solid, liquid, or gaseous states. This means that, for the same tissue, there are different material models that are valid for the specific conditions of deformation, temperature and pressure.

Therefore, it is unreasonable to expect that any single constitutive relation should describe totally a particular tissue. In other words, diverse constitutive relations can be equally useful for describing the behaviour of individual tissues depending on the conditions of interest.

In the particular case of biological soft tissues, there is no tissue that exhibits a truly elastic response. However, there are many conditions under which the assumption of elasticity is both reasonable and useful. Toward this end, one of the most interesting observations with regard to the behaviour of many soft tissues is that they can be preconditioned under cyclic loading. That is, as a biological tissue is alternatively loaded and unloaded, the stress versus stretch curves tend to shift to the right, with decreasing hysteresis, until a near-steady-state response is obtained (see figure 2.4). Fung (Fung1993), for instance, suggested that this steady-state response could be modelled by separately treating the loading and unloading curves as nearly elastic or *pseudo-elastic*.

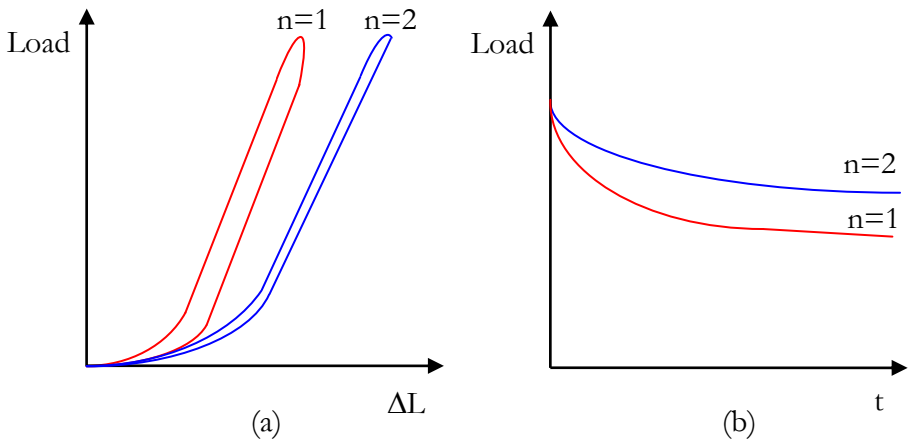

Figure 2.4. An example of the preconditioning effect: (a) load-elongation and (b) relaxation curves of the first two cycles (Fung1993).

In practice, except in the case of muscular tissues, the hysteresis is often small. Thus, it is possible to approximate reasonably well the mean response between the loading and the unloading responses using a single elastic descriptor, similar to what is done to describe rubber elasticity. Many parallels between tissue and rubber elasticity likely result from the long-chain polymeric microstructure of both classes of materials, thus these fields can borrow ideas from one another (Treloar2005).

Whereas a measured linear stress-strain response implies a unique functional relationship, the nonlinear, anisotropic stress-strain responses exhibited by most soft tissues typically do not suggest a specific functional relationship. In other words, one must decide whether the observed characteristics are best represented by polynomial, exponential, or more complex stress-strain relations. Common forms of stress-strain relations in rubber elasticity and soft-tissue modelling are those who represent accurately hyperelastic behaviours, for example, neo-Hookean (Wu2001, Harders2003, Martins2006), Mooney-Rivlin (Hirota2001, Wu2001, Hu2004, Martins2006), and Ogden (Hu2004, Martins2006, Gao2010) material models.

For this reason, it is generally accepted that considering the behaviour of soft tissues as linearly elastic, in the case of small deformations, and hyperelastic for large deformations is enough to characterize them in the surgery simulation field. Even more, if the behaviour of the tissue is assumed to be similar for the whole model, then it is acceptable to use uniform properties. However, some applications require more detailed models and in those cases it can be more realistic to use non-uniform properties.

2.3 INTRODUCTION TO MODELLING METHODS

The characteristics observed and idealized in a behaviour model have to be incorporated into a mathematical framework. In general, real processes in nature are continuous with respect to space and time. Modelling continuous processes using computers necessarily leads to problems that use data that computers can represent, that is, discrete data. This involves working with limited accuracy. Therefore all problems have to be parameterized in a discrete state vector. The problem is then generally solved with a numerical integration technique that approximates the solution at discrete time steps.

A discrete problem representation as necessary for the computer can be achieved in two ways: (1) a continuous problem formulation can be discretized or (2) the problem itself can be formulated in a discrete way. Both approaches are common in biomechanical modelling.

2.3.1 CONTINUOUS APPROACH

The continuous approach requires special mathematical formulations to solve the deformation field since the object can hardly ever be studied with

a finite number of parameters. Until the arrival of the FEM continuous systems were solved analytically, but this was affordable only when the geometry or the boundary conditions were simple. FEM formulation caused a big change in the way the continuum problems were solved since it allows finding approximate solutions of partial differential equations as well as integral equations.

Several branches of computational mechanics can be distinguished depending on the focus of attention. A typical classification of static analysis is based on the discretization method by which the continuous mathematical model is subdivided in space. This classification leads to three methods: FEM, Boundary Elements Method (BEM) and Finite Differences Method (FDM).

For linear elastic problems FEM currently dominates the scene and BEM, although it is less used, is steadily gaining ground in some application fields. For nonlinear problems the dominance of FEM is overwhelming. FDM achieves efficiency and accuracy when the geometry of the problem is regular, but they are not well suited to study solids with complex contours. Thus, FDM in deformable body study has virtually disappeared from practical use except for a few simple problems.

The main advantage of BEM approach is that it only requires a mesh on the surface of the model but do not a volumetric inner mesh. However, BEM techniques have several disadvantages over FEM. The most limiting issue is that BEM makes strong hypotheses about the nature of the elastic material: only homogeneous and isotropic linear elastic materials can be modelled. Another important point is that BEM cannot compute the displacement of any interior point, which can be a limitation when data about internal structure displacements are needed.

As computing internal deformations can be necessary and the nonlinear material models are very common in soft-tissue simulation, in this thesis only the FEM has been considered.

2.3.2 DISCRETE APPROACH

The discrete approach considers the deformable object as a finite collection of elements interconnected to each other at specific points. The essential characteristic of these systems is that their deformation can be exactly defined using a finite number of parameters, namely, the displacements of the points where the different elements are connected. Therefore, the

equilibrium of the system can be represented using the equations of equilibrium in the directions of the deformations.

There are few discrete approaches used in medical applications. The most popular ones are the MSM, Discrete Element Method (DEM) and Smoothed-Particle Hydrodynamics (SPH). DEM and SPH are mesh-free methods that study inter-particle interactions. This makes them especially suitable for the simulation of solids at atomic-scale and fluids. In turn, MSMs have network organization and are able to define complex structures such as non-homogeneous and layered models. Therefore, the MSM is preferable to DEM and SPH when simulating soft-tissue deformations.

As DEM and SPH are not very common in soft-tissue simulation, in this thesis only the MSM has been considered.

2.4 FINITE ELEMENT METHOD (FEM)

The FEM is a numerical analysis technique for obtaining approximate solutions to a wide variety of engineering problems. Although it was originally developed to study stresses in complex structures, it has been extended and applied to the broad field of continuum mechanics. One of these fields being the study of soft-tissue mechanics.

The objective of the FEM applied to deformable body simulation is to solve the differential equations provided by the theory of elasticity. This theory will not be explained since its details are out of the scope of this thesis. Just say that this theory defines the *material law* as a relation between the stress and the strain, which can be linear or nonlinear depending on properties of the material. For further information on the theory of elasticity the reader is referred to the work of Zienkiewicz et al. (Zienkiewicz2005).

In the continuum based approach, the continuous medium replaces discrete arrays of atoms and molecules with a continuous distribution of matter. Fields and properties defined at every mathematical point in the medium are continuous, with continuous derivatives, except at a finite number of surfaces separating regions of continuity. To work with the continuum, the fundamental concept applied by FEM to study mechanical response is the spatial discretization of this continuous medium.

The body being analysed is divided into a finite collection of contiguous and disjointed regions called elements. These elements are

connected to each other at a finite number of points known as nodes. In this way, the unknown displacements that are necessary to calculate the deformation become a finite set of parameters to be solved: de displacement of the nodes.

Each finite element has associated some interpolation functions that define the displacement of any internal point in function of the displacement of the nodes of that finite element. Consequently, solving the mechanical problem just in the nodes of the finite elements gives the approximated displacement field of the whole continuous solid. This idea can be applied because the equations that govern the global object also govern the behaviour of the elements.

In this way, it is possible to transform the initial continuum object with an infinite number of degrees of freedom that is governed by differential equations into a system with a finite number of degrees of freedom. The way that the discretized object describes the behaviour of the original body is by a system of equations that can be either linear or nonlinear.

2.4.1 LINEARITY IN THE MATHEMATICAL FORMULATION OF FEM

One frequent source of confusion in the formulation of FEM is its linear or nonlinear nature. It is important to distinguish between material model nonlinearity and mathematical nonlinearity. The former refers to the material law, that is, the relation between the stress and strain that shows a certain body. While the latter corresponds to the type of equations found during the resolution of a specific problem.

There are different sources of mathematical nonlinearity. Then, having nonlinear material models leads to nonlinear mathematical equations but the contrary is not necessarily true. That is, having nonlinear equations does not mean that the behaviour of the body is nonlinear.

The behaviour of a body is governed by an equation that relates the stress ($\boldsymbol{\sigma}$) with the strain ($\boldsymbol{\varepsilon}$):

$$\boldsymbol{\sigma} = f(\boldsymbol{\varepsilon}) \tag{2.1}$$

For an isotropic linear elastic material operating under small deformations and displacement this relation is defined by an elasticity matrix ($\mathbf{D}$) whose coefficients are constant:

$$\boldsymbol{\sigma} = \mathbf{D}\boldsymbol{\varepsilon} \tag{2.2}$$

And the corresponding system of static equilibrium equations obtained applying the FEM is:

$$\mathbf{F} = \mathbf{K}\mathbf{U} \tag{2.3}$$

where **F** is the vector that contains the forces caused by the interaction between the body and its surrounding, **K** is the stiffness matrix and **U** is the vector that contains the nodal deformations.

However, this linear behaviour is just an idealization. In general, during the deformation of a body caused by certain loads its stiffness changes. There are two fundamental factors that make stiffness nonlinear: material and geometry. Without analyzing these concepts in depth, just say that stiffness changes with the deformation state if the relation between the stress and strain of the material is not constant (material nonlinearity) or if the deformations are large enough to consider the effects of the modification of the shape of the body (geometric nonlinearity).

On the other hand, if the change in stiffness is small enough, it makes sense to assume that neither the shape nor material properties change at all during the deformation process. This assumption is the fundamental principle of linear elastic analysis.

That means that throughout the entire process of deformation, the analyzed model retained whatever stiffness it possessed in its undeformed shape prior to loading. Regardless of how much the model deforms, whether the load gets applied in one step or gradually, and no matter how high may be the stresses that develop in response to that load, the model retains its initial stiffness.

This behaviour changes upon entering the world of nonlinear analysis, because it involves abandoning the assumption of constant stiffness. Instead, stiffness changes during the deformation process and the stiffness matrix must be updated as the nonlinear solver progresses through an iterative solution process. Those iterations increase the amount of time it takes to obtain accurate results.

A key component of nonlinear FEM is the solution of the nonlinear algebraic systems of equations that arise upon discretization. Frequently, dealing with this kind of system leads to convergence problems. This difficulty is overcome by the use of an incremental analysis. Briefly speaking, the analysis starts from an easily computable solution, for

example, the linear solution, and then goes on by trying to follow the behaviour of the system as actions applied to it are changed by small steps called *incrementa*. The previous solution is used as a starting point for the iterative solution-search procedure.

Considering the huge difference that exists between linear and nonlinear FEM, it can be useful to divide the state of the art related to FEM in two different groups. Therefore, the following sections will present the most relevant works related to soft body modelling taking into account the linearity of the resulting FEM formulation.

2.4.2 LINEAR FEM IN SOFT BODY MODELLING

In the section where the characteristics of soft living tissues were analyzed (see section 2.2) it was mentioned that linear elasticity, isotropy and homogeneity are not frequently observed properties in real biological tissues. Moreover, their assumption can lead, in some cases, to serious errors in the estimated mechanical behaviour. However, it is the simplest material model definition and it has been widely applied (Bro-Nielsen1998, Müller2002, DiMaio2003, James2003, Berkley2004, Hauth2004, Wu2004, Lee2006, Georgii2008).

Adopting this material model and considering that the deformations and the displacement that are suffering the deformable bodies are small simplifies dramatically the mathematical formulation of the FEM. As the stiffness matrix depends on the material properties, geometry and restraints, under the linear analysis assumption the study of the behaviour of the body becomes as simple as solving a linear system of equations (see equation 2.3).

That is, the stiffness of the model never changes. Consequently, those equations are assembled and solved just once, with no need to update anything while the model is deforming. Thus, linear analysis follows a straight path from problem formulation to completion and it produces results in a matter of seconds or minutes, even for very large models.

Many authors (DiMaio2003, James2003, Berkley2004, Wu2004, Lee2006) simplify as much as possible the behaviour of deformable bodies in order to apply the linear elasticity approach. In this kind of models the deformations vector and the forces vector are related by constant matrices either in the quasi-static or static case (see equation 2.3), where there is just a stiffness matrix, as in the dynamic case (see equation 2.4), where

additionally there is an influence of the mass matrix (**M**) and the damping matrix (**C**):

$$\mathbf{F} = \mathbf{M}\ddot{\mathbf{U}} + \mathbf{C}\dot{\mathbf{U}} + \mathbf{K}\mathbf{U} \qquad 2.4$$

Regarding the numerical resolution scheme applied to solve these systems using static, quasi-static or dynamic formulations depends on the application and interactive-time requirements. For example, simulating cutting and tearing generally requires a dynamic model to accurately capture the viscoelastic properties of soft tissue when topology changes. On the other hand, simulating large deformations or stress-relaxation may only require at most a nonlinear static model owing to the well-damped nature of soft tissue (Sundaraj2004).

There are several techniques based on computation optimization to help solving faster the linear FEM. Focusing the attention on the quasi-static approach, the preferred optimization strategies are preprocessing and condensation. In simulations where external forces are deforming a body without changing its topology, it is easy to set out a preprocessing strategy by calculating previously the ***LU*** decomposition of the stiffness matrix (Zhuang1999, Berkley2004, Delingette2004). This way, calculating the system deformations is reduced to a simple backward-forward substitution operation.

One important point to consider in linear FEM is that, in some cases, only the deformation of the visible surface nodes is of interest, while knowing the evolution of internal nodes is not needed. This idea was first exploited by Bro-Nielsen (Bro-Nielsen1998) and later on used by other researchers (DiMaio2003, Berkley2004, Delingette2004, Wu2004, Lee2006) (see figure 2.5). Bro-Nielsen showed that the linear system of equations (see equation 2.3) can be simplified by means of condensation, or the elimination of internal nodes from the system of equations, leading to a smaller system. The first step consists in decomposing the displacement and load vector as well as the stiffness matrix according to external (*e* subscript) and internal (*i* subscript) nodes:

$$\begin{bmatrix} \mathbf{F}_e \\ \mathbf{F}_i \end{bmatrix} = \begin{bmatrix} \mathbf{K}_{ee} & \mathbf{K}_{ei} \\ \mathbf{K}_{ie} & \mathbf{K}_{ii} \end{bmatrix} \begin{bmatrix} \mathbf{U}_e \\ \mathbf{U}_i \end{bmatrix} \qquad 2.5$$

Then, assuming that in typical applications the external forces acting over internal nodes ($\mathbf{F}_i$) are null and combining both blocks of equations it

is possible to calculate the displacements of the external nodes without computing the internal ones:

$$\mathbf{F}_e = \left(\mathbf{K}_{ee} - \mathbf{K}_{ei}\mathbf{K}_{ii}^{-1}\mathbf{K}_{ie}\right)\mathbf{U}_e \qquad 2.6$$

This kind of computation is specifically useful when there is not topology modification and the stiffness matrix does not change. In this case, the factorization of the condensed matrix that multiplies the $\mathbf{U}_e$ vector can be preprocessed.

Although this strategy is focused on solving the displacements of the external surface, it also allows studying the interior of the body. If it is necessary to know the evolution of the internal nodes their displacements can be computed as follows:

$$\mathbf{U}_i = -\mathbf{K}_{ii}^{-1}\mathbf{K}_{ie}\mathbf{U}_e \qquad 2.7$$

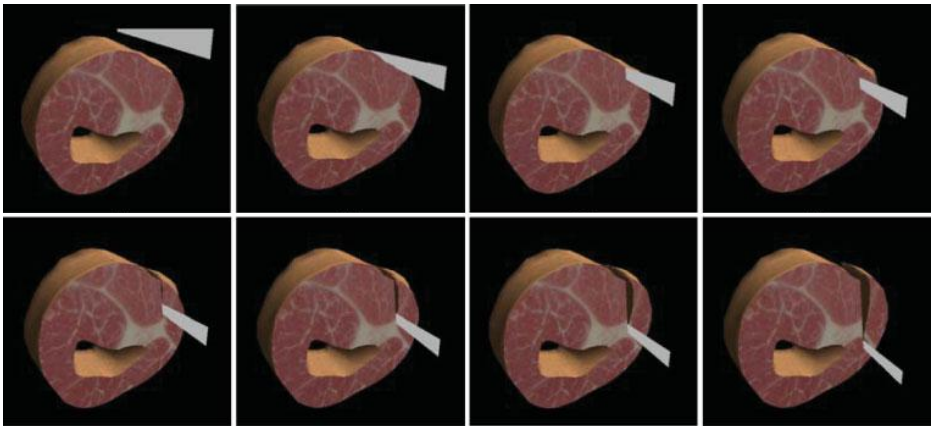

Figure 2.5. A sequence of an interactive cutting process using a hybrid condensed FEM with GPU acceleration (Wu2004).

The combination between the previously enumerated hypotheses needed for linear analysis with preprocessing and condensation strategies allows developing very computationally efficient simulations. However, those advantages come at the expense of two important limitations. The first one is accuracy. As mentioned in previous sections soft tissue can be hardly assumed to be linear elastic. The second limitation is that linear models that use the infinitesimal strain tensor are not invariant with respect to rotations. That is, when a deformable model undergoes a rigid solid rotation, the computed deformation changes even though no forces are

applied (see figure 2.6). In the case of a global rotation of the object, the problem can be solved with a specific change of the reference frame. However, the effectiveness of this solution is lost when only one part of the object undergoes a rotation, which is the case in general.

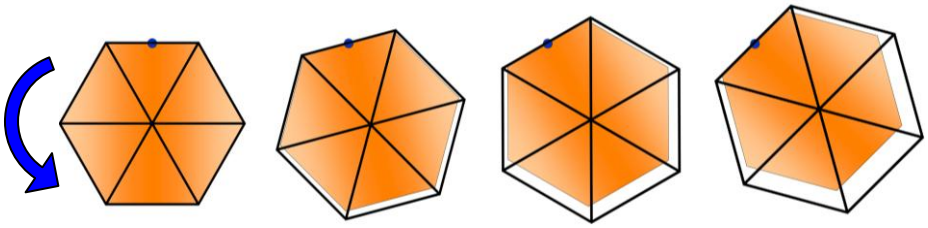

Figure 2.6. Volume variation of a linear elastic model under pure rotations (wireframe).

To eliminate the artificial forces that appear in this kind of models some authors have proposed using the corotational method (Müller2002, Hauth2004, Nesme2005, Georgii2008). Basically it consists in rotating the finite elements into a configuration that best matches its reference configuration, such that the rigid body motions of the elements are eliminated before the strain is computed. This way, the elimination of the geometrical nonlinearity is achieved.

To consider element rotations in the FEM, some modification have to be introduced to the previous equations. These modifications maintain the linearity of the mathematical formulation. However, the difficulty relays on the computation of the rotations of the elements in an accurate and stable way.

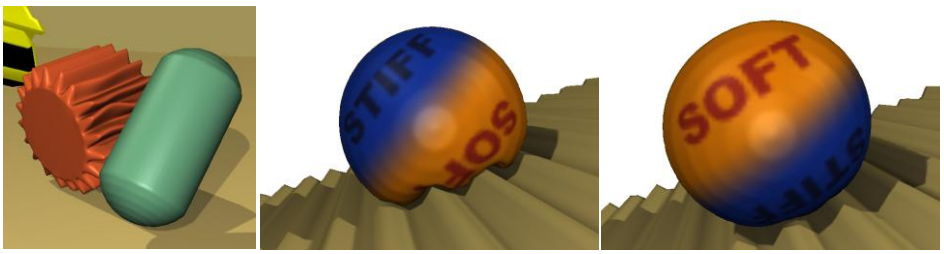

Figure 2.7. Simulation of deformable models by representing the object with a rigid core covered by a deformable layer (Galoppo2006).

Another interesting approach was proposed by Galoppo et al. (Galoppo2006) who derived an implicit yet highly parallelizable solution to dynamic deformations using linear elasticity theory (with separation of rigid

motion), continuum Lagrangian mechanics, FEM discretization, and constraint-based contact response with Lagrange multipliers. They assumed that a simulated object can be modelled as a rigid core covered by a layer of deformable material, and that the deformation field of the surface can be expressed as a function in two-dimensional, parametric atlases (see figure 2.7).

2.4.3 NONLINEAR FEM IN SOFT BODY MODELLING

As mentioned before, nonlinear FEM can have different sources of nonlinearity. In any case, the mathematical formulation is much more complex than in the case of linear analysis. This complexity has made difficult the use of nonlinear FEM formulations to interactive virtual reality tools that require topology changes. However, in the last years, taking advantage of the computer evolution, some interesting solutions have been proposed.

Most of the nonlinear material models used in tissue simulation belong to the group of hyperelastic materials. A hyperelastic or Green elastic material is a type of constitutive model for ideally elastic material for which the stress-strain relationship derives from a strain energy density function. The hyperelastic material is a special case of a Cauchy elastic material.

Hyperelastic material models are well suited to describe the behaviour of materials whose stress-strain relationship can be defined as nonlinearly elastic, isotropic and incompressible. These properties match with the main characteristics of most of living tissues.

One alternative to solve the problem that appears in linear elasticity during rotations (see figure 2.6) is to adopt the Saint Venant-Kirchhoff elasticity. This model is the simplest hyperelastic model since it is just an extension of the linear elastic material model to the nonlinear regime. It works well under large displacements but it is limited to small strains. As the strain-energy function is no longer a linear function of the displacement field the relation between strain and stress is no more linear. Other hyperelastic material models such as Neo-Hookean, Mooney-Rivlin, Ogden and Arruda-Boyce, are able to simulate soft body deformations under large displacements as well as large strains.

In the field of computer graphics, Wu et al. (Wu2001) proposed using nonlinear FEM for the realistic simulation of deformable objects for

applications such as surgery training (see figure 2.8). They particularly focused on Neo-Hookean and Mooney-Rivlin models. To achieve real-time simulations they suggested applying mass-lumping to diagonalize the mass matrix in the dynamic equilibrium equation (see equation 2.4). Additionally, they implemented an adaptative mesh algorithm to provide sufficient detail where required while minimizing unnecessary computation.

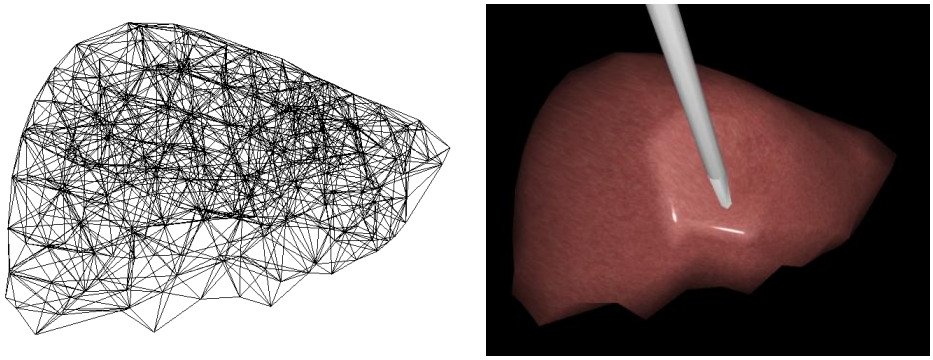

Figure 2.8. Tetrahedral liver model simulated using nonlinear FEM (Wu2001).

At the same time Hirota et al. (Hirota2001) adopted Mooney-Rivlin and Veronda models to simulate contact with human body. They introduced a novel penalty FEM based on the concept of material depth, the distance between a particle inside an object and the boundary of the object. By linearly interpolating precomputed material depths at node points, they analytically integrated contact forces over contact surfaces without raising computational cost.

In view of the limitations corresponding to previous FEM algorithms, some researchers (Miller2007, Taylor2007, Comas2008, Joldes2009) propose using the Total Lagrangian Explicit Dynamics algorithm (TLED) for nonlinear models (see figure 2.9), where all variables are referred to the original configuration of the system. This approach, unlike the updated Lagrangian formulation, allows the preprocessing of all the derivatives respect to the original configuration and eliminates the necessity to rotate (Cauchy) incremental stresses before addition. Although the simulation of nonlinear bodies using this approach is faster, computation remains complex and its capability for solving deformations in real-time applications has been only demonstrated using relatively small models (Joldes2009).

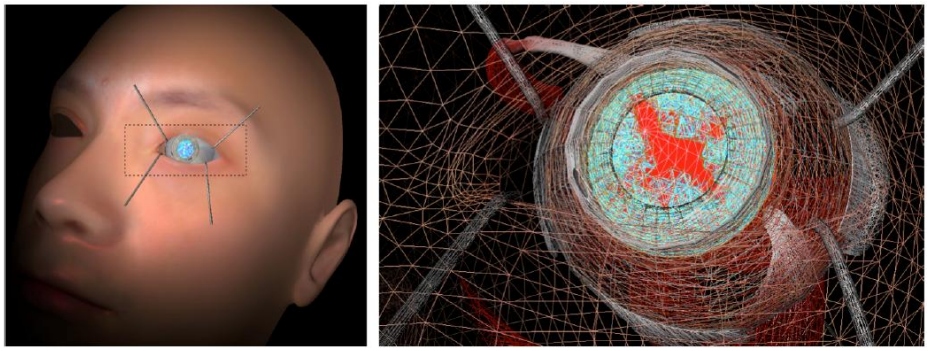

Figure 2.9. Cataract surgery simulation: (a) global view of the operating scene and (b) illustration of the complexity of the meshes involved in the simulation (Comas2008).

An important drawback of traditional FEM has been their computational cost when making topology changes. This limitation has usually made many authors prefer other simulation models such as MSMs to the FEM. Recently, the Extended Finite Element Method (XFEM) has been proposed to simulate interactive cuttings of deformable objects in virtual environments (Jeřábková2009). This method can be implemented with any kind of FEM in order to perform cuts. However, the improvement in the cutting calculation is accompanied by an increase in the evaluation of the deformations where no cuts are present because they use enriched elements. In particular, the tests published by Jeřábková et al. (Jeřábková2009) show that this technique is between 2.2 and 4 times slower when simulating deformable models without topology changes than the standard FEM approach.

Figure 2.10. Simulation of large cloth deformations using nonlinear FEM (Volino2009).

Apart from medical applications, other disciplines have also adopted nonlinear FEM. For instance, Volino et al. (Volino2009) proposed adapting strain-stress laws to simulate large deformations of cloth (see figure 2.10). Their model can be viewed as a particle system, through simple explicit relationships relating material strains and stresses to particle positions and forces. It avoids intermediate computations as much as possible, such as the coordinates transformations used in the corotational approach.

The mathematical development of the nonlinear FEM is quite complex and needs to introduce many concepts related to strain-energy functions, and stress and strain tensors. As these concepts are out of the scope of this thesis, for an extensive discussion on the underlying issue, the reader is referred to the book written by Holzapfel (Holzapfel2000) about nonlinear solid mechanics.

2.4.4 FINAL REMARKS

The FEM is a mathematical tool that allows solving a wide range of problems, from deformation studies to heat transfer. Its formulation depends on the underlying physical laws of the problem and the corresponding framework. Concerning the field of soft-tissue simulation, the formulation becomes increasingly complex and more computationally costly when more detailed material and geometrical models are used.

The simplest framework corresponds to the linear elasticity assumption (see section 2.2), which gives the advantage of applying well-known techniques to accelerate the computation and work in real time (Bro-Nielsen1998, DiMaio2003, Berkley2004, Wu2004, Lee2006). As linear elasticity gives unrealistic solutions under relevant rotations some authors have proposed the corotational approach (Müller2002, Hauth2004, Nesme2005, Georgii2008). However, realistic surgical simulators require handling large displacement and deformations as well as stress-strain relations closer to the real behaviour of living tissues.

Nonlinear FEM approaches are more suitable but with the drawback that their formulation is more complex and the techniques adopted to accelerate linear FEM are no longer valid when accurate results are desired. Recently, an efficient algorithm called TLED (Miller2007, Taylor2007, Comas2008, Joldes2009) has been applied to soft-tissue simulation, which allows the development of real-time applications by using preprocessing and parallelization techniques. However, this approach is not unconditionally stable and therefore is not suitable for certain simulation applications.

Although a keen effort has been done to develop real-time applications using nonlinear FEM, they still face the problem of handling topological changes in real time because, in some cases, this makes avoiding the advantages of preprocessing and evaluating new integrals. In this sense, XFEM (Jeřábková2009) could be a good solution but still has not been demonstrated its ability to work in real time with nonlinear material models.

2.5 MASS-SPRING MODEL (MSM)

MSMs are physically based models with simple structure and relatively small computational cost. Consequently, many operations like large deformations and topology modifications can be simulated easily. These characteristics make them suitable for interactive-time applications and parallel computing. Therefore, it is very common to find them in many applications involving facial animation (Platt1981, Waters1987, Terzopoulos1990, Kähler2003, Wang2009a), artificial animal animation (Miller1988, Tu1994) ,cloth simulation (Terzopoulos1988, Lafleur1991, Breen1994, Provot1995, Baraff1998, Desbrun1999, Garcia2007, Kaldor2008), biomechanical analysis (Nedel1998, Bourguignon2000, Hong2006), and surgery simulation (Meseure2000, Teschner2000, Brown2001, Choi2004, Teschner2004, Steinemann2006, Vafai2010).

In this kind of models the object is modelled as a collection of point masses linked by springs in a lattice structure (see figure 2.11). That is, their representation is discrete, contrarily to continuum based approaches.

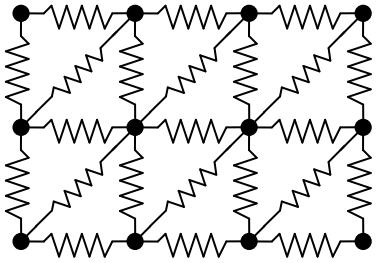

Figure 2.11. A schematic representation of a regular 2D MSM.

Following the idea of classical mechanics, MSMs represent a body by a single or multiple point masses that have no extension and hold the complete mass of the body. The external forces applied to the body are concentrated in the point masses as well. In this way, every continuous body can be transformed into a system of distributed point masses.

These models include a mesh of springs that interconnect those point masses representing the elastic behaviour of the bodies. The spring mesh can have many different configurations depending on the geometry of the object and the topology selected to represent the elasticity properties. There are mainly two types of meshes: polyhedral meshes and nearest neighbour meshes. The polyhedral meshes fill the volume of the body with polyhedrons that can be regular or not. In some applications, regular meshes are preferable since they allow controlling better the elastic response of the body. Irregular meshes, on the contrary, have the advantage of allowing mesh refinement in those areas where the required resolution is higher. On the other hand, nearest neighbour meshes (see figure 2.12) make the elastic connections with a fixed number of nearest neighbours or with all the neighbours that are closer than a certain distance.

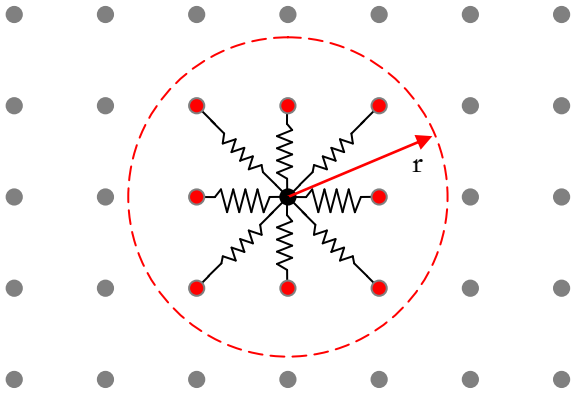

Figure 2.12. A schematic representation of 2D MSM where the connectivity is governed by an *influence distance*.

Regardless of the mesh type, when the model interacts with the environment new boundary conditions appear on the surface of the body. Generally, depending on the interaction type, the new surface conditions can be expressed in two ways: a set of forces exerted over some point masses or a collection of displacements imposed to some point masses. In any case, this new conditions cause the change of the length of the springs inducing forces that act over each point mass of the MSM.

Typically, the elastic connection between the point masses is modelled using Hookean or linear springs, that is, the force exerted by the spring that connects two generic nodes i and j is proportional to the elongation of the spring, $k_{(i,j)}$ being the corresponding stiffness coefficient

and $l_{(i,j)}^{0}$ its rest length. Calling $\mathbf{x}_i=(x_i, y_i, z_i)^T$ and $\mathbf{x}_j=(x_j, y_j, z_j)^T$ to the position of the *i*-th and *j*-th particles the resulting connection force is:

$$\mathbf{f}_{(i,j)} = k_{(i,j)}\left(\left\|\mathbf{x}_i - \mathbf{x}_j\right\| - l_{(i,j)}^{0}\right)\frac{\mathbf{x}_i - \mathbf{x}_j}{\left\|\mathbf{x}_i - \mathbf{x}_j\right\|} \qquad 2.8$$

In some few cases, this relation is not directly proportional and the force adopts other type of expressions. For instance, Cooper et al. (Cooper1997) proposed the following expression:

$$\mathbf{f}_{(i,j)} = k_{(i,j)}\left(\left\|\mathbf{x}_i - \mathbf{x}_j\right\| - \frac{\left(l_{(i,j)}^{0}\right)^2}{\left\|\mathbf{x}_i - \mathbf{x}_j\right\|}\right)\frac{\mathbf{x}_i - \mathbf{x}_j}{\left\|\mathbf{x}_i - \mathbf{x}_j\right\|} \qquad 2.9$$

Teschner et al. (Teschner2000) and Wang et al. (Wang2009a) also modified the equation 2.8 and proposed several expressions by assuming that the stiffness value could vary in function of the elongation.

Given any of those force definitions the equilibrium shape of the deformable body is always reached when the sum of all forces acting over each node are null. If only the final equilibrium state of the MSM is required then, it is enough to define the stiffness values of the springs.

However, if the transition from rest state to the deformed state is also required then, it is necessary to study the dynamic evolution of the body and usually a damping factor is added to the model in order to improve the stability and performance of the system. The ways to consider the effect of damping are manifold: including dampers aligned with the springs (Nogami2004), introducing forces as if the point masses where immerse in a fluid that makes a resisting force to motion directly proportional to the velocity of the particles (Kähler2003) or changing in an ad-hoc manner the time integration expression (Rasmusson2008). The models that consider damping are called Mass-Spring-Damper Models (MSDMs).

When some point mass is moved the springs attached to it are strained and forces are exerted on adjacent point masses. In the dynamic simulations these forces induce acceleration to those point masses and change their positions accordingly. The acceleration of a generic point mass *i* with mass m_i is governed by Newton's Second Law:

$$m_i\ddot{\mathbf{x}}_i - c_i\dot{\mathbf{x}}_i - \sum\mathbf{f}_{(i,j)}^{s} = \sum\mathbf{F}_i^{ext} \qquad 2.10$$

where c is the damping coefficient, $\mathbf{f}_{(i,j)}^{s}$ the force of the spring that connects particle i and j and $\mathbf{F}_i^{ext}$ the external forces acting over the i-th particle. Note that the term of the damping effect can be different because some authors consider just the velocity of the particle (Baraff1998, Brown2001, Bhasin2006, Rasmusson2008) while others the relative velocity with respect to the neighbour particles (Cooper1997, Nogami2004, Zerbato2007).

As solving these systems might be impossible, it is typical to use the following numerical integration methods: explicit (e.g. forward Euler, Runge-Kutta, and Verlet), implicit (backward Euler, and Baraff and Witkin method), and combined methods (e.g. Gear predictor-corrector). Generally speaking the explicit methods are simple but need small time steps for stability while the implicit methods are more complex and stable. These methods are valid for solving MSMs as well as FEM.

2.5.1 EQUILIBRIUM COMPUTATION

As in the case of continuum-based approach, the resolution scheme applied to solve discrete systems can be static, quasi-static or dynamic. The selection of the method depends on the application and its interactivity requirements, and has to take into account the stability and efficiency of the resolution during the entire simulation.

In some static problems, just the final state of the simulation needs to be considered; it is not necessary to calculate the real transition of the body from the rest state to the final deformed state. An example of such application is the simulation of the final appearance of a patient after undergoing maxillofacial surgery. In this case, it is not necessary to simulate the whole surgical process. Instead, it is sufficient to specify the changes suffered by the bone due to the surgery and study directly the final state of the different layers of soft tissue in order to evaluate the aesthetic effects on the skin.

In the case of considering dynamic simulations, if the change in the external conditions is slow enough to achieve the equilibrium almost immediately, the dynamic evolution of the simulation can be considered as a succession of static states. Consequently, time integration can be avoided and the static solution can be applied in every time step. In other words, the deformation evaluation becomes into a quasi-static study when dynamic inertial and damping forces can be neglected. This assumption is reasonable when displacements are not fast and the deforming soft objects have

relatively high damping parameters, which is usually the case for most biological tissues (Sundaraj2004).

When quasi-static formulation cannot be applied, it is necessary to compute the deformations by solving the dynamic equations. The easiest way is to solve them numerically using time integration methods based on finite differences (Haile1992) like Euler, Runge-Kutta, Verlet, and Gear's predictive-corrective methods.

Apart from these approaches, Brown et al. (Brown2001) proposed a scaling factor of the force acting over a point mass to approximate the solution of the dynamic problem (see equation 2.11). In this way, the particle moves along the resulting force to a position where, theoretically, the sum of the forces is smaller. Ideally, the value of the scaling factor should be chosen as large as possible such that the solving method converges rapidly. The value of this factor depends on the specific characteristics of the simulation and requires experimental trials.

$$\mathbf{x}_i(t+1) = \mathbf{x}_i(t) + \alpha \sum \mathbf{f}^s_{(i,j)}(t) \qquad 2.11$$

Another way to compute the equilibrium state is by studying the problem from an energetic point of view. Instead of focusing the attention on the forces acting over the point masses it concentrates the study on the energy of the springs connected to each particle (E_s). This energy, for the case of a linear spring, is proportional to the quadratic value of the elongation:

$$E_s = \frac{k_{(i,j)}}{2}\left(\left\|\mathbf{x}_i - \mathbf{x}_j\right\| - l^0_{(i,j)}\right)^2 \qquad 2.12$$

Usually this kind of approach includes additional energy terms that refer to constrains that penalize some unnatural behaviours like volume change or external surface change (Teschner2004). In those cases the most common technique to calculate the equilibrium is to find the minimal value of the accumulated energy in the model.

2.5.2 MSM IN SOFT BODY MODELLING

Probably, one of the first applications using MSMs was facial animation. Platt et al. (Platt1981) and Waters (Waters1987) developed facial animation tools using static approaches. Soon after, Terzopoulos et al. (Terzopoulos1990) improved this application by representing the cutaneous

tissue, subcutaneous tissue, and muscle layer with a dynamic trilayered model. Similarly, Chadwick et al. (Chadwick1989) developed dynamic models to model skin, fat and muscle of computer generated characters.

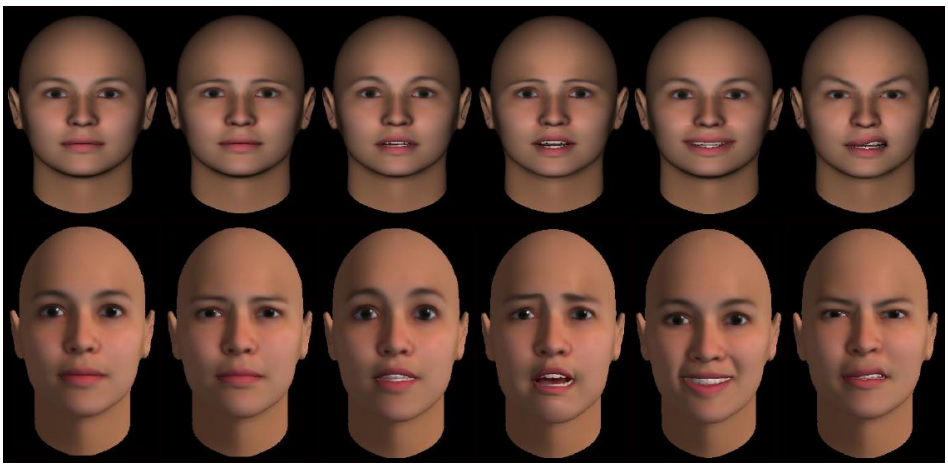

Figure 2.13. A facial animation example using MSMs (Wang2009a).

The MSMs adopted in facial animation were increasingly becoming more complex. Kähler (Kähler2003) for instance developed MSMs based on anatomic data and included human head growth models. On the other hand, Wang et al. (Wang2009a) proposed nonlinear spring constants and extended the muscle model of Waters to improve the combination of multiple muscle actions and to generate realistic expressions (see figure 2.13).

Figure 2.14. Artificial worm locomotion simulation using MSMs (Miller1988).

Artificial animal animations appeared a little bit after than facial animations. It began with studies about locomotion of simple artificial animals as snakes, worms (see figure 2.14) and fishes (Miller1988, Tu1994). In these models, spring rest lengths vary over time to simulate muscle actuation. Besides, they identified the most common problem associated

with the simulation of deformable objects using MSMs namely, stiffness parameter identification.

The cloth modelling field has also benefited by the development of MSMs. Lafleur et al. (Lafleur1991) combined the method proposed by Terzopoulos et al. (Terzopoulos1988) with a collision response algorithm to simulate realistic cloth movements. Provot (Provot1995) also developed a physically based modelling technique by introducing constraints to the classical MSM based on the rate of deformation to solve the problem of excessive deformation when simulating a hanging cloth.

Breen et al. (Breen1994) presented a particle system to model cloth. They suggested that, as cloth is a mechanism of warp and weft fibres, MSMs are more appropriate than FEM techniques for modeling cloth. Using measured data from the Kawabata Evaluation System, they proposed specific energy functions for stretching, bending and trellising to improve the animation of static drape of real materials.

Figure 2.15. Fast simulation of cloths using MSMs (Baraff1998).

Few years later Baraff et al. (Baraff1998) described a cloth simulation system that was able to take large time-steps without numerical instabilities. They used implicit integration to enforce constraints on individual cloth particles and applied a modified conjugate gradient method to solve the sparse linear system of equations. This approach improved significantly the previous cloth simulation formulations (see figure 2.15). Desbrun et al. (Desbrun1999) also focused their attention on the time integration scheme.

They proposed alleviating the need to solve the linear system through the use of a predictor-corrector approach.

More recently, García et al. (Garcia2007) presented a MSM based approach to simulate the interaction of a hyperelastic textile tissue with a forming body. The fabric was represented by rectangular meshes of springs to enable the model behaving orthotropically and therefore making possible to simulate realistically the warp and weft properties. Kaldor et al. (Kaldor2008) presented a cloth modelling method specifically developed for knitted fabric simulation which considered energetic terms equivalent to spring energies. They studied in depth the behaviour of knits and the interactions of yarns and they propose an implicit-explicit integrator, with yarn inextensibility constraints imposed using efficient projections (see figure 2.16).

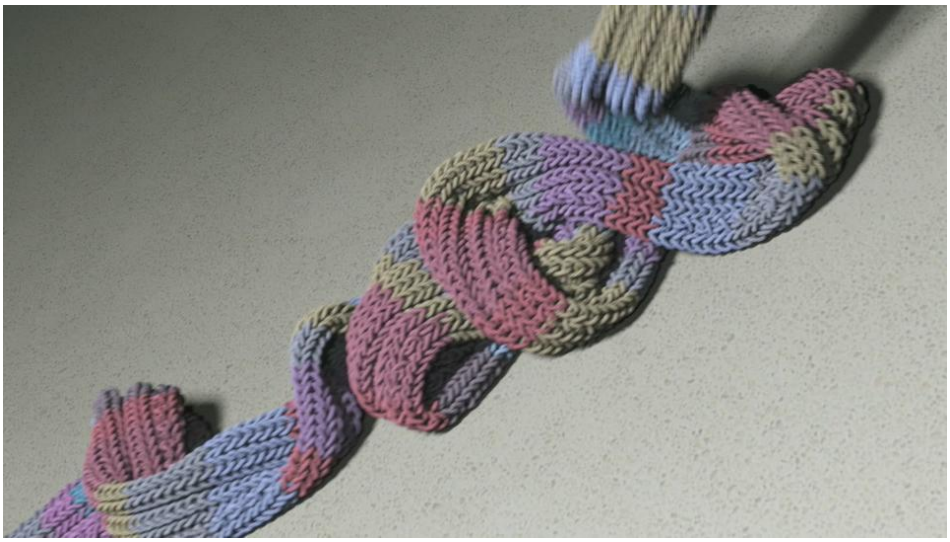

Figure 2.16. Simulation of the falling of a scarf modelled at the yarn level (Kaldor2008).

Apart from facial animation and cloth simulation, many medical branches such as biomechanics and surgery have adopted discrete models to make simulations. In biomechanical modelling, MSMs were used by Nedel et al. (Nedel1998) to simulate muscle deformations. Muscles were represented at two levels: action lines and muscle shape. Their shape was deformed using a MSM. Apart from linear springs, angular springs were also introduced in order to control the volume of muscles during deformation and smooth out mesh discontinuities.

As realistic simulation of biological tissues requires more accurate results than pure animation approaches a lot of research work has been done on MSMs to improve various aspects of the material being simulated. Bourguignon et al. (Bourguignon2000), for instance, proposed controlling isotropy or anisotropy of elastic tissues such as heart and liver. They allowed the user to specify the mechanical properties of the material, everywhere in the model, independently from the mesh geometry and topology.

Other authors have focused their work on the volume preservation problem. Hong et al. (Hong2006) proposed a fast volume preservation method to improve the simulation of incompressible models. They applied their method, for instance, to the simulation of muscle deformations when flexing the forearm at the elbow joint (see figure 2.17).

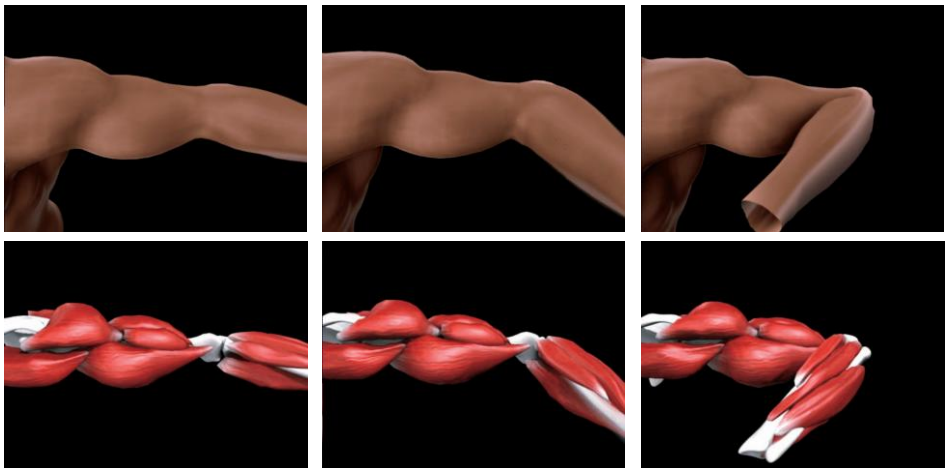

Figure 2.17. Simulation of muscle deformations when flexing the forearm at the elbow joint (Hong2006).

In surgical simulation, Meseure et al. (Meseure2000) proposed a deformable body model in order to simulate the dynamic behaviour of human organs in surgical simulators. It was based on a spring surface mesh, fitted with a virtual rigid component which did not interact with the environment and provided the structure with a rigid behaviour. Brown and Montgomery (Brown2001) developed an efficient algorithm to solve MSM for microsurgery simulation. Assuming that the deformations are local they reduced calculations by using a wave-propagation technique that automatically stops computation when deformations become below a

threshold. Using this algorithm, they achieved real-time performance in a suturing vessel surgery. A similar approach was proposed by Choi et al. (Choi2004) to accelerate the simulation computation and achieve the frame rate required for haptic interaction.

MSMs are also applied in craniofacial surgery. Teschner et al. (Teschner2000) presented a patient specific model taking into account the nonlinear and incompressible behaviour of living tissues. The system was able to simulate bone cutting and bone realignment with integrated interactive collision detection. Additionally, it handled soft-tissue deformation and cutting due to the application of surgical instruments. Later on they proposed an energy based approach with which they could simulate elastic and plastic deformations at interactive rates (Teschner2004). Their model was able to handle a large variety of material properties ranging from stiff to fluid-like behaviour. The key point of their approach was to incorporate volume and surface area preservation energy terms.

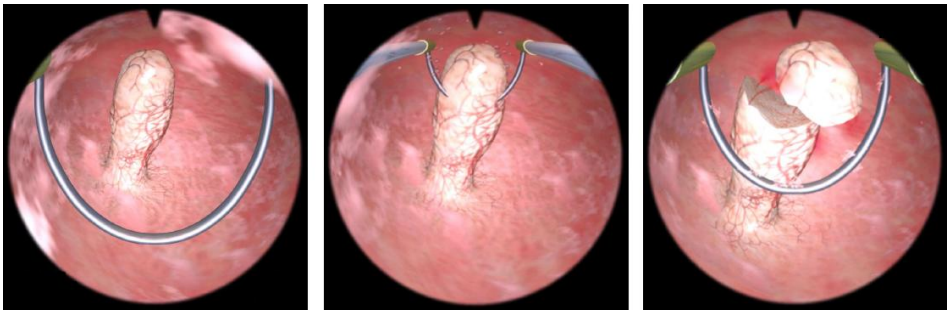

Figure 2.18. Ablating a polyp in a hysteroscopy simulator where the deformable objects are represented by tetrahedral meshes and simulated by a MSM (Steinemann2006).

Within the framework of a hysteroscopy simulator (see figure 2.18), Steinemann et al. (Steinemann2006) developed a hybrid cutting approach for tetrahedral meshes. With their method, they closely approximated arbitrary, user-defined cut surfaces while avoiding the creation of small or badly shaped elements, thus strongly reducing stability problems in the subsequent deformation computation.

Other simulation tools such as interactive virtual dissections (Vafai2010) have also adopted MSMs. In this case they used a surface MSM enriched with *home springs* that pulled the surface to its rest state.

2.5.3 FINAL REMARKS

Generally speaking, MSMs are easy to construct, physically based models. They allow real-time simulations even when the model has to handle user interactions that involve topology changes. Another well-known advantage is their ability to deal with both large displacements and large deformations. Additionally, their discrete formulation permits adopting easily parallel computing and implementing them in multiprocessor computers and graphics processing units (GPUs) (Georgii2005a, Tejada2005, Rasmusson2008).

As it has been shown in the previous section, these characteristics have caused the fast propagation of MSMs to all of the simulation fields related to graphical and interactive applications. They are widely used in character animation, cloth simulation, biomechanical studies and, more recently, surgery simulation.

They have shown to be very flexible since they have adapted their parameters and topology to fit the increasing level of the requirements of new applications. For instance, some authors have adopted multiphasic (Keeve1998, Garcia2007, Wang2009a) and nonlinear expressions of the stiffness (Cooper1997, Teschner2000, Chen2007, Basafa2008, Cui2009, Wang2009a) in order to make more realistic models or have implemented energy based formulations (Teschner2004) to preserve some properties. When well tuned, they have been able to define properties such as non-homogeneity (Morris2008), anisotropy (Bourguignon2000, Bianchi2004, Choi2004), surface preservation (Teschner2004) and volume preservation (Teschner2004, Georgii2005, Hong2006).

However, MSMs have also some drawbacks. These models are tuned through their spring parameters and it is difficult to find methods to assign proper values for these constants. Only a few works have derived directly the MSMs parameters from measured material properties. Furthermore, although it has been done for particular cases, it is difficult to express certain constraints (like incompressibility and anisotropy) in a natural way.

2.6 DISCUSSION

Along the discussion of the following points important decisions about the deformable model will be taken. First, the level of accuracy that a simulator can achieve will be discussed in order to select models according to that level. Secondly, the material model will be selected taking into account

accuracy and linearity issues. To finish, the deformable body model itself will be selected considering the previous decisions. The decisions taken in these three points will be totally conditioned by the objectives mentioned in section 1.4.

2.6.1 ACCURACY

When defining the accuracy needed for a medical simulator, it is important to specify whether the application requires using accurate patient-specific data or just approximate properties.

Accurate patient-specific data can be interesting when the information obtained from the simulation may be decisive in the definition of a real surgery. In the case of the resection of several brain tumours, for instance, the surgeon needs to plan ahead performing the actual surgery which is the best area to perform a craniotomy to better access the unhealthy tissues with the smaller risks and potential damages. In some cases the spatial location of the tumours can be enough to decide the path to follow during the intervention but in other cases simulating previously the whole surgery can help in the planning.

On the other cases, the objective of the simulation can be to take some decisions that do not specifically depend on the mechanical properties of the tissue of particular patients, but only based on the specific geometrical properties. Then, the simulator can offer friendly tools where tissues are deforming but that use generic approximated properties. This can be the case of surgical training programs or simulations whose only objective is to define the sequence of the operation.

Certainly, the most critical case is the first one, when patient-specific data is needed, because in this case surgery planning and simulation can be decisive. As discussed in section 2.1 the best approach to obtain specific data is to make *in vivo* measurements. Non invasive techniques, such as ARFI and ultrasounds, can be applied before surgery and provide the surgeons with useful information to plan the intervention. However, they usually give punctual information and do not provide the whole necessary stress-strain curve since the studied range of deformations may not be as wide as the deformations that take place during surgery. That is, they are not accurate when defining the whole response of the tissue.

Invasive techniques, in turn, provide information of the behaviour of the studied tissue with two main drawbacks: only the physically accessible

area can be tested and the data can be only collected from the surface. Even more, invasive methods can only be applied during the surgery, which limits dramatically its usefulness in the surgery planning and simulation process, and increases the risk of causing injuries to patients.

Additionally, a real surgery is anything but predictable. During the operation the body of the patient is suffering an *attack* that causes physical and physiological reactions. In theory physical reactions might be predicted using accurate material models, but the problem is that physiological changes modify the mechanical properties of living tissues.

The mechanical properties of brain, for instance, change due to known and unknown physical and physiological phenomena (Schiavone2009). Therefore, using very accurate models makes only sense when the physiological reactions can be evaluated and predicted.

However, it is not justified developing such accurate models when relevant uncertainties are originated by some of the following issues:

- Physiological reaction will change substantially the mechanical properties and can not be predicted.
- The tissue is non-homogeneous and mechanical parameters can be calculated only in a certain small area of the whole region of interest.
- Time elapsed between the mechanical properties acquisition and the intervention (in some cases even months) can vary substantially those values.
- The available instruments do not allow obtaining accurate values.
- In an *ex vivo* measurement, the layered and non-homogeneous nature of the tissue makes impossible to obtain useful information about the mechanical response of a whole organ from the extracted sample.
- The only available data are medical images such as MRI and CT which do not give mechanical response information (in most of the cases) and low geometrical resolution.
- The simulation needs to be made before the surgery which eliminates the possibility to use *in vivo* measures during surgery.

In these cases, it is hard to define reliable patient-specific mechanical properties and, frequently, it is necessary to use data sets of other patients.

For this reason, the quality of the simulation is always determined by the quality of the available input data apart from the accuracy of the deformable model itself.

2.6.2 MATERIAL MODEL

Although obtaining patient-specific data has been proved to be hard, the model has to be able to adapt its behaviour to the available data. In some cases there will be detailed information while in other cases the information will be partial. Moreover, in some situations it is necessary to use generic data sets to define the mechanical response of the virtual body.

As mentioned in previous sections, most of the mechanical experiments performed to obtain the behaviour of biological tissues show that they generally exhibit non-uniform, anisotropic, quasi-incompressible, nonlinear plastic-viscoelastic material properties. However, these characteristics are usually simplified due to the lack of real data obtained using *in vivo* experiments (see section 2.1).

Taking into account the conclusions reached in section 2.2, it is reasonable to consider that the behaviour of living tissues is linearly elastic only when small deformations are considered, while hyperelastic material models are preferable when working under larger deformations. Therefore, the proposed model has to be able to describe linear elastic responses as well as hyperelastic behaviours such as those defined by neo-Hookean, Mooney-Rivlin, and Ogden material models. In addition, handling different compressibility rates is also a requirement since not all the tissues are incompressible.

2.6.3 DEFORMABLE MODEL

Two main approaches have been presented in previous sections: FEM and MSM. The wide presence of both formulations in medical field shows that both are good candidates. Logically, each one of them has its own advantages and disadvantages. The decision of which one is most suitable for a particular task has to be driven by analyzing the objectives defined in the first chapter. Summarizing, those objectives were: real-time simulation, accurate response, mechanical feedback, nonlinear and non-homogeneous material model, generic and patient-specific model and admit user interaction such as palpation and cutting.

Concerning the response of the model, both approaches can simulate deformations and provide mechanical feedback to the interactions of the user such as palpation and cutting.

In relation with the material model, in the previous sections has been shown that both models can approximate linear and nonlinear behaviour as well as uniform and non-uniform properties. Those characteristics can be either generic or patient-specific.

Thus, the key points for the selection are the computation time required to compute those simulations and whether they fulfil the condition of real-time performance, and the accuracy of the model when simulating the behaviour of actual living tissues.

With regards to the computation time constraint, approximating linear or nonlinear elastic behaviours using MSMs leads to the same model in both cases but with different spring coefficients. However, the formulation can change significantly when considering the FEM. Therefore, it is better to study separately both cases in order to compare their performance.

In the simulations performed by Zhou et al. (Zhou2009) with linear elastic FEM models working under small deformations, the computation times were 45% larger than the ones observed in the MSM approach. When they considered large deformations the MSM is at least 2.5 times faster. They performed this comparison without making cuts to the deformable model. Taking into account topological changes would probably increase the difference between both approaches, since the linear FEM needs recalculating the stiffness matrices that define the behaviour of the deformable model.

Although it is very hard to find two equivalent implementations of MSMs and nonlinear FEM, there are two works that can be assumed to be very similar because they were published the same year, both are implemented in GPU and they show their performance using a similar number of degrees of freedom.

Rasmusson et al. (Rasmusson2008) presented a MSDM of a heart with 88347 degrees of freedom. Their implementation in the GPU reached 5515 fps. On the other hand, Comas et al. (Comas2008) presented a GPU implementation of a TLED using a cube with 89373 degrees of freedom (considering also the fixed nodes which probably reduces the unknowns in 2883) and obtained a simulation performance of 1000 fps. This means that

MSDM simulated five times faster than the nonlinear FEM under similar conditions.

Regarding accuracy, the FEM formulation is much more robust and versatile. It allows defining explicitly properties such as compressibility ratio, complex stress-strain relations, anisotropy, etc. In turn, MSMs have provided good results only in particularly tuned models. Given some behaviour laws it is not straightforward how to obtain the corresponding MSM. Apart from the contribution of Lloyd et al. (Lloyd2007) for designing MSMs from linear FEM there has been little work done in this field. Even less bibliography can be found about how to approximate hyperelastic behaviours using MSMs.

However, as it has been seen above (see sections 2.1 and 2.6.1), independently of the deformable model, the accuracy of the simulations is always constrained by the capability of obtaining reliable data of living tissues, with which to feed a model.

Taking into account the differences in the computation times and considering that in this kind of simulations the real-time performance is the most important constraint (Delingette2004), in this thesis the MSM is selected to model soft tissues.

2.7 CONCLUSIONS

The behaviour of living tissues is very complex and several detailed material models have been proposed to describe them (Fung1993). However, in the everyday practice of surgery simulation, these mechanical properties are hard to obtain for many reasons. For instance, their value changes during surgery, technology applied to obtain them only provides data of a limited area, there is no way to analyze the behaviour of the tissue accurately or data are not available on time since they can only be obtained during surgery.

The consequence is that using complex formulations that sacrifice computation velocity can lead to simulations that are not more accurate than those achieved with simpler models.

On the other hand, real-time performance is a mandatory requirement for interactive surgery simulators. If this condition is not satisfied it does not matter if the model is accurate or not, since the perception of the surgery will be unnatural. Thus, knowing the limitations

for the acquisition of the mechanical properties of the tissue, real-time performance becomes the most important requirement and accuracy is subordinated to it. The MSM provides a computationally less expensive model for elastic models than other approaches such as them FEM. This means that MSM are more likely to achieve real-time performance and for this reason, the MSM has been adopted as the deformable model in this thesis.

The main drawback of MSMs is the difficulty of obtaining the right parameter values that make the model behave accurately. As it will be explained in the following chapter, there are several methods to calculate the stiffness coefficients of MSMs but none of these techniques is suitable for fulfilling the objectives of this work. Therefore, the efforts in this thesis will be focused on proposing new methods to design MSMs that provide fast and realistic simulations in the field of medical applications.

CHAPTER 3

STUDY AND PROPOSALS OF MSM DESIGNING METHODS

MSMs are the most popular discrete models and they can be an interesting alternative to continuum-based simulations since they avoid many of the difficulties that have other simulation techniques. There are three major advantages that make these models attractive: simple mathematical formulation, great versatility for topological changes, and a computation structure well-suited for parallelizing in multicore computers and graphics processing units (GPUs).

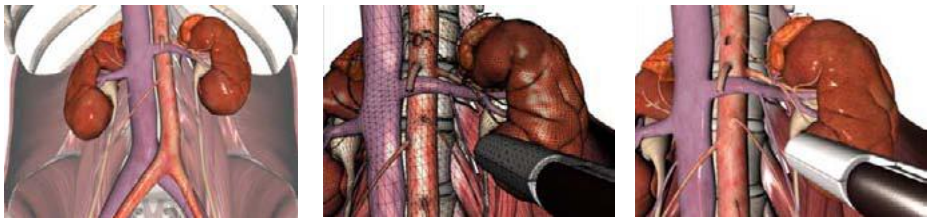

(a) Kidney and vessels (b) Mesh (c) Local hilum section

Figure 3.1. Example of a virtual laparoscopic nephrectomy simulator (Zhou2009).

One of the main drawbacks of these models is that it is difficult to design them to describe with accuracy the mechanical behaviour of actual deformable bodies. The main reason is that their formulation usually does not offer an easy way to express the constitutive relations of the material.

However, the parameter versatility of MSMs allows choosing suitable parameters to develop realistic simulators (Zhou2009) (see figure 3.1).

Many authors have presented improvements in the MSM designing field in order to make realistic simulations. Some of them have proposed new methods to obtain the stiffness coefficients of the springs while others have suggested modifying the traditional model, for example, by including external forces or considering nonlinear springs.

A detailed review of the existing approaches will be presented in the following section. After analyzing their virtues and drawbacks, new MSM designing strategies will be proposed. To finish the chapter, some generic information related to the considered MSM will be presented: node numbering, point mass evaluation, spring nomenclature and some guidelines for assembling cubical MSMs.

3.1 STATE OF THE ART IN MSM DESIGN

Obtaining parameters like stiffness coefficients still remains a big challenge in MSM design. There are many methods to find the stiffness values and the topological configuration that allow describing certain behaviour in a satisfactory way. The main contributions in this area come from the fields of cloth simulation, surgical simulation, and body animation.

An interesting classification of MSM derivation methods was proposed by Lloyd et al. (Lloyd2007). They divided these methods into two groups: data-driven techniques and analytical derivation methods. The former methods estimate the model parameters using deformations measured in experiments, real or virtual, as reference data. The latter approaches obtain analytical expressions for the spring coefficients using a physical model as a reference.

In data-driven strategies a second subdivision can be made attending to the available knowledge of the body whose behaviour must be reproduced. According to this idea, three different approaches stand out when designing MSMs: pure data-driven approach, nonlinear and piecewise linear springs, and constraint-based simulation. Likewise, analytical derivation can be subdivided into two different strategies: estimation from material science and derivation from discretized formulation of continuum.

The next sections will describe the state of the art in realistic parameter derivation using this classification.

3.1.1 DATA-DRIVEN STRATEGIES

Data-driven MSM design strategies are based on the fitting of the deformation of the MSM to some reference data by modifying the stiffness coefficients and, in some cases, the topology as well. It is typically used when the only available information about the behaviour of a body comes from a set of mechanical tests. These data can be obtained measuring experimentally the deformations of a real body or by taking as a reference the deformations of another simulation model, such as FEM model.

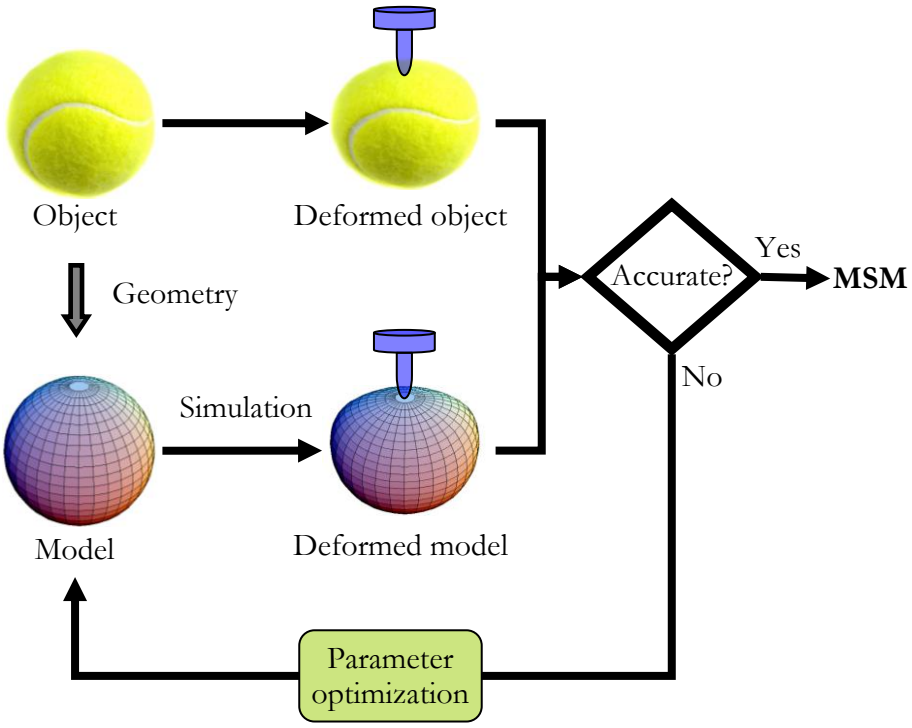

Figure 3.2. The process of obtaining the parameters of a MSM in the data-driven strategies.

The pure data-driven approach does not require any previous information about the intrinsic behaviour of the body apart from the test data (see figure 3.2). In other words, it does not matter if the body is linear elastic or hyperelastic; compressible or incompressible; the parameter derivation method will obtain the constants and configuration best-suited for the specific input-data. Thus, the attention is focused on the parameter optimization method.

However, since most biological soft tissues have a nonlinear mechanical response, some authors have tried to incorporate this behaviour into the traditional MSM using nonlinear springs and piecewise linear springs. That is, considering that the force of a spring is not linearly related with its elongation or, at least, not with a constant coefficient. Thus, the difference of this approach with a pure data-driven strategy is that the behaviour of the body is analyzed before establishing the MSM type.

Another data-driven approach is based on the definition of constraints that control the behaviour of the simulation. The knowledge of how a certain body behaves and which are its natural characteristics allows extending traditional MSM with constraints that simulate these observed properties. The additional information can be just a qualitative description that comes from plain observation or it can have a quantitative meaning obtained through experimental studies. Some bodies, for instance, do not change their volume during the deformation process, thus, incompressibility constraints can be used to enrich the model. As this information cannot be explicitly included in the initial virtual deformable model it is considered in the simulation stage.

Usually, in constraint-based simulations the deformation computation is formulated from an energetic point of view. For this reason, solving this kind of models usually requires a minimization of the total energy of the system.

3.1.1.1 Pure Data-driven Approaches

One of the first pure data-driven approaches was proposed by Louchet et al. (Louchet1995). They adopted genetic algorithms for the identification of the internal parameters of physically-based fabric models. These heuristic methods are inspired by evolutionary biology and consist of a set of model parameters that evolve using three main processes: selection, mutation, and crossover. In this particular case, they considered a MSM simulation based on fixed parameters as the reference deformation.

Later, Nogami et al. (Nogami2004) extended the traditional MSM with two additional dampers and identified the parameters using genetic algorithms as well as other randomized algorithms. Bianchi et al. (Bianchi2004) suggested an approach based on genetic algorithms where MSM derivation takes as a reference shearing and stretching tests of linear elastic FEM models. Their main contribution was the simultaneous identification of mesh topology and spring stiffness values. A similar work

was presented by Völlinger et al. (Völlinger2009) who identified the spring constants and simultaneously optimize the topology of the mesh adopting evolutionary algorithms. Besides, Zerbato et al. (Zerbato2007) proposed a non-homogeneous model with great amount of degrees of freedom because the stiffness coefficients and viscosity values for each tetrahedron were different. Since their value depended on Young's modulus, the goal of the genetic algorithm was the optimization of that modulus.

Deussen et al. (Deussen1995), Choi et al. (Choi2004) and Morris et al. (Morris2008) suggested a method based on simulated annealing to identify the coefficients of the MSM. This technique is a generic probabilistic method that achieves a global optimization of the problem. The former used stretching and shearing tests based on linear elastic theory, while the latter takes as reference uniform and non-uniform elastic material deformations.

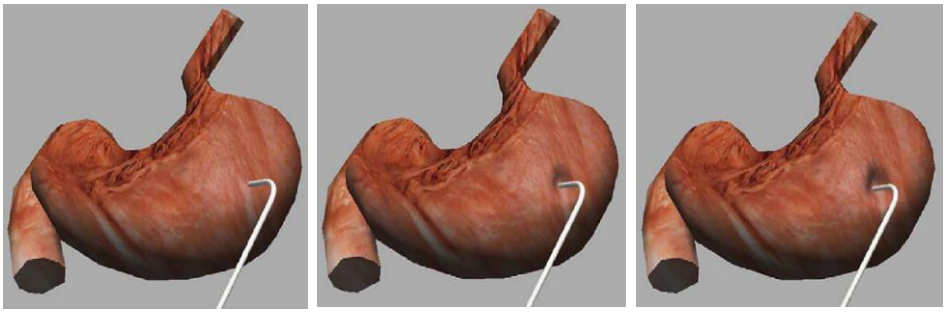

Figure 3.3. Interactive stomach model obtained using simulated annealing (Choi2004).

All methods presented above share the same basic idea. They identify the parameters of a MSM through an optimization process that tries to make the behaviour of the body match the general behaviour of the body. These methods are appropriate tools for solving complex nonlinear problems. However, their main disadvantage is that they usually require a long computation time. Simulated annealing has the additional problem of high sensitivity to the parameters of the optimization method (Deussen1995).

3.1.1.2 Nonlinear and Piecewise Linear Springs

An additional problem in the design of MSM is the definition of the spring behaviour. Usually these springs are modelled using linear springs. However, in some works the initial model of MSM with linear springs was

modified in order to obtain more realistic simulations. Cooper and Maddock (Cooper1997), for instance, suggested using nonlinear springs. They proposed a stiffness expression based on the idea that, as the spring length tends to zero, the spring exerts a reaction force which should tend to infinity. Although this expression does not usually have a polynomial form, their nonlinear springs have polynomial formulation. Teschner et al. (Teschner2000), for instance, proposed several polynomial coefficients to compute soft-tissue deformation caused by surgical procedures using multi-layered spring configuration. More recently, some authors have proposed using nonlinear coefficients based on the Duffing's equation (Chen2007, Cui2009) and the nonlinear behaviour of the skin (Wang2009a).

Another interesting approach is to consider that the behaviour of the spring is piecewise linear. This type of springs has the advantage of keeping force computation simple but with behaviours closer to nonlinear bodies (Garcia2007, Keeve1998). This approach can also be combined with piecewise nonlinear formulation (Basafa2008).

3.1.1.3 Constraint-based Simulation

The simplest MSMs are based on the fact that most bodies respond with internal restitution forces that try to restore their shape to the initial stage when they are deformed by external forces. However, this does not in principle guarantee the correct behaviour of other mechanical properties, such as volume conservation. In addition to this inter-particle distance conservation, Gayle et al. (Gayle2005) relied on the ideal gas law in order to satisfy the volume preservation constraint. Likewise, Teschner et al. (Teschner2004) considered volume preservation energies and completed the model with external surface preservation condition. In a similar way, Hong et al. (Hong2006) included volume preservation forces acting on the surface of the body to obtain more realistic simulations.

Breen et al. (Breen1994) proposed a physically-based technique for predicting the drape of woven fabrics taking as a reference various tests of a cloth sample in a Kawabata fabric testing device. The energy function that they propose does not take into account area and volume preservation. Instead, they consider the influence of two bending energies, repulsion and stretching (equivalent to the natural distance preserving term), and gravity effects.

Another interesting contribution similar to other constraint-based simulations is the hybrid approach for tetrahedral meshes suggested by

Lloyd et al. (Lloyd2007). They extended the traditional MSM by adding volume preserving forces and obtained the stiffness parameters using a minimization strategy. In this way, they introduced additional degrees of freedom to the system in order to improve their initial approach.

This kind of strategy can correct some unnatural responses and give visually plausible results but they will rarely give accurate values if they are designed using only trial and error techniques. Therefore, they have to be combined with other types of MSM designing methods.

3.1.2 ANALYTICAL DERIVATION APPROACH

As it has been shown above, data-driven approaches define the parameters of a MSM by simulating the model and comparing its resulting behaviour with external data, obtained from experiments or from other models. In contrast, analytical methods perform the derivation using analytical expressions of the behaviour of MSMs.

One approach to model analytically a MSM is based on the analysis of the behaviour of the model as an actual material under specific loads, and therefore, closely matches the analysis of material science. In this case a parametric analysis of the behaviour of the MSM allows obtaining the relationship between the parameters of the mesh, such as spring stiffness, and the properties of the material to be simulated.

Another analytical approach is based on a discrete formulation of the continuum. These techniques try to match the properties of the MSM to the properties of methods such the FEM, for example, by finding a linearized MSM model that produces elements with a stiffness matrix similar to that from linear FEM.

3.1.2.1 Estimation from Material Science

Following the material science approach, Maciel et al. (Maciel2003) obtained analytical expressions of the stiffness of hexahedral meshes from the elastic modulus and the uniaxial elongation test. Their parameters depend on the angular configuration of each deformed stage of the cube.

In the cloth modelling field, Wang et al. (Wang2005) developed a model composed by preloaded springs for solving problems of bending, stretching and shearing of clothing. With that aim, they proposed starting from the mathematical formulation of a MSM that describes those mechanical behaviours and then obtaining the stiffness values of the model.

Similarly, Baudet et al. (Baudet2009) proposed designing 2D and 3D MSMs using elongation and shearing experiments. The objective of this method is to reliably represent the mechanical properties of deformable objects starting from their definition: Young's modulus, Poisson's ratio and shear modulus. Their model includes, apart from spring forces, some correction forces.

3.1.2.2 Derivation from Discretized Formulation of Continuum

The analytical reasoning strategy based on the FEM formulation was started by Gelder (Gelder1998) who proposed to derive a set of expressions from geometrical and physical restrictions. He attempted to find a MSM equivalent to a triangular linear FEM model linearizing the system of equations of the MSM. He concluded that there was no solution to equating the stiffness matrix of linear elastic triangular elements to the corresponding stiffness matrix of the linearized equations of MSM.

Figure 3.4. Cloth simulation using particle systems derived from continuum mechanics (Etzmuss2003).

However, Lloyd et al. (Lloyd2007) demonstrated that there was a particular case in which both stiffness matrices were equal: equilateral

triangles with Poisson's ratio equal to 1/3. Although this case is just a particular case, they proposed a general method to obtain approximated stiffness values for any type of triangle even for rectangular meshes but maintaining Poisson's ratio equal to 1/3. Additionally, they proposed the minimization of the distance between the stiffness matrices to derive approximated tetrahedral models with Poisson's ratio equal to 1/4.

Etzmuss et al. (Etzmuss2003) proposed the calculation of the forces that act over a particle system from continuum mechanics by linearization, the choice of a local reference frame, and successive finite difference discretization (see figure 3.4). Although the derivation is made starting from linearized Green's strain tensor the resulting model is invariant under rotations.

Delingette (Delingette2008) established a formal link between springs and continuum mechanics through the introduction of biquadratic springs. Furthermore, he showed that any isotropic hyperelastic membrane can be expressed as a function of the two invariants of the strain tensor and therefore can be expressed in terms of tensile and angular biquadratic springs.

More recently, Xu et al. (Xu2010) proposed a modified MSM based on the 3D finite strain nonlinear anisotropic elasticity theory. Their model is able to describe typical behaviours of living tissues such as incompressibility, nonlinearity and anisotropy. They also incorporated into the soft-tissue model the nonlinear viscoelasticity by using numerical schemes.

3.1.3 DISCUSSION AND CONCLUSIONS

Data-driven methods adjust the parameters of a MSM to behave as close as possible to a reference model. In most of the cases, the resulting parameters are not exportable to other meshes since they are obtained for a specific body, an exclusive topology, and some particular tests. Thus, it is not easy to obtain useful generic parameter values from such techniques. However, in the case of soft tissue, typically there is not analytical information of the behaviour of the body. Then, testing the actual body and adjusting the virtual deformable body to those data becomes mandatory.

On the contrary, analytical methods offer parameters that are calculated for a certain material models and are not limited to a specific

sample body. Consequently, they provide more exportable results than the previous methods.

Data-driven strategies can be useful, for instance, to design virtual models for a learning simulator in which the object is not going to be modified and where the interactions are going to be known in advance. However, if the model has to be modified because the application is patient-specific or the resolution and the topology of the object can be arbitrarily changed then, analytical methods are preferable.

Once a data-driven method is selected an important disadvantage comes through: the time spent in obtaining the parameter of the model. Usually, they adopt evolutionary or simulated annealing techniques to avoid local minima and give global optimal values, which require long searching times due to the size of the search space. Additionally, their performance is governed by some parameters that are hard to define, for instance, mutation probability, population size or annealing schedule.

Concerning the disadvantages found in analytical methods presented above is that some of them derive MSMs that are more complex than the models that use only linear springs with constant stiffness values. Building more complex MSMs might increase the accuracy of the simulation but they lead to models that are harder to calculate. Enclosed in this group are those who add external forces (Etzmuss2003, Baudet2009) or angular springs (Delingette2008), and those who change the stiffness values of the springs depending on the angles of the deformed cube (Maciel2003). On the contrary, the approach suggested by Gelder (Gelder1998) and followed by Lloyd et al. (Lloyd2007) keeps the simplicity of traditional models.

3.2 MSM DESIGN PROPOSAL

As stated before, surgery oriented applications can use diverse information to build deformable models. When available, it is better to obtain analytical information and design models that perform accurately. Otherwise, data-driven methods offer the possibility to make some tests and derive from them the desired parameters. As both methods can be useful to design surgery simulators it is necessary to propose methods in both branches in order to improve the existing ones and overcome their drawbacks.

The methods presented previously are very different from one another and, a priori, it might be considered that all of the approaches are compatible with the objectives of this thesis. However, it is important to

stress one fundamental point: the proposed models must allow computing the deformations fast and accurately. Considering complex MSM designs is hardly justified since one of the main advantages against FEM would be lost. Thus, the effort has to be focused on obtaining models that perform as accurately as possible, but maintaining the mathematical simplicity to exploit their advantages.

This remark rules out directly those data-driven methods that are based on nonlinear and piecewise linear springs. It also reduces dramatically the available analytical approaches since, except from the works of Gelder (Gelder1998) and Lloyd et al. (Lloyd2007), all of them build models with complex characteristics. On the contrary, constraint-based approaches are compatible with the idea of mathematical simplicity since they only have influence during the simulation, not on the MSM design itself. In other words, they allow using the conventional MSMs as ground models and introduce some constraints that make the model perform more realistically. For example, they can be very useful to avoid the collapse of the elements of the model.

According to the topology of the mesh, most of the methods listed previously are focused on calculating the spring stiffness values for the particular case of tetrahedral meshes. The main reason is that using tetrahedra makes it possible to build easily any type of 3D virtual body found in surgical simulators. However, it is not possible to fill an object using equally sized tetrahedra. That is, each tetrahedron requires different edge sizes and angles. This variety of elements leads to complex design methods, like topology identification techniques, since meshes with identical mass and spring constants still behave quite differently depending on the overall topology (Bianchi2003, Völlinger2009).

Some of the difficulties found in the MSM design can be avoided choosing another type of elements. Regular meshes like cubical grids, for instance, allow using one unique type of element to fill the body simplifying a lot the parameter identification, at least in the case of homogeneous materials.

Another important advantage of cubical meshes is the possibility of making symmetric configurations of point masses and springs in the three orthogonal directions perpendicular to the faces of the cube. This makes the model respond equally in those directions.

Most of the continuum-based deformable models used in the simulations of living tissues consider isotropic or orthotropic material models. The main reason is that obtaining anisotropic models requires the determination of many unknown parameters for which more specific experiments and more complex formulations are needed. In practice, in the case of patient specific models for instance, the available information to build the model is limited to CT and MRI data which makes almost impossible to provide enough information to define complex material models. Thus, it is reasonable to make the same assumption when using MSMs and adopt symmetrical cubical meshes whose behaviour is orthotropic.

Taking all these considerations into account in this thesis two new methods are proposed to design accurate and fast deformable models based on cubical MSMs:

1- A new analytical method for linear elastic material models based on the linearization of the equilibrium equations of the MSM. In this method the linearized system is equated to the linear FEM model with the particularity that it allows obtaining the stiffness coefficients for any values of Young's modulus and Poisson's ratio.

2- A new analytical method that is based on the study of the nonlinear behaviour of cubical MSMs. This method adjusts the parameters of the MSM in such a way that it behaves like some reference nonlinear elastic material. According to the bibliographic review, there is no published method for deriving analytically cubical models from hyperelastic material models.

CHAPTER 4

MSM DESIGN FROM LINEAR ELASTIC MATERIAL MODELS

As already mentioned in section 2.2, it is usual in continuum based approaches to assume that biological tissues display a linear elastic behaviour when the material is working under small deformations. Setting this simplification in the case of discrete models such as MSMs is more difficult because there is no underlying formulation to define the global material model. Therefore, the main challenge of this chapter is the search for a cubical MSM that behaves like a linear elastic material.

The first approach to accurately simulate the properties of elastic materials using a MSM was due to Gelder (Gelder1998). This work proposed an analytical reasoning strategy based on the FEM formulation. First, he searched for a MSM with a triangular mesh equivalent to a linear elastic FEM by linearizing the system of equations of the MSM. This approach did not provide a positive result and he concluded that there is no possible solution that equates the stiffness matrix of a linear FEM to the corresponding stiffness matrix of the linearized equations of MSM.

Afterwards, he proposed the derivation of a set of expressions from geometrical restrictions obtaining a stiffness value that depends on the elastic modulus, the rest length of the edge, and the area of the triangle. Although the derivation is valid only for Poisson's ratios equal to zero, he

suggested that no observable difference in quality was detected within a range between 0 and 0.25.

Later on, Lloyd et al. (Lloyd2007) demonstrated that there is a particular case in which both stiffness matrices are equal: equilateral triangles with Poisson's ratio equal to 1/3. Although this case is just a particular situation, they proposed a general method to obtain approximated stiffness values for any type of triangle even for rectangular meshes but maintaining Poisson's ratio equal to 1/3. However, in 3D problem, they did not find any exact solution to make both matrices equal for the case of tetrahedral meshes. For this reason, they proposed the minimization of the distance between the stiffness matrices to derive approximated tetrahedral models with Poisson's ratio equal to 1/4.

The methods presented in both works (Gelder1998, Lloyd2007) are based on the linearization of the equations of the MSM around the equilibrium position, which makes them valid only for small deformations. In other words, the usefulness of these methods in the field of surgery simulation, where the deformations and displacements are large, is limited. However, it can be an interesting first approximation when attempting to build deformable models. Even though linear elastic material models are far from the actual behaviour of living tissues the assumption of small deformations has been widely adopted in soft body simulation (Bro-Nielsen1998, Müller2002, DiMaio2003, James2003, Berkley2004, Hauth2004, Wu2004, Lee2006, Georgii2008).

Keeping in mind the limitations of the results that can be obtained from the linearization approach, this procedure will be followed in this thesis to make a first approximation to the design of deformable models. Special attention will be paid in the definition of the method to some weak points detected in the method proposed by Gelder (Gelder1998) and Lloyd et al. (Lloyd2007).

First, both works suggest that the best way to make the linearized MSM behave like the linear FEM is by achieving the same element values in both stiffness matrices one to one. As in most cases there is not an exact solution Lloyd et al. (Lloyd2007) propose minimizing the difference between each element. However, an eigenvalue- and eigenvector-based approach can provide a deeper analysis of the quality of the approximation because it allows studying the direction and magnitude of the transformations that produce both stiffness matrices.

Second, there are two main material parameters in linear elastic FEM: Young's modulus and Poisson's ratio. The work of Lloyd et al. focuses on finding an exact solution to the stiffness matrices equating process. Thus, they limit the variability of Poisson's ratio to the value that produces the smallest error. However, this magnitude has to be, in principle, a free parameter in the deformable model design.

Finally, Gelder studies the particular case of 2D triangles and tetrahedron meshes while Lloyd et al. focus on the analysis of 2D triangle, rectangle, and tetrahedron meshes. However, neither work studies 3D cubical MSM elements.

For these reasons, a new method is developed in this thesis based on the study of the eigenvectors and eigenvalues of the linearized cubical MSM, which is able to deal with any value of Poisson's ratio and Young's modulus. It is important to remark that the linearized model is only used to obtain the stiffness coefficients of the MSM but not to compute the real deformations. That is, the MSM used in any simulation will be nonlinear. For this reason, from now on, this method is called the *linear method* although it provides the parameters of a nonlinear model.

4.1 METHOD DESCRIPTION

As it has been seen, one possibility to derive a MSM whose behaviour is equivalent to a linear FEM is by linearizing the spring force as a function of the node positions and equating the linearized MSM equations with the FEM equations (see figure 4.1). This results in a linear approximation around the current configuration of the element.

Four steps are necessary to derive the spring coefficients of a single cubical MSM before the whole body is assembled. First, the element stiffness matrix must be calculated analytically using the FEM. Second, the equations of the MSM have to be obtained. Then, these equations are linearized and the linear stiffness matrix is calculated. Finally, the stiffness matrices of both MSM and FEM are compared. Normally, a linearized MSM with the same stiffness matrix as the linear FEM of the same geometry cannot be found, making it necessary to find the parameters that minimize the difference between them.

It is important to mention that this analytical method works over a single element. It does not consider the whole mesh of the deformable model. This makes the MSM design method independent of the mesh

topology. Thus, after identifying the parameters of one cube, the elements are assembled in order to build the complete deformable model.

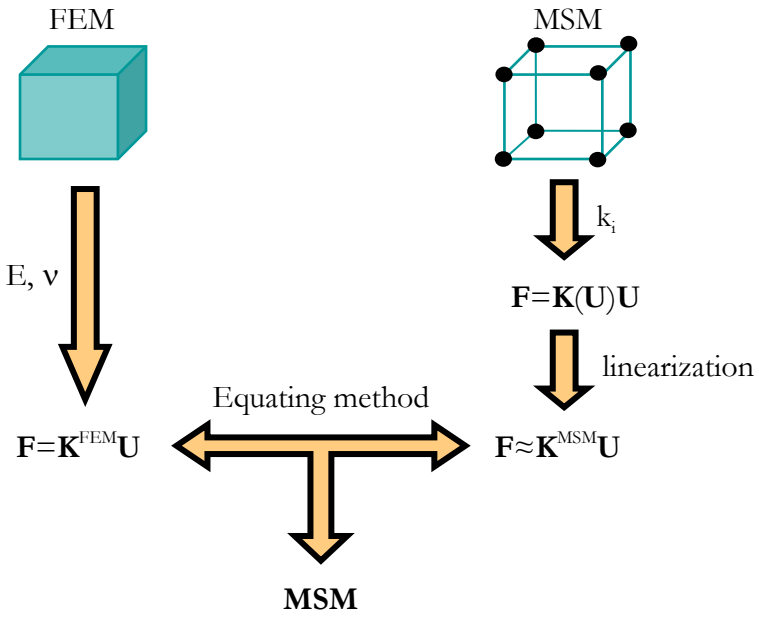

Figure 4.1. Method to obtain a cubical MSM from linear elastic FEM.

4.1.1 LINEAR ELASTIC FEM

In the FEM, the continuous model is spatially discretized by dividing it into a set of interconnected regions, called elements. The deformation field is approximated by interpolation functions associated with each element. For the linear FEM formulation, a cubical element with 8 nodes and trilinear interpolation is used. The equilibrium equations have the following form:

$$\mathbf{F} = \mathbf{K}^{FEM}\ \mathbf{U} \tag{4.1}$$

where **F** is the vector of 24 forces applied at the nodes (3 components for each node), **U** is the vector of the nodal displacements and $\mathbf{K}^{FEM}$ is a symmetric 24x24 matrix known as the element stiffness matrix.

As the objective in this section is to obtain the stiffness matrix $\mathbf{K}^{FEM}$ the theoretical background for the FEM will be only briefly outlined. The reader is referred to the work of Zienkiewicz et al. (Zienkiewicz2005) for further details.

For a linear elastic material the stiffness matrix depends on the elasticity matrix (**D**). This matrix is constant and depends only on two parameters:

$$\mathbf{D} = \begin{bmatrix} \lambda+2\mu & \lambda & \lambda & 0 & 0 & 0 \\ \lambda & \lambda+2\mu & \lambda & 0 & 0 & 0 \\ \lambda & \lambda & \lambda+2\mu & 0 & 0 & 0 \\ 0 & 0 & 0 & \mu & 0 & 0 \\ 0 & 0 & 0 & 0 & \mu & 0 \\ 0 & 0 & 0 & 0 & 0 & \mu \end{bmatrix} \quad 4.2$$

The λ and μ coefficients are the Lamé parameters whose values depend on the Young's modulus and Poisson's ratio:

$$\lambda = \frac{E\nu}{(1+\nu)(1-2\nu)} \quad 4.3$$

$$\mu = \frac{E}{2(1+\nu)} \quad 4.4$$

Following the *Serendip* formulation (Zienkiewicz2005), three local coordinates (ξ, η and ζ) centred in a cube are used to define the interpolation functions (see figure 4.2), whose values vary between -1 and 1. Thus, the resulting cube in the local coordinates has an edge length of 2.

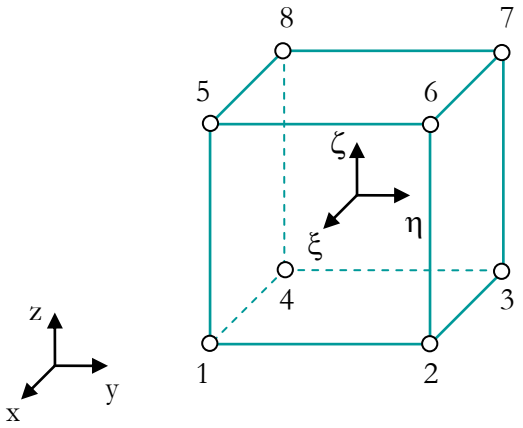

Figure 4.2. The cubical element represented using normalized local coordinates ξ, η and ζ.

Calling the coordinates of node i as ξ_i, η_i and ζ_i and taking into account that the element is a cube with 8 nodes and linear interpolation the corresponding functions of interpolation are:

$$N_i = \frac{1}{8}(1+\xi\xi_i)(1+\eta\eta_i)(1+\zeta\zeta_i) \quad i=1,...,8 \tag{4.5}$$

The strain state is defined by the strain-displacement matrix (**B**). The block columns of **B** can be calculated by taking the derivative of the interpolation function with respect to the global Cartesian coordinates in the following way:

$$\mathbf{B_i} = \partial \begin{bmatrix} N_i & 0 & 0 \\ 0 & N_i & 0 \\ 0 & 0 & N_i \end{bmatrix} = \begin{bmatrix} \frac{\partial N_i}{\partial x} & 0 & 0 \\ 0 & \frac{\partial N_i}{\partial y} & 0 \\ 0 & 0 & \frac{\partial N_i}{\partial z} \\ \frac{\partial N_i}{\partial y} & \frac{\partial N_i}{\partial x} & 0 \\ 0 & \frac{\partial N_i}{\partial z} & \frac{\partial N_i}{\partial y} \\ \frac{\partial N_i}{\partial z} & 0 & \frac{\partial N_i}{\partial x} \end{bmatrix} \quad i=1,...,8 \tag{4.6}$$

Finally, the stiffness matrix can be obtained computing the following volumetric integral:

$$\mathbf{K}^{FEM} = \int_v \mathbf{B}^{\mathbf{T}}\mathbf{D}\mathbf{B}dv \tag{4.7}$$

4.1.2 LINEARIZED MSM

In order to obtain a MSM equivalent to the linear FEM described above, first, it is necessary to obtain an expression that relates the applied forces with the resulting deformations.

The numbering of the vertices of the hexahedral elements follow the conventions typically used in FEM texts. That is, the element is represented by an ordered set of vertices from 1 to 8, where the point masses are placed. These vertices are connected to each other by linear springs. Considering the requirement of symmetric configuration three types of springs are defined to connect each of the vertices of the cube with the remaining

seven vertices: edge springs with k_e stiffness (e.g. between vertices 1 and 2), face diagonal spring with k_f stiffness (e.g. between vertices 1 and 6) and internal diagonal springs with k_d stiffness (e.g. between vertices 1 and 7). The graphic representation of the different springs and the node numbering are shown in figure 4.3.

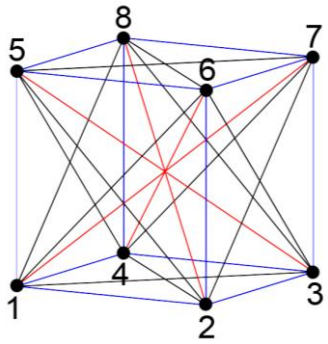

Figure 4.3. Node numbering and spring distribution in the cube. Edge springs in blue, face diagonal springs in black and internal diagonal springs in red.

Every elastic force that connects the 8 point masses of the cubical MSM is modelled using linear springs. That is, the force exerted by the spring that connects two generic nodes i and j is proportional to the elongation of the spring, $k_{(i,j)}$ being the corresponding stiffness coefficient and $l_{(i,j)}^{0}$ its rest length. Calling $\mathbf{x_i}=(x_i, y_i, z_i)^T$ and $\mathbf{x_j}=(x_j, y_j, z_j)^T$ to the positions of the nodes i and j, the force at node i exerted by the spring that connects it with the node j can be computed as:

$$\mathbf{f}_{(i,j)} = k_{(i,j)}\left[\left(\mathbf{x}_i - \mathbf{x}_j\right)\left(1 - \frac{l_{(i,j)}^{0}}{\left\|\mathbf{x}_i - \mathbf{x}_j\right\|}\right)\right] \qquad 4.8$$

For a given spring, the force acting at node j is the same as at node i but with the opposite direction:

$$\mathbf{f}_{(j,i)} = -\mathbf{f}_{(i,j)} \qquad 4.9$$

Although the relation between the force and the elongation is constant, the evaluation of this force leads to a nonlinear formulation. The reason is that the computation of the length of the spring in the deformed state is a Euclidean distance. Thus, the assembly of the 28 springs that compose the cube produces a system of nonlinear equations.

As deformations are considered small, the final positions of the nodes are close to their initial positions. Consequently, the system of equations that governs the behaviour of the MSM can be linearized around the rest state. The same approach was adopted by Lloyd et al. (Lloyd2007) to obtain triangular, rectangular, and tetrahedral elements.

A first order approximation of the equations at the rest state is adopted to linearize the system of equations. In addition, a generic spring will be studied first to simplify the formulation and then the assembly of all the system will be performed.

The linearized expression of the force of the spring that connects nodes *i* and *j* around the rest nodal positions ($\mathbf{x}_i^0$, $\mathbf{x}_j^0$) is:

$$\mathbf{f}_{(i,j)} \approx \mathbf{f}_{(i,j)}\Big|_{\mathbf{x}_i^0,\mathbf{x}_j^0} + \nabla\mathbf{f}_{(i,j),\mathbf{x}_i}\Big|_{\mathbf{x}_i^0,\mathbf{x}_j^0}\left(\mathbf{x}_i - \mathbf{x}_i^0\right) + \nabla\mathbf{f}_{(i,j),\mathbf{x}_j}\Big|_{\mathbf{x}_i^0,\mathbf{x}_j^0}\left(\mathbf{x}_j - \mathbf{x}_j^0\right) \qquad 4.10$$

The first term of the linearized expression is null because it refers to the resulting forces at the rest state. The second and third terms can be calculated by computing partial derivatives and substituting $\mathbf{x}_i$ and $\mathbf{x}_j$ with $\mathbf{x}_i^0$ and $\mathbf{x}_j^0$ respectively.

The process concerning the assembly of the equations of the 28 springs that compose the single cube is straightforward and will not be detailed. In any case, this linearization allows computing approximately the equilibrium of a MSM under the hypothesis of small deformations around the initial rest position with a system of equations of the following form:

$$\mathbf{F} = \mathbf{K}^{MSM}\ \mathbf{U} \qquad 4.11$$

As in the case of FEM, **F** is the vector of 24 forces applied at the nodes (3 components for each node), **U** is the vector of the displacements of the nodes and $\mathbf{K}^{MSM}$ is the symmetric 24x24 stiffness matrix obtained from the linearization. This matrix has a structure of 8x8 blocks, each block being a 3x3 matrix. The blocks located in the diagonal of the matrix correspond to the sum of the spring forces exerted at each node. The blocks not contained in the diagonal, in turn, define the stiffness relation between only two particular nodes.

The submatrices located at the diagonal have the form:

$$\mathbf{K}_{ii}^{MSM} = \sum_{j=1,8} \frac{k_{(i,j)}}{\left(l_{(i,j)}^0\right)^2}\left(\mathbf{x}_i^0 - \mathbf{x}_j^0\right)\left(\mathbf{x}_i^0 - \mathbf{x}_j^0\right)^T \quad i = 1...8 \qquad 4.12$$

While the submatrices not contained in the diagonal have the form:

$$\mathbf{K}_{ij}^{MSM} = -\frac{k_{(i,j)}}{\left(l_{(i,j)}^0\right)^2}\left(\mathbf{x}_i^0 - \mathbf{x}_j^0\right)\left(\mathbf{x}_i^0 - \mathbf{x}_j^0\right)^T \quad i,j = 1...8 \quad i \neq j \qquad 4.13$$

Note that the stiffness values of the springs $k_{(i,j)}$ can be only of three types: edge (k_e), face diagonal (k_f) or internal diagonal (k_d) springs.

4.1.3 STIFFNESS MATRICES EQUATING PROBLEM

The objective of the present method is finding the values of the free parameters of the MSM so that it behaves in a way equivalent to linear FEM, at least when the model is working under small deformations around the initial rest configuration. The MSM has been already linearized and written in matricial form (see equation 4.11) which is similar to the FEM system (see equation 4.1). The equivalency between both mathematical formulations makes possible to propose methods that allow obtaining an approximate MSM from the linear elastic FEM.

Both models transform the nodal displacements into force vectors using a stiffness matrix whose elements are constant. Note that the transformation that makes $\mathbf{K}^{FEM}$ depends on two parameters because a linear elastic material is defined by the Young's modulus and Poisson's ratio. However, the proposed MSM has at most three parameters to adjust its behaviour: k_e, k_f, and k_d (see figure 4.4).

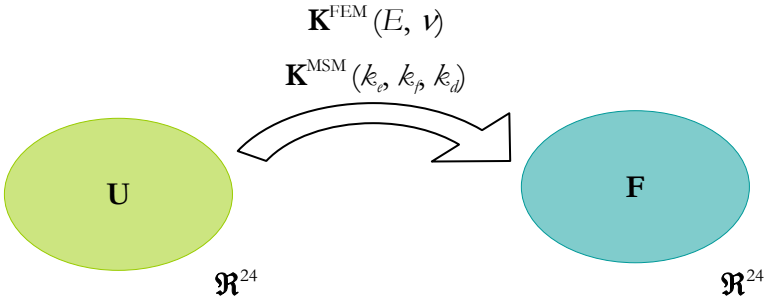

Figure 4.4. Linear transformation mapping each displacement vector **U** in $\mathfrak{R}^{24}$ to the force vector **F** in $\mathfrak{R}^{24}$.

In the ideal case, given any displacements vector $\mathbf{U} \in \mathfrak{R}^{24}$ both stiffness matrices would transform this **U** into the same **F** and the method

proposed to obtain the parameters would have to be valid for any E and ν. In general, finding the stiffness coefficients of the MSM that fulfil this requirement is not possible since the problem has not an exact analytical solution.

The method of Lloyd et al. (Lloyd2007) consists in making the submatrices of $\mathbf{K}^{FEM}$ symmetric before solving the equating problem. The main drawback of this approach is that the Poisson's ratio needs to be fixed to a specific value, which limits extremely its usability. For this reason, it is necessary to develop a new method to find the spring coefficients that make both stiffness matrices as similar as possible for any value of ν.

In the following section the approach followed by Lloyd et al. (Lloyd2007) to calculate the most suitable constants will be presented and then a new method based on the eigenproblem study will be proposed.

4.1.3.1 Matrix distance approach

Lloyd et al. (Lloyd2007) obtained an analytical exact solution to the equating problem for equilateral triangles and rectangles. However, as the stiffness parameters of the MSM are not enough to equate both matrices they increased the number of degrees of freedom of the problem by considering also as output variable the Poisson's ratio. In the particular case of triangles and rectangles, the Poisson's ratios that make the submatrices of $\mathbf{K}^{FEM}$ symmetric are 1/3 and 1/4 respectively. In the case of rectangles they even had to increase the number of variables by considering prestrained springs.

In other words, they force $\mathbf{K}^{FEM}$ to have the same form as the stiffness matrix of the linearized MSM by selecting a particular value for Poisson's ratio. However, including ν in the set of design parameters limits the usefulness of the method because it admits as input parameters any value of E but a unique ν. Therefore, this method is able to find MSMs equivalent to only certain linear elastic material models.

In the case of regular tetrahedra, apart from the three stiffness parameters and ν, they included volume preserving forces. However, the equating problem still did not yield an exact solution. Therefore, they proposed a minimization approach to obtain the best possible approximations, and divided the method into two steps: first the value of ν that makes both stiffness matrices have similar form is selected and then the minimization is performed. Calling $\mathbf{C}$ to the difference between the

linearized MSM and FEM stiffness matrices (see equation 4.14) the optimization strategy consists in minimizing the Frobenius norm of **C** (see equation 4.15).

$$\mathbf{C} = \mathbf{K}^{FEM} - \mathbf{K}^{MSM} \tag{4.14}$$

$$\min \|\mathbf{C}\|_F = \min \sqrt{\sum_{i=1}^{24}\sum_{j=1}^{24} |c_{ij}|^2} \tag{4.15}$$

However, using this strategy it is difficult to understand the physical meaning of the Frobenius norm of **C** and even more difficult to interpret the obtained results. In turn, analyzing the transformation that makes each stiffness matrix in certain characteristic directions provides a more detailed view of the physical behaviour of the model.

4.1.3.2 Eigenproblem approach

In this thesis a new approach is proposed to find the most suitable parameters of the cubical MSM. In particular, it is focused on the study of the eigenproblem of the stiffness matrices.

Taking as reference the stiffness matrix of the FEM, the study of the eigenproblem provides the **V** and **D** square matrices that satisfy the following equation:

$$\mathbf{K}^{FEM}\mathbf{V} = \mathbf{V}\mathbf{D} \tag{4.16}$$

The columns of **V** are the eigenvectors ($\mathbf{v}_n$) of $\mathbf{K}^{FEM}$ and **D** is a diagonal matrix whose values correspond to the eigenvalues (λ_n) of $\mathbf{K}^{FEM}$.

As **V** is an orthogonal matrix ($\mathbf{V}^T=\mathbf{V}^{-1}$) the vector of displacements **U** can be computed as follows:

$$\mathbf{U} = \left(\mathbf{K}^{FEM}\right)^{-1}\mathbf{F} = \mathbf{V}\mathbf{D}^{-1}\mathbf{V}^T\mathbf{F} \tag{4.17}$$

As both the stiffness matrices of the FEM and the linearized MSM are symmetric, their eigenvectors are orthogonal. This means that the 24 eigenvectors of each matrix form an orthogonal basis of the space of **U**. Analyzing the transformations suffered in those directions is equivalent to studying all the possible displacements vectors since the rest of them are linear combinations of this basis.

Consequently, analyzing the eigenproblem of the stiffness matrices is equivalent to studying the effects of applying different deformations in the specific directions that define the whole behaviour of the model.

In this approach the reference system is the FEM model, and therefore the eigenvectors of $\mathbf{K}^{\text{FEM}}$ will be the directions in which the equivalence will be studied. The error obtained in the MSM when performing the linear transformation in the principal directions defined by $\mathbf{K}^{\text{FEM}}$ can be computed as follows:

$$\mathbf{e}_n\left(k_e,k_f,k_d\right)=\mathbf{K}^{MSM}\mathbf{v}_n-\mathbf{K}^{FEM}\mathbf{v}_n \quad n=1...24 \tag{4.18}$$

The strategy proposed to optimize these transformations is the minimization of ϕ using a least squares method, ϕ being:

$$\phi\left(k_e,k_f,k_d\right)=\sum_{n=1}^{24}\left\|\mathbf{e}_n\right\|^2 \tag{4.19}$$

This new strategy based on the study of the eigenvectors of $\mathbf{K}^{\text{FEM}}$ is consistent with the minimization of the Frobenius norm of difference between $\mathbf{K}^{\text{MSM}}$ and $\mathbf{K}^{\text{FEM}}$ proposed by Lloyd et al. (Lloyd2007). This equivalence is proved in equation 4.20 taking into account that $\mathbf{C}$ is a real matrix and $\mathbf{V}$ orthogonal ($\mathbf{V}^{\text{T}}=\mathbf{V}^{-1}$).

$$\begin{aligned}\phi\left(k_e,k_f,k_d\right)&=\sum_{n=1}^{24}\left\|\mathbf{K}^{MSM}\mathbf{v}_n-\mathbf{K}^{FEM}\mathbf{v}_n\right\|^2=\left\|\mathbf{K}^{MSM}\mathbf{V}-\mathbf{K}^{FEM}\mathbf{V}\right\|_F^2\\&=\left\|\mathbf{CV}\right\|_F^2=tr\left(\left[\mathbf{CV}\right]^*\left[\mathbf{CV}\right]\right)=tr\left(\left[\mathbf{CV}\right]^T\left[\mathbf{CV}\right]\right)=tr\left(\mathbf{V}^T\left[\mathbf{C}^T\mathbf{CV}\right]\right)\\&=tr\left(\mathbf{C}^T\mathbf{CVV}^T\right)=tr\left(\mathbf{C}^T\mathbf{C}\right)=\left\|\mathbf{C}\right\|_F^2\end{aligned} \tag{4.20}$$

However, the approach proposed in this thesis provides more information about the obtained MSM as it will be seen in section 4.2.2.

The main advantage of this method is that it allows making an analysis of the deformation modes of both mechanical models. It consists in identifying the shapes of the deformations and the stiffness of the model in those directions. In particular, the eigenvectors of the stiffness matrices determine the shapes of these deformation modes, while the eigenvalues are used to determine the stiffness associated to them. The orthogonality property of the eigenvectors allows decoupling the behaviour of the model so that the system can be represented as linear combination of the

eigenvectors. That is, any deformation of these mechanical models is a superposition of their eigenmodes.

As the FEM and linearized MSM can be decomposed in eigenmodes it is possible to evaluate the quality of the approximation by analyzing the similarity between their corresponding modes. The more similar the modes are the more similar the mechanical models will behave. In the ideal case, both models would have their eigenvectors parallels to one another and the corresponding eigenvalues with the same magnitude.

4.2 RESULTS

As mentioned before, linear elastic material models are defined by two parameters: E and ν. From equations 4.2, 4.3 and 4.4 can be deduced that the elastic matrix $\mathbf{D}$ depends on E and ν but with the particularity that Young's modulus multiplies all the elements of the matrix. Thus, the stiffness matrix $\mathbf{K}^{FEM}$ (see equation 4.7) can be rewritten as a product of E and a matrix.

On the other hand, all the elements of $\mathbf{K}^{MSM}$ are proportional to the spring constants (see equation 4.12 and 4.13). The consequence of these properties of $\mathbf{K}^{FEM}$ and $\mathbf{K}^{MSM}$ is that the stiffness coefficients of the MSM have to be proportional to E. A similar reasoning can be made with the length of the cube edge L_0. In this way, the study of the equivalence between stiffness matrices is simplified since E and L_0 are no longer free parameters to be identified.

In turn, there is no way to consider an equivalent proportionality with respect to the Poisson's ratio. Taking these considerations into account, the parameters of the MSM can be rewritten using three pseudo-stiffness k_i' constants which are non-dimensional factors:

$$k_i = \frac{L_0}{2} k_i' E \quad i = e, f, d \tag{4.21}$$

To derive the values of these parameters from the linear elastic FEM the minimization method described in the previous section (see equation 4.19) is applied. In order to handle this minimization in an easy way, the resolution is particularized for certain values of ν. The range of Poisson's ratios between 0 and 0.5 is divided into discrete values using increments of 0.05. The resulting pseudo-stiffness values are detailed in table 4.1.

Poisson's ratio (ν)	Edge springs (k_e')	Face diagonals (k_f')	Internal diagonals (k_d')
0.00	0.155	0.206	0.119
0.05	0.153	0.206	0.121
0.10	0.153	0.208	0.125
0.15	0.154	0.214	0.132
0.20	0.158	0.223	0.141
0.25	0.166	0.239	0.156
0.30	0.179	0.265	0.179
0.35	0.205	0.312	0.220
0.40	0.260	0.410	0.303
0.45	0.432	0.714	0.555
0.49	1.826	3.166	2.585

Table 4.1. The pseudo-stiffness coefficients of edge springs, face diagonal springs, and internal diagonal springs obtained from linear FEM for different Poisson's ratios.

These pseudo-stiffness values depend only on the Poisson's ratio. Defining a particular MSM requires taking into account the expression that relates them with k_i (see equation 4.21) and choosing coherent units for L_0 and E.

Note that the highest value of ν has been taken 0.49 instead of 0.5 because the elements of the stiffness matrix corresponding to the linear elastic FEM tend to infinite as the model approaches incompressibility.

4.2.1 SENSIBILITY TO THE POISSON'S RATIO

There are several ways to study the influence of the Poisson's ratio on the quality of the approximation. One of them is to subject a single cubical MSM to certain forces and compare the resulting deformations with respect to the corresponding FEM simulations. Another way to evaluate the approximation is to analyze the residual error of the minimization.

4.2.1.1 Uniaxial tensile test

The most common experiment used to obtain the mechanical properties of some sample is the uniaxial tensile test (see figure 4.5). Therefore, an interesting way to analyze the effect of ν on the deformation error of the model is testing a single cube made up with the derived spring constants and study how it behaves in both axial and transversal directions.

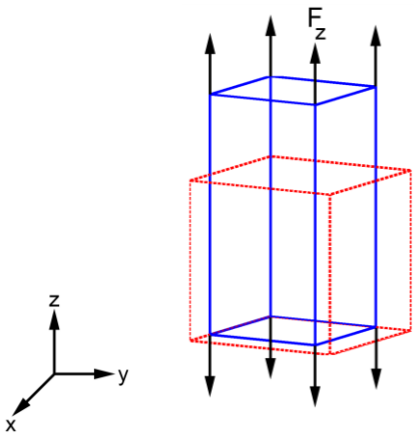

Figure 4.5. The appearance of the MSM subject to uniaxial tensile forces.

Different definitions of stress and strain are used in solid mechanics. Although these magnitudes are defined for a continuum context, in a tensile test it is possible to define an equivalent relation in the discrete domain, assuming that the total applied load over a face is the sum of the external nodal forces. The resulting engineering stress in z axis equation 4.22 in the present tensile test may be defined as the relation between the applied load ($4F_z$) and the original cross-sectional area.

$$\sigma_z = \frac{4F_z}{L_0^2} \qquad 4.22$$

Likewise, the engineering strain equation 4.23 along the *i* axis may be estimated as the relation between the elongation and the original reference length of the spring.

$$\varepsilon_i = \frac{L_i - L_0}{L_0} \qquad 4.23$$

It is also interesting to study the Poisson's ratio equation 4.24, that measures the relation between the strain in the transversal direction (ε_x or ε_y) and the strain along the axial direction (ε_z) when a pure uniaxial test in z axis is performed.

$$\upsilon = -\frac{\varepsilon_x}{\varepsilon_z} = -\frac{\varepsilon_y}{\varepsilon_z} \qquad 4.24$$

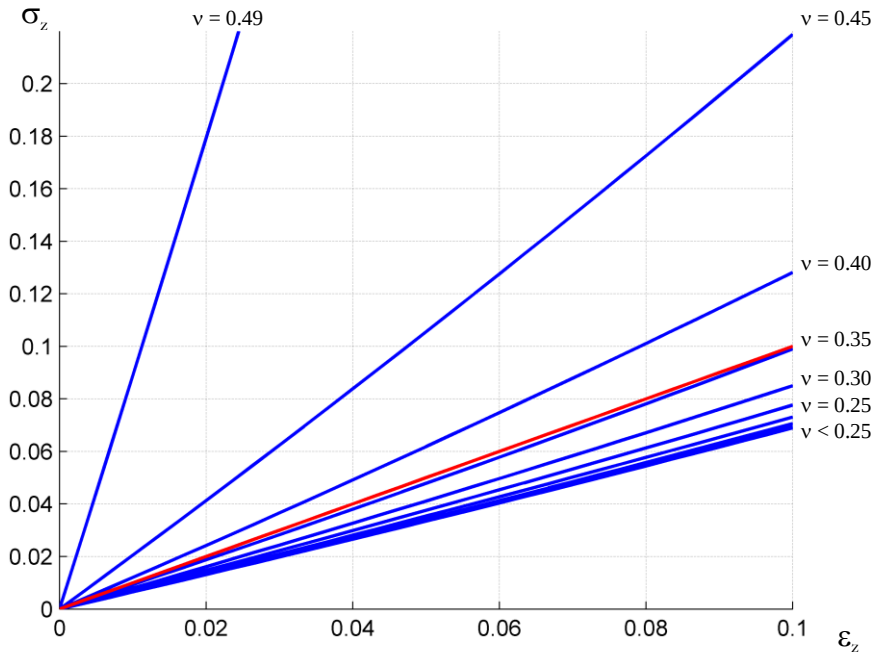

Figure 4.6. Stress-strain curves of the linear FEM (in red) and MSM (in blue) for a uniaxial tensile test. The MSM shows a dependency with the Poisson's ratio. The stress value is expressed per unit of elasticity module.

Taking into account these magnitudes figures 4.6 and 4.7 show the results of tensile tests performed to MSMs designed using the values of

table 4.1. Note that although the parameters have been obtained using the linearized model, these tests are applied to the original MSM. In all the cases the model is pulled until the elongation raises a value of 10% in the axial direction. In order to avoid the scaling influence of E on the deformation as well as on the error, this parameter is taken equal to 1. In particular, figure 4.6 shows the stress-strain curves of the linear FEM and the MSM in the axial direction for all the Poisson's ratios displayed in table 4.1.

Note that the curves shown in figure 4.6 that correspond to the MSM are not perfect straight lines although they look so. The reason for this is that the response of the MSM is calculated by computing the nonlinear equations (see equation 4.8) and not the linearized system. The fact that these lines are fairly straight demonstrates that it is logical to assume that the behaviour of MSMs is close to linear when they work under small deformations.

When Poisson's ratio is around 0.35, the derived spring constants behave in the axial direction very much like a linear elastic FEM but a considerable error appears when other values are selected. Below this value the cube behaves more softly and the deviation increases when Poisson's ratio decreases, 31% softer would be its worst. On the other hand, analyzing Poisson's ratios greater than 0.35, it can be seen that the sample behaves more stiffly than the original one. This error gets even worse the more ν approaches incompressibility. For example, a MSM obtained from linear elastic FEM with Poisson's ratio of 0.40 is 28% stiffer than that reference model.

Taking into account the same experiments, figure 4.7 shows the transversal strain in function of the tensile strain for the linear FEM and the MSM for all the Poisson's ratios displayed in table 4.1. That is, this figure shows how good the approximation in the transversal direction is.

Figure 4.7 allows completing the analysis of the error in uniaxial tensile tests associated to the parameter derivation method in function of ν. Although in the reference FEM model the Poisson's ratio varies from 0 to 0.49 with increments of 0.05, the obtained MSMs show very different behaviours. All of them have a relation between the transversal strain and the tensile strain in the range of 0.25 and 0.3.

That is, even though the proposed method is able to approximate accurately the behaviour in the axial direction for ν=0.35 it is not capable of describing correctly the strain caused in the transversal direction.

Conversely, for ν=0.275 the transversal behaviour is approximated accurately while the axial response turns 20% softer.

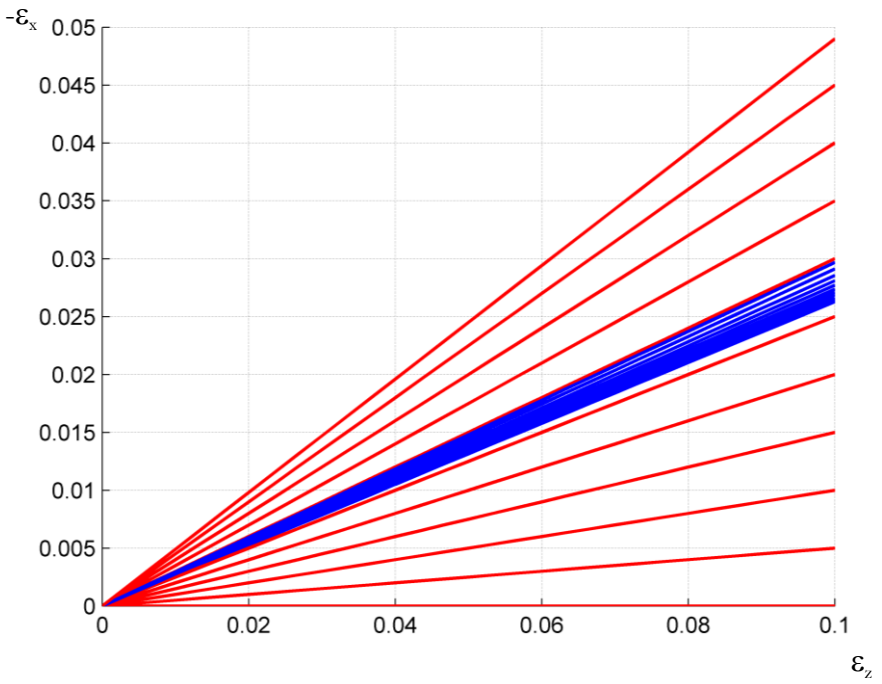

Figure 4.7. Transversal strain versus tensile strain curves of FEM (in red) and MSM (in blue) for a uniaxial tensile test.

In summary, in the case of considering the axial response in a uniaxial tensile test then, the best ν is 0.35. In turn, if the relation between the axial and the transversal deformations is analyzed then, the optimum value becomes 0.275.

4.2.1.2 Residual error of the minimization

Another way to analyze the best approximated reference parameters is studying the residual error of the proposed minimization process. Figure 4.8 shows the 2-norm value of the residual error at the solution in function of the Poisson's ratio.

The curve of the residual error remains quite planar for Poisson's ratios below 0.35. Although in this whole range the error is small the

minimum value is located at approximately 0.2, which means that at this specific value both matrices are *closer*. However, the error shown by this value in the uniaxial tensile test suggests that ν=0.2 does not correspond to the best approximation.

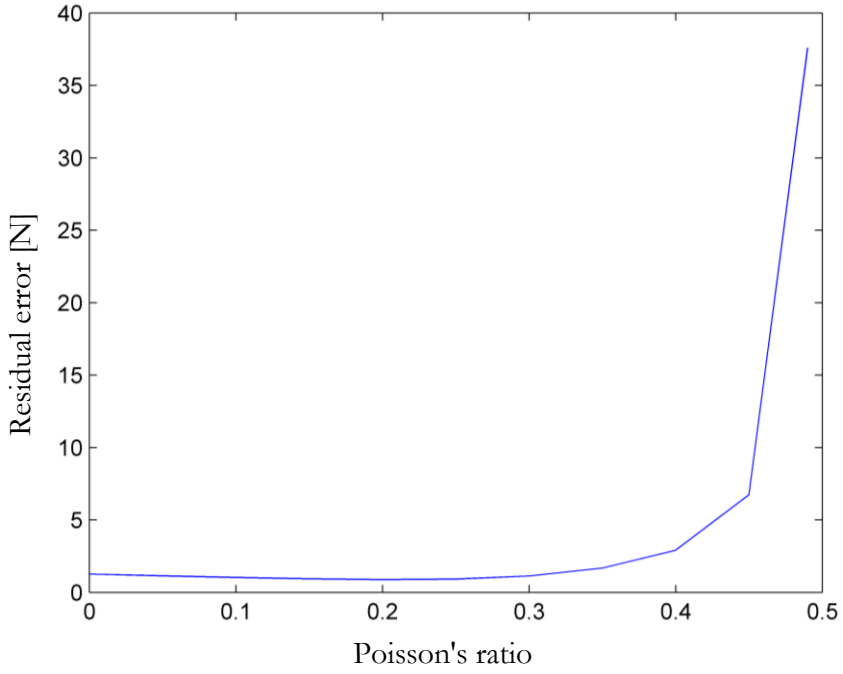

Figure 4.8. Residual error of the minimization approach in function of the Poisson's ratio.

On the other hand, the optimum Poisson's ratios obtained in the tensile experiments (0.275 and 0.35) display small residual error. This makes them the best candidates for approximating accurately the behaviour of linear elastic material models.

4.2.2 ANALYSIS OF THE EIGENPROBLEM

The eigenproblem approach allows analyzing the results of the proposed method from a point of view that is different from the direct study of the generic response of the model itself. It provides specific information about the response of the model in a group of directions that represent its whole behaviour. This information makes it much easier to evaluate how close the FEM and the linearized MSM are. In particular, the study will be focused on the identification of *equivalent* subspaces and the evaluation of the quality of

the approximation of the obtained MSM by using a specifically defined metric. This approach will help identifying the optimum value for the Poisson's ratio.

The same set of Poisson's ratios in the range of 0-0.5 that are detailed in table 4.1 will be analyzed since the previous section provided several optimum values for ν. Before starting with the complete study, some aspects of the eigenproblem study will be introduced. In order to illustrate this concepts the case of ν=0 is adopted. For other values of ν the procedure would be same.

4.2.2.1 Eigenspaces

The stiffness matrix of the FEM has a set of 24 eigenvectors and each of them has associated an eigenvalue. Due to the symmetry of this matrix, the eigenvectors are orthogonal to one another and they form a basis of the space of **U**. Some of these eigenvectors have associated the same eigenvalue and form, together with the zero vector, subspaces of **U** called *eigenspaces*. The dimension of these eigenspaces is given by the number of eigenvectors that have the same eigenvalue, also known as the *geometric multiplicity* (μ) of the eigenvalue.

The stiffness matrix of the linearized MSM has also the same characteristics as the stiffness matrix of the FEM. Therefore, its collection of eigenvectors can also be subdivided in orthogonal eigenspaces.

In order to show this concepts in a practical example, table 4.2 shows the eigenvalues and their geometric multiplicity for the case of ν=0. This table is organized in increasing order of the eigenvalues.

	λ_1	λ_2	λ_3	λ_4	λ_5	λ_6	λ_7	λ_8	λ_9
FEM	$0_{(6)}$	$0.17_{(2)}$	$0.22_{(3)}$	$0.5_{(6)}$	$0.67_{(1)}$	$1_{(6)}$	-	-	-
MSM	$0_{(6)}$	$0.21_{(2)}$	$0.31_{(3)}$	$0.34_{(3)}$	$0.52_{(2)}$	$0.62_{(3)}$	$0.72_{(3)}$	$0.82_{(1)}$	$1.37_{(1)}$

Table 4.2. Eigenvalues and their geometric multiplicity (the number in brackets) for ν=0.

This information allows identifying the number of eigenspaces that each stiffness matrix uses to define the space **U** and their dimension. In any case, the sum of all of them is 24 which is the dimension of the space of **U**.

In particular, the FEM that corresponds to ν=0 has 6 eigenspaces while the corresponding linearized MSM has 9. That is, the way in which they describe the solution is different. The reason for this is that the MSM cannot behave exactly as the linear FEM, only in an approximate way.

In particular, the shapes of the eigenmodes corresponding to the linear FEM with ν=0 are displayed in figure 4.9 except from the first eigenspace which is the one that describes the rigid body displacements. Four of these shapes have well-known physical meaning. The 2nd eigenspace describes the deformations that take place in a torsion test, the 3rd one refers to the side warping, the 4th one corresponds to bending experiments and the 6th one refers to the shapes obtained in shear tests. The fifth eigenspace does not have a simple physical interpretation.

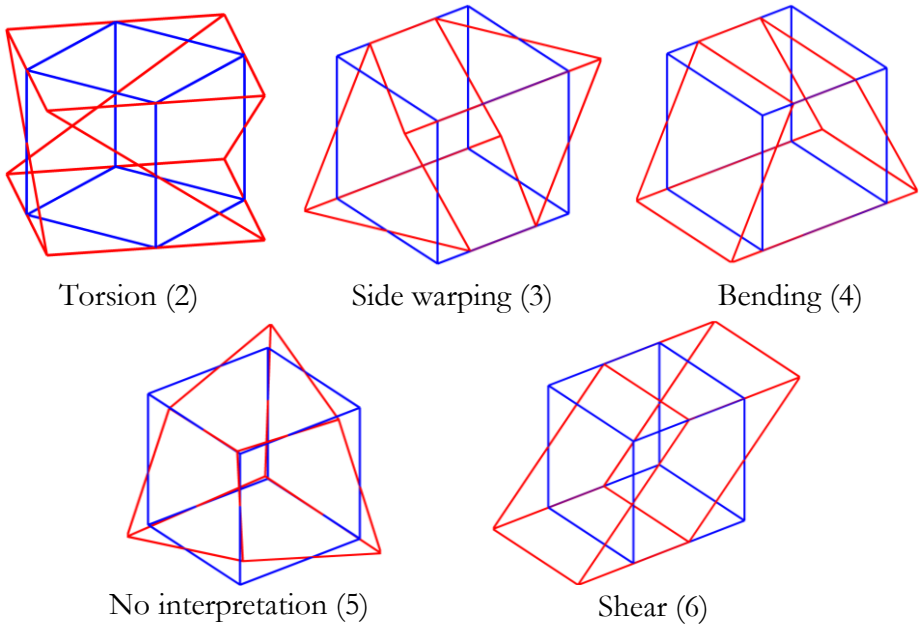

Figure 4.9. Some shapes of the eigenmodes of the linear elastic FEM when ν=0. In brackets the number that identifies the eigenspace.

The minimization strategy proposed in this chapter adjusts the parameters of the MSM in order to design a model whose modes are as similar to the modes of the FEM as possible. Depending on the quality of the obtained linearized MSM, some shapes will be the same in both models

and the others different. The eigenspaces that describe the same subspace of **U** will be considered equivalent eigenspaces.

In particular, the adjusted linearized MSM and the FEM corresponding to $\nu=0$ have three equivalent eigenspaces. Following the numbering of the eigenspaces of the FEM, these are the 1st (rigid body displacements), 2nd (torsion) and 5th (no interpretation) ones. Apart from these shapes the MSM has another six that are detailed in figure 4.10. The 5th eigenspace describes the deformations obtained in stretching experiments while the 9th one can be seen as a scaling deformation. The other four eigenspaces do not have a simple physical interpretation.

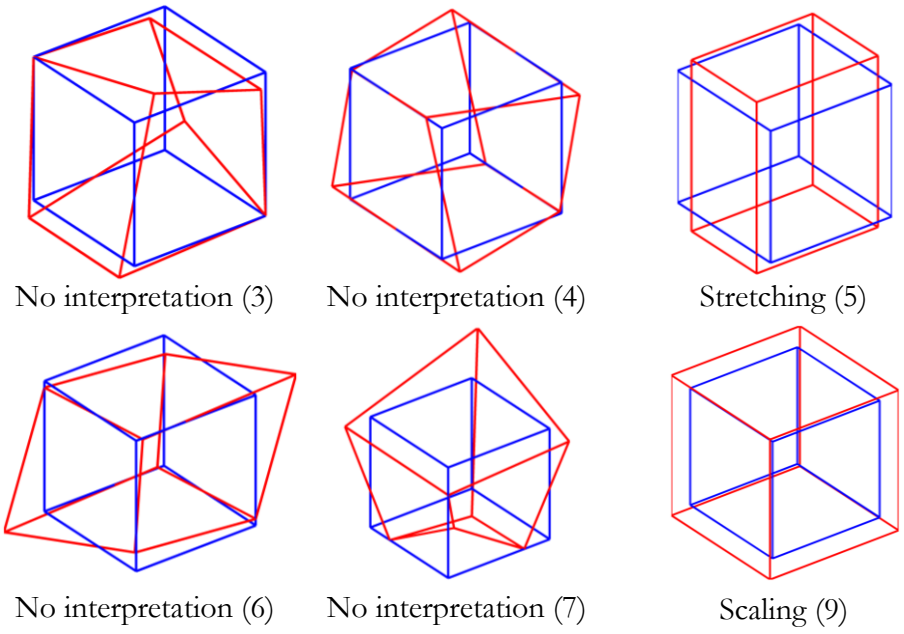

Figure 4.10. Some shapes of the eigenmodes of the linearized MSM for $\nu=0$. In brackets the number that identifies the eigenspace.

Analyzing the shapes of the eigenmodes allows identifying which are the eigenspaces that the proposed method has achieved to describe correctly. However, it does not evaluate how good the approximation of the other eigenmodes is. In other words, the similarities between the eigenspaces of both systems and the coupling of their eigenspaces are not still quantified.

4.2.2.2 Projection of the eigenvectors

With the aim of evaluating the quality of the approximation of the derived MSM, each eigenvector of the linearized MSM is projected onto each eigenvector of the linear FEM. This allows completing the information provided by the identification of the modes made in the previous section and checking whether the eigenspaces of both systems describe similar shapes or not.

If an eigenvector of the linearized MSM has projection only onto a single eigenvector of the FEM then both eigenvectors are collinear. In turn, if it has projections onto a set of multiple eigenvectors it is a linear combination of those eigenvectors of the FEM. In this way it is possible to study the level of coupling between the different eigenspaces of the FEM and the linearized MSM.

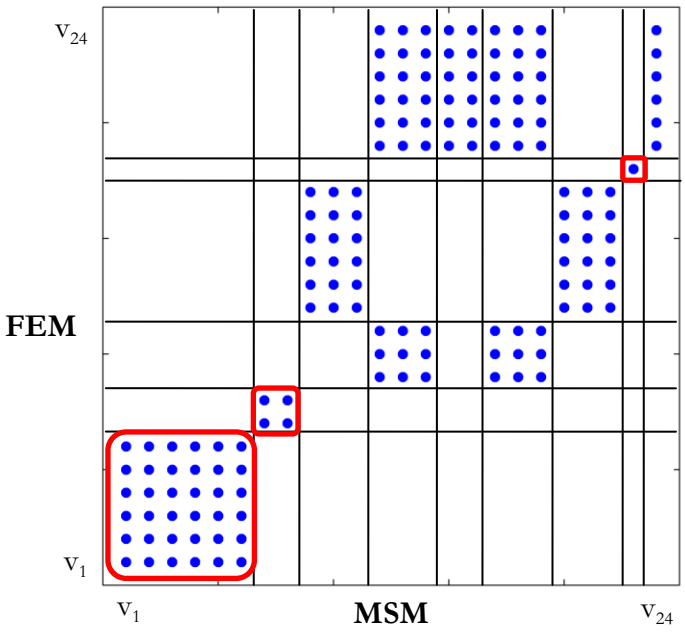

Figure 4.11. Projection of the eigenvector of $\mathbf{K}^{MSM}$ on the eigenvectors of $\mathbf{K}^{FEM}$ for the case of ν=0. The horizontal axis refers to the eigenvectors of the $\mathbf{K}^{MSM}$ while the vertical axis refers to the ones of FEM. Both axes are ordered in increasing value of their respective eigenvalues. Red blocks refer to equivalent subspaces.

The projections of some eigenvectors onto the others are represented graphically using a dot diagram. In particular, the data relative to the

projections of the eigenvectors for the case of ν=0 is represented in figure 4.11. The horizontal axis refers to the eigenvectors of the linearized MSM while the vertical axis refers to the eigenvectors of the FEM. Both axes are ordered in increasing value of the respective eigenvalues. In this diagram, each dot indicates that the corresponding eigenvector of the FEM and the linearized MSM have a projection different to 0, that is, they are not orthogonal to one another.

4.2.2.3 Identifying equivalent eigenspaces

The key idea to identify the equivalent eigenspaces using the projection techniques is the fact that any linear combination of the eigenvectors belonging to an eigenspace is also an eigenvector of the system and belongs to same eigenspace. Therefore, if an eigenvector of the linearized MSM has projections only onto the set of eigenvectors of a specific eigenspace of the FEM then, this vector is also an eigenvector of the FEM. When this happens to all the eigenvectors of a particular eigenspace then this eigenspace is equivalent in both models.

In figure 4.11, the vertical and horizontal lines delimitate the eigenspaces of the $\mathbf{K}^{MSM}$ and the ones of the $\mathbf{K}^{FEM}$ respectively. In the particular case of ν=0, there are three equivalent eigenspaces in both systems. These eigenspaces have the particularity that the eigenvectors of $\mathbf{K}^{MSM}$ have projections only on the eigenvectors of certain eigenspace of $\mathbf{K}^{FEM}$, but are orthogonal to the rest of the eigenspaces. The following equivalent eigenspaces can be identified in figure 4.11: a 6-dimensional eigenspace that corresponds to rigid body movements, a two-dimensional space that describes torsion-like deformations and an eigenspace formed by a single eigenvector with simple physical interpretation.

On the other hand, the 4th eigenspace of the FEM is coupled with two eigenspaces of the linearized FEM. The shapes are equivalent in both models since they are orthogonal to the rest of the eigenspaces. That is, six eigenvectors of the FEM form an equivalent basis to six eigenvectors of the linearized MSM. However, the two eigenspaces corresponding to $\mathbf{K}^{MSM}$ have associated different eigenvalues. This makes them not to be exactly equivalent eigenspaces.

The remaining eigenspaces of $\mathbf{K}^{FEM}$ do not have an equivalent eigenspace in $\mathbf{K}^{MSM}$. The third eigenspace of $\mathbf{K}^{FEM}$ which has dimension 3 for example, is coupled with two eigenspaces of $\mathbf{K}^{MSM}$ (4th and 6th) that

contain 6 eigenvectors. In the case of the FEM, a force applied in a certain direction contained in the third eigenspace of $\mathbf{K}^{FEM}$ causes a deformation in the same direction. In turn, this force causes a force in a different direction when applied to the MSM.

The information regarding the equivalent eigenspaces was correctly obtained in the identification of the shapes made in section 4.2.2.1. However, the projection method allows in addition to indentify fairly equivalent eigenspaces and the level of coupling between the shapes that are not equivalent.

4.2.2.4 Obtaining the optimum Poisson's ratio

In the case of a linearized MSM totally equal to a linear elastic FEM, all the eigenspaces of the $\mathbf{K}^{FEM}$ would have their equivalent ones in the $\mathbf{K}^{MSM}$ and the corresponding eigenvalues would be the same. In such case, the dot diagram would have a diagonal shape. This distribution of the projections of the eigenspaces in the diagram can be used to measure how far from the ideal stiffness matrix the obtained MSM is.

In this thesis, it is proposed to measure the quality of the approximation by calculating the distance between the equivalent subspaces and their ideal position in the diagram. To this end a new metric h is defined based on the dot diagram (see equation 4.25). In particular, this magnitude weights these distances by giving more importance to the eigenspaces whose eigenvalue is greater:

$$h = \sum_{i=1}^{N} \frac{i}{N} \frac{1}{d_i + 1} \qquad 4.25$$

N is the total number of eigenspaces of $\mathbf{K}^{FEM}$ while d_i is the number of eigenvectors that separates a given equivalent eigenspace from its ideal position in the diagram. When an eigenspace corresponds exactly to the ideal case then the distance is 0; for this reason, using d_i+1 as the measure of the distance is proposed. An example of this metric is given in figure 4.12 for the case of ν=0.

In order to indentify the best approximation it is necessary to apply this technique to the whole range of Poisson's ratios described in table 4.1. The dot diagrams corresponding to the different ν values are displayed in appendix A.

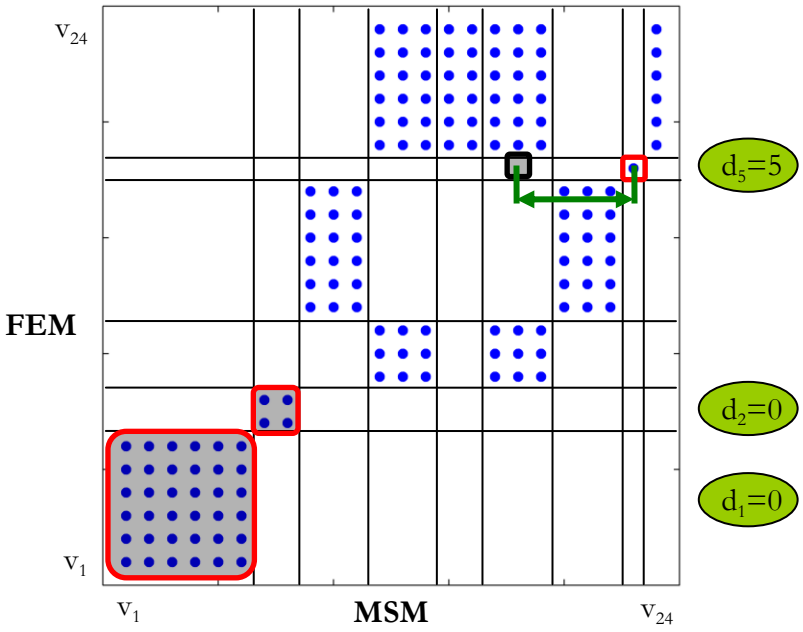

Figure 4.12. Distance between equivalent eigenspaces and their ideal positions for ν=0.

Table 4.3 contains the metric computed using these diagrams for each linearized MSM depending on the Poisson's ratio.

ν	0.00	0.05	0.10	0.15	0.20	0.25	0.30	0.35	0.40	0.45	0.49
h	**0.64**	1.73	1.73	1.73	1.72	1.72	1.65	**2.01**	1.74	1.97	1.97

Table 4.3. Quantification of the quality of the approximation for the different values of ν.

From the eigenspace projection point of view, ν=0.35 leads to the best approximation of the model while ν=0 corresponds to the worst one. This conclusion reasserts the observations made in section 4.2.1 where the best Poisson's ratio was suggested to be the one that could approximate better the axial response in the uniaxial tensile test.

4.2.2.5 Additional comments

One remarkable issue is that all the obtained MSMs have the two eigenspaces that correspond to the smallest eigenvalues equivalent. Those eigenspaces define pure translations and rotations and torsion deformations.

In addition, except for the case of Poisson's ratio 0, all the MSMs share the same last eigenspace. This is one-dimensional eigenspace and corresponds to the largest eigenvalue. That is, the response of the model in the direction of the eigenvector that defines this subspace has the largest gain. The effect of exciting the cube in the direction of this eigenvector is equivalent to scaling the model (see figure 4.10).

Apart from these common equivalent eigenspaces, other three eigenspaces appear in most of the equivalence analyses. Two of them are three-dimensional whereas the other one needs only an eigenvector to define the eigenspace. However, their distribution in the graph of projections is different and in some cases they even do not appear. Using the magnitude *h* makes it easier to identify the best approximation.

Finally, it is important to stress the idea that the three ways proposed to analyze the quality of the approximation (uniaxial tensile test, residual error and eigenproblem study) are complementary. The information they provide helps to better understanding the behaviour of the obtained MSMs and identifying the most suitable value of Poisson's ratio.

4.3 EXPERIMENTS

The study of the MSM derived from linear elastic FEM that has been performed in the previous section was focused on the evaluation of a single cubical element. However, it is necessary to test multi-element bodies in order to validate the method proposed in this thesis. In addition, the eigenproblem analysis refers to the study of the linearized MSM which is only valid around the rest state and does not provide information about the behaviour of the model for larger deformations.

For these reasons, it is necessary to study different deformation states of a more realistic MSM with multiple elements to make a complete evaluation of the model. In particular, six tests that consider axial, shear and torsion forces have been chosen to evaluate the performance of the MSM.

4.3.1 DESIGN OF THE CUBICAL MSM

The model selected for the simulations is a cube with 10x10x10 elements (1 mm^3 each). Concerning its mechanical properties, the proposed method to design MSMs is able to provide stiffness coefficients for any value of Young's modulus and Poisson's ratio. Therefore, the validation is made using different material models.

In particular, the reference material model is described by a Young's modulus of 300 KPa and different Poisson's ratios, detailed in table 4.1. This will make it possible to identify the Poisson's ratio that provides the most accurate results and assess the conclusions of sections 4.2.1 and 4.2.2. Additionally, ν=0.49 will help studying the quasi-incompressible condition which is a frequent assumption in living tissue modelling.

The considered hexahedral mesh is composed by a collection of interconnected cubes. In this mesh there are different kinds of neighbour conditions since the assembly of cubes involves merging faces and edges. When two cubes share a face, both of them are contributing to the stiffness of that face, which means that the values of k_e and k_f of both cubes have to be added. If the merging process involves sharing just an edge then k_e will be added but not k_f. The same idea is behind the assembly of matrices in FEM. Some generic examples of cube assemblies are shown in figure 4.13. The assembly of the multielement model used for the simulations is built by following these rules of stiffness contribution.

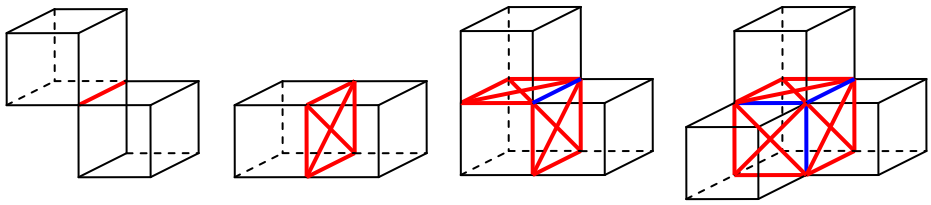

Figure 4.13. Four examples of multiple contributions to the spring stiffness due to cube assembling. In red, springs whose stiffness is the sum of two values. In blue the case in which three springs are involved.

4.3.2 DESCRIPTION OF THE EXPERIMENTS

The proposed experiments are divided into two sets of three tests. The first set of experiments is specifically designed to produce small deformations while the second, in turn, large deformations. The only difference between both sets is the amount of force applied but in both cases, the force configuration is the same. In this way, the MSM can be evaluated for small deformations (around the linearization point) as well as large deformations (farther from the rest state). Independently of the deformation amount, these simulations are calculated using the nonlinear equations (see equation 4.8).

Following the typical experiments performed in material science these tests are focused on tensile, shear and torsion forces where the bottom faces (z_0=0) are fixed (see figure 4.14):

- **Test 1**: each node belonging to the top face is subject to a vertical force $\mathbf{F}_{Ai}$. The total force acting over the face is 121 times $\mathbf{F}_{Ai}$.
- **Test 2**: each node belonging to the top face is subject to a horizontal force $\mathbf{F}_{Si}$. The total force acting over the face is 121 times $\mathbf{F}_{Si}$.
- **Test 3**: each node belonging to the edges of the top face is subject to forces that cause an anti-clockwise moment with respect to the z axis. The force applied on each edge is $11\mathbf{F}_{Ti}$. In the vertices exists the combined effect of the two corresponding edges.

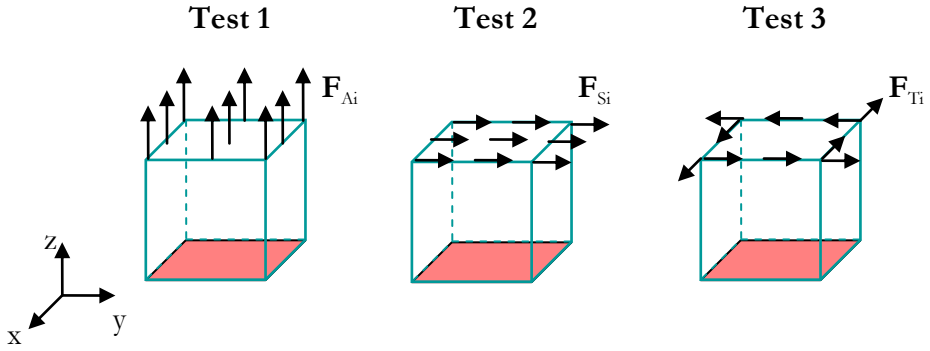

Figure 4.14. Description of the three tests used in the validation of the MSM. The bottom face is kept fixed and the forces act on the top face (tests 1 and 2) or top edges (test 3).

The particular values of the forces that are applied in the different tests are detailed in table 4.4.

	Test 1 ($\mathbf{F}_{Ai}$)	**Test 2 ($\mathbf{F}_{Si}$)**	**Test 3 ($\mathbf{F}_{Ti}$)**
Small deformations	10	2	5
Large deformations	50	10	25

Table 4.4. Nodal forces of the different experiments given in $x10^{-3}$ N.

4.3.3 EXAMPLE OF SIMULATIONS

In this section the results of the simulations are presented, with the aim of explaining the validation strategy and proposing measurements to evaluate the quality of the performance of the MSM. In addition, the range of deformations caused by the two sets of experiments will justify the value of the forces detailed in table 4.4.

In particular, from the available Poisson's ratios, the value of 0.25 is chosen for the six experiments. Based on the results obtained in section 4.2, the stiffness constants of a MSM derived from the linear elastic material model with L=1 mm, E=300 KPa and ν=0.25 are:

$$\begin{aligned} k_e &= 25\,N/m \\ k_f &= 36\,N/m \\ k_d &= 23\,N/m \end{aligned} \qquad 4.26$$

The behaviour of this MSM in the six experiments is compared with the results obtained with the *Abaqus*[1], software for finite element analysis, using a linear elastic FEM with E=300 KPa and ν=0.25.

In order to better compare these results, the corresponding final deformed states of the MSM and the FEM are displayed in superimposed images in figure 4.15. The visual comparison of the results of the MSM with the FEM simulations gives a qualitative idea of the accuracy of the obtained deformations for the particular case of ν=0.25.

In the three tests corresponding to small deformations, the displacements of the MSM nodes are larger than the FEM. This means that, in the case of ν=0.25, the obtained MSM behaves softer than the reference model. This characteristic is coherent with the stress-strain curves of tensile experiment performed with a single element (see figure 4.6), the cube showed to be softer for ν below 0.35.

In any case, these simulations show that the general behaviour of the proposed MSM is quite similar to the performance of the FEM in both small and large deformations. However, it is necessary to make a quantitative measurement of the error in order to evaluate more precisely the quality of the designed model.

[1] http://www.simulia.com/products/abaqus_fea.html

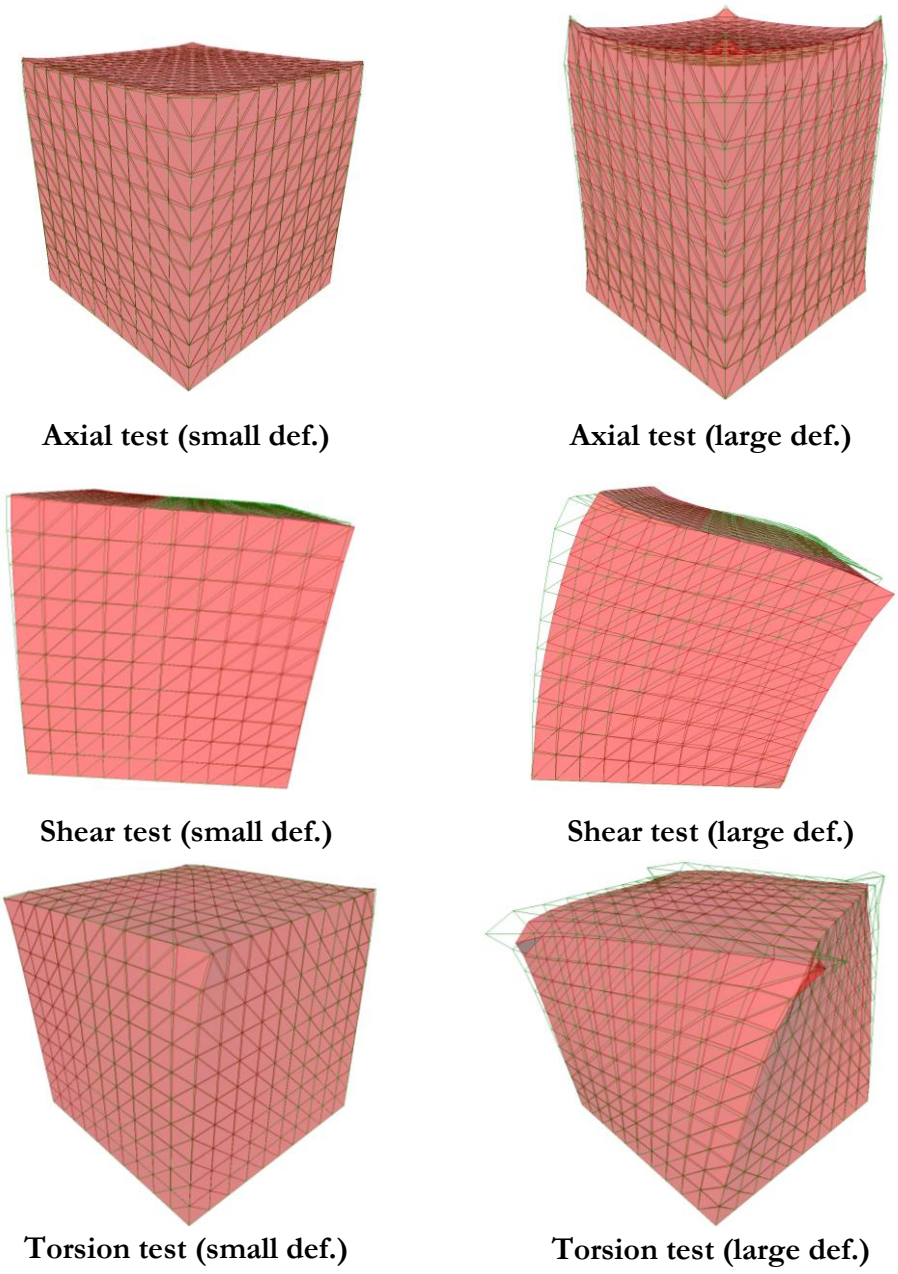

Figure 4.15. Simulation of deformable bodies using MSM, red mesh, and FEM, green wire-frame (E=300 KPa, ν=0.25). Left column small deformations and right column large deformations. From top to bottom: axial, shear and torsion tests (details in figure 4.14).

4.3.4 ERROR MEASUREMENT

One way to make the quantitative evaluation of the quality of the simulations is to define some representative measurements and compute their error with respect to the FEM results.

In the case of the tensile test the height of two particular nodes of the top face is studied: L_1 and L_2. These are the z coordinates of the centre node and a vertex of the top face respectively (see figure 4.16).

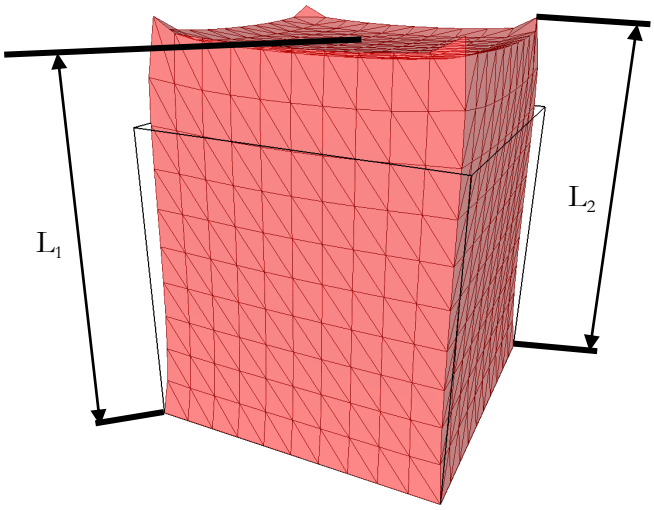

Figure 4.16. Magnitudes selected to measure the error in the axial tensile test. L_1 stands for the centre node in the top face while L_2 corresponds to any vertex of the top face.

The second test corresponds to a shear test, and therefore, in this case the most representative measurements are the angles of the left (α_1) and right (α_2) faces. These angles are measured considering the rotation of the vertices of the top face with respect to the analogous vertex of the bottom face (see figure 4.17).

In the case of the torsion test, the most meaningful measurement is the rotation of the top face. Therefore, the angle described by two nodes is proposed: the rotation of the middle node of an edge of the top face (β_1) and the rotation of a vertex of the top face (β_2). Both angles correspond to the rotation of the segment that connects them to the centre of the top face (see figure 4.18).

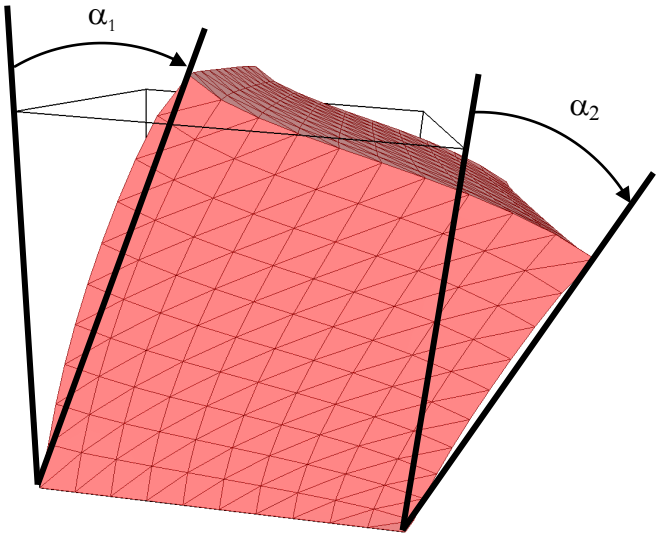

Figure 4.17. Measurement of the error in the shear test.

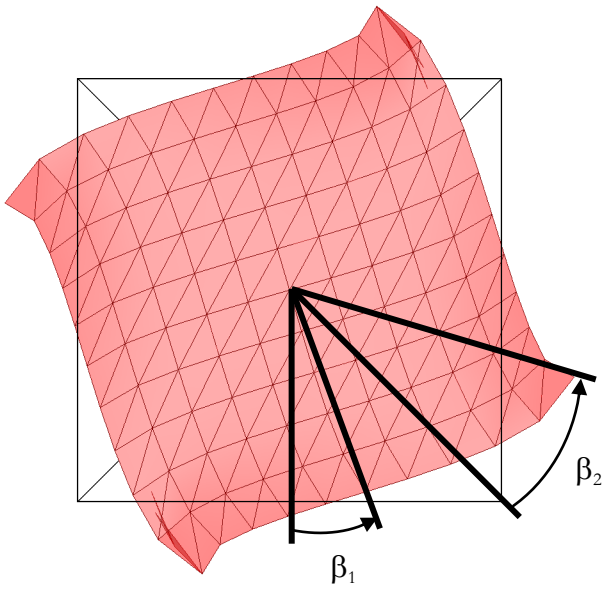

Figure 4.18. Measurement of the error in the torsion test.

In order to evaluate the accuracy of the simulations performed with the MSM the relative errors (r) of these measurements (m) with respect to the results obtained with the FEM are calculated:

$$r = \frac{m_{MSM} - m_{FEM}}{m_{FEM}} \times 100\% \qquad 4.27$$

As the experiments have been divided into two sets regarding the resulting displacements, the study is divided in two cases attending to this distinction: small and large deformations.

4.3.5 ACCURACY OF THE MSM UNDER SMALL DEFORMATIONS

Table 4.5 shows the errors obtained in the simulation of the three tests corresponding to small deformations. In this case the minimum error belongs to MSMs obtained from ν=0.3 and ν=0.35. For these values the best results are obtained for the axial experiment where the error is below 0.6% while shear tests have an error up to 12%. Torsion tests for ν=0.3 and 0.35 show errors below 6% except for the rotation of the vertex node for ν=0.35 whose error is around 22%. Note that for the same experiment the error of the middle point of the edge of the top face is 1.5% for ν=0.35.

	Poisson's ratio				
	0.20	**0.25**	**0.30**	**0.35**	**0.49**
L_1 (axial)	1.25%	0.97%	0.59%	**0.05%**	-3.02%
L_2 (axial)	1.30%	0.85%	**0.26%**	-0.57%	-5.29%
α_1 (shear)	34.16%	24.83%	11.52%	**-4.91%**	-90.14%
α_2 (shear)	32.95%	21.54%	9.89%	**-6.67%**	-90.58%
β_1 (torsion)	4.13%	2.76%	**0.97%**	-1.54%	-19.91%
β_2 (torsion)	21.84%	8.00%	**-5.63%**	-22.28%	-92.98%

Table 4.5. Relative errors for different experiments and Poisson's ratios under small deformations.

The results of the experiments performed with ν=0.2 are less accurate, reaching the shear test errors values around 33%. The errors

corresponding to the axial test are around 1.25%. In the case of the torsion test the error of the vertex for ν=0.2 and 0.35 is similar.

Analyzing the magnitude of the errors and the corresponding sign it can be seen that they are totally consistent with the analysis made in sections 4.2.1 and 4.2.2 about the Poisson's ratio sensibility. That is, for MSMs obtained for ν below 0.35 the resulting model gets softer than the reference FEM as the Poisson's ratio decreases. For material models close to incompressibility the method becomes much stiffer and very inaccurate in the case of shear and torsion tests.

These results highlight the importance of analyzing also the eigenproblem instead of focusing just on the residual value of the minimization. As it was concluded in that analysis, the best design was expected for Poisson ratios around 0.35.

4.3.6 ACCURACY OF THE MSM UNDER LARGE DEFORMATIONS

Table 4.6 displays the relative errors corresponding to the large deformation tests.

	Poisson's ratio				
	0.20	**0.25**	**0.30**	**0.35**	**0.49**
L_1 (axial)	**0.36%**	3.22%	-2.59%	-4.95%	-12.48%
L_2 (axial)	-1.48%	**-1.02%**	-7.94%	-12.01%	-20.97%
α_1 (shear)	38.02%	28.62%	16.69%	**0.69%**	-89.64%
α_2 (shear)	32.77%	22.30%	9.34%	**-7.40%**	-90.95%
β_1 (torsion)	2.50%	0.95%	**-0.68%**	-2.77%	-12.46%
β_2 (torsion)	9.99%	**-0.01%**	-7.95%	-24.20%	-92.23%

Table 4.6. Relative errors for different experiments and Poisson's ratios under large deformations.

As deformations increase the MSM becomes stiffer and under large deformations the errors vary with respect to the case of small deformations. This effect is reasonable taking into account that MSMs are nonlinear models. For axial tests the minimum errors are achieved with ν=0.2 and 0.25 while in the case of shear experiments ν=0.35 is more accurate. The MSM obtained for ν=0.25 and 0.30 perform better in torsion tests. These values have to be taken carefully because they are based on large deformations, that is, far from the linearization point.

Considering the general performance in the proposed simulations it can be concluded that the MSM derived from ν=0.35 behaves more accurately than the other models. Except from the angle that corresponds to the vertex in the torsion test it shows a relative error below 7% for small deformations and below 12.5% for large deformations.

4.3.7 QUASI-INCOMPRESSIBLE MATERIAL MODEL

Under small and large deformations the approximation of the MSM when the reference material model is quasi-incompressible is not accurate. In this section it is proposed to analyze whether the optimal value of Poisson's ratio can be a better choice. Therefore, ν=0.35 will be taken as input parameter to model nearly incompressible materials.

	Small deformations	**Large deformations**
L_1 (axial)	0.18%	0.57%
L_2 (axial)	-0.44%	-4.46%
α_1 (shear)	-2.93%	-2.94%
α_2 (shear)	-5.57%	-6.90%
β_1 (torsion)	-1.89%	-3.84%
β_2 (torsion)	-28.65%	-28.65%

Table 4.7. Errors of the MSM obtained from ν=0.35 with respect to incompressible FEM.

Table 4.7 displays the relative errors of the MSM, with parameters E=300 KPa and ν=0.35, when compared to the behaviour of a linear elastic FEM with E=300 KPa and ν=0.49.

These tensile, shear and torsion experiments show that the MSM derived from ν=0.35 simulates accurately the behaviour of a nearly incompressible material. Independently of the range of deformations, it shows a relative error below 7%, except from the measure of the angle that corresponds to the vertex in the torsion test. In this case the error is around 30%.

These errors are clearly below the results obtained for a MSM derived from ν=0.49. Therefore, for simulating incompressible material models it is recommended to adopt the MSM derived from ν=0.35.

4.4 DISCUSSION

Given a pair of reference values (E, ν) that define a linear elastic material model the method proposed calculates the stiffness coefficients of a MSM that approximates its behaviour. As the quality of the simulations is influenced by the Poisson's ratio it is necessary to discuss the outcome of the analyses presented above: uniaxial tensile tests, residual error of the minimization, eigenvalue and eigenvector analysis and multi-element experiments.

The MSM was subject to a uniaxial tensile test in order to evaluate how accurately it approximates the parameters of the reference FEM. This allows obtaining the equivalent Young's modulus (E_{MSM}) and Poisson's ratio (ν_{MSM}) of the discrete model. The results show that the input parameter ν influences the values of E_{MSM} and ν_{MSM}, while E only influences E_{MSM}. In addition, independently of the value of the reference ν, the resulting ν_{MSM} is always ranged between 0.25 and 0.30. As the influence of ν over E_{MSM} is high, it is more important to obtain accurate values of E_{MSM} instead of trying to approximate ν_{MSM}. In particular, Young's modulus is accurately described when the reference material model has a Poisson's ratio around 0.35.

From the point of view of the residual error of the minimization process, the smallest error corresponds to ν=0.2 which has been shown to

be less accurate in the tensile test than when using ν=0.35. Specifically, it behaves 32% softer than the reference model.

On the other hand, the eigenproblem study also indicates that ν=0.35 should provide more accurate MSMs because their equivalent eigenspaces are closer to their ideal position in the eigenvector projection graph. For this value, only two of the eight eigenspaces of the FEM have no equivalent eigenspace in the stiffness matrices of the linearized MSM.

Consequently, uniaxial tensile tests and eigenproblem analysis conclude that the optimum value is ν=0.35 while the residual error determines that it should be ν=0.20. This discrepancy is solved with the experiments performed using multi-element bodies. They assert that ν=0.35 is the most accurate value.

4.5 CONCLUSIONS

In this chapter a new method to derive cubical MSMs from linear elastic FEM has been proposed. The main characteristics of this method are:

- Given any value for the input parameters Young's modulus and Poisson's ratio, the method proposed provides the stiffness coefficients needed to build a cubical MSM that approximates that behaviour.

- Although the method provides MSMs for any linear elastic FEM the quality of the approximation depends on ν. That is, in practice, the usefulness of the method is limited to some specific values of ν. In particular, the most accurate results correspond to the range between 0.30 and 0.35.

- Below ν=0.35 the obtained MSM behaves softer than the reference FEM while above this value the model becomes stiffer.

- The value of E does not influence the quality of the model since the stiffness coefficients of the MSM are proportional to this parameter.

- The proposed method is based on the study of the MSM around the initial rest position. Therefore, it is valid for small deformations. As deformations increase the difference between the MSM and the FEM increases.

- Under small deformations, the MSM obtained from ν=0.35 is the most accurate one. In five of the six results obtained in tensile, shear and torsion experiments the relative error is below 7%.

- Under large deformations ν=0.30 is the optimum value. In this case, the relative error is below 17% in the six results compared.

- The optimum value of ν has been correctly predicted by the tensile test analysis and the eigenproblem study. However, focusing only on the analysis of the residual error of the minimization can lead to wrong interpretations.

- Although incompressible materials are out of the range of useful Poisson's ratios, it is possible to use the MSM obtained from ν=0.35 to represent the incompressible behaviour. Experiments show that this value gives accurate simulations. Independently of the range of deformations, the relative errors of five of the six results compared are bellow 7%.

- The three ways proposed to analyze the quality of the approximation (uniaxial tensile test, residual error and eigenproblem study) are complementary and help to better understand the behaviour of the obtained MSM.

The main conclusion reached in this chapter is that discrete nonlinear models such as cubical MSMs are able to approximate quite accurately the behaviour of linear elastic FEM with any value of Young's modulus and a Poisson's ratio between 0.30 and 0.35. When the material model is nearly incompressible adopting ν=0.35 provides also good results.

CHAPTER 5

MSM DESIGN FROM HYPERELASTIC MATERIAL MODELS

In the previous chapter a new method to derive cubical MSMs from linear elastic FEM has been proposed. Considering biological soft tissues, however, a linear elastic material is an assumption that usually is valid only for small deformations. When deformations are large, the behaviour of these materials generally becomes nonlinear. Taking advantage of the nonlinear behaviour of MSMs, the main objective of this chapter is to study the possibility of building a cubical MSM that behaves like the nonlinear elastic material models used in soft-tissue simulation.

The bibliographic review presented in chapter 3 shows that there is no analytical method for obtaining a cubical MSM based on nonlinear material models. The closest study belongs to Delingette (Delingette2008) who proposed a discrete model to simulate nonlinear membranes. This lack of methods opens a challenging field that is tackled in this chapter.

The MSM designs described in section 3.1 focus their attention on the continuum, either, using the results of their simulations as reference data or taking their mathematical formulation as the starting point for analytical derivations. Following such a continuum-based methodology without analyzing previously the behaviour of MSMs can lead to two basic problems: unreasonable approximations and high complexity.

The first problem refers to the enforcement of an unnatural behaviour. That is, if cubical MSMs have a response that is totally different from some reference data obtained from FEM simulations it makes no sense to search for the parameters that best approximate its behaviour, because the quality of the approximation will never be good. Thus, it is necessary to analyze first if the model has the capability of describing the desired behaviour and then, adjust the coefficients to obtain a model as accurate as possible, within the limits of the model.

The second problem is related to the complexity of the model. Delingette (Delingette2008), for instance, proposed a discrete model equivalent to nonlinear membranes whose mathematical derivation is based on a continuum formulation. This method provides a model that contains extremely complex expressions, even though the considered elements are bi-dimensional. The consequence of this is that the obtained discrete model can lose the advantage of the computation efficiency that MSMs have over the FEM.

For these two reasons, it is proposed to change the focus from the continuum to the discrete field. In this way, it is possible to develop methods to derive cubical MSMs from material models that have similar behaviour to them. With this objective, the following sections will start studying the intrinsic behaviour of cubical MSMs and then, a new MSM design strategy that defines consistent parameters will be developed. As this method is based on the nonlinear behaviour of MSMs, from now on, it is called the *nonlinear method*.

5.1 METHOD DESCRIPTION

Let us assume a cubical MSM with edge length L_0 where the point masses are placed on the eight vertices as shown in figure 5.1.a. To ensure the maximal number of degrees of freedom and the same behaviour along the x, y, z axes the same three types of linear springs presented in section 4.1.2 are used: edge springs with stiffness k_e, face diagonal spring with stiffness k_f and internal diagonal springs with stiffness k_d. Note that adopting the same value of k for all the springs of the cubical MSM would lead to a model with less capability for approximating the behaviour of real soft tissues.

The study of the behaviour of cubical MSMs will be focused on the study of their response under uniaxial tensile loads as this is a common experiment performed to characterize living tissues (Chui2004, Hu2004,

Martins2006, Zhong2007, Kim2008, Ma2009, Brunon2010). The same experiments were adopted to evaluate the resulting MSM in the previous chapter (see section 4.2.1.1).

The z axis indicates the direction along which the tensile stress is applied and x and y axes are considered as the transversal directions. Accordingly, L_x, L_y and L_z denote the lengths of the deformed cube along the corresponding axes.

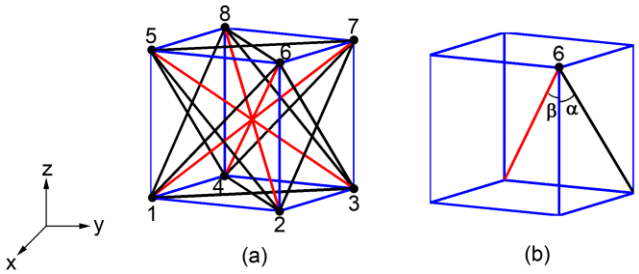

Figure 5.1. (a) The configuration of the essential MSM cube showing the point masses and springs. In blue edge springs, in black face diagonal springs and in red internal diagonal springs. (b) α defines the direction of diagonal springs contained in the lateral faces and β the direction of internal diagonal springs.

Once the cube is defined, there are many ways to characterize the mechanical properties of the MSM. Two different points of view are proposed to study its behaviour: a qualitative reasoning and a quantitative evaluation. With this aim, the MSM is tested as if it were a sample of an actual material, and the behaviour of the cube is studied by performing a uniaxial tensile test and evaluating the response in both the axial and the transversal directions.

In this situation, because of the symmetries, the deformations along the x and y axes are identical; thus, in the tensile test the two faces of the cube that are subject to the external forces keep their square shape whereas the other four faces turn into rectangles. Consequently, it is enough to study one unique node. Considering node number 6 for example, two angles can be defined to better describe the spring configuration. The first, α, is the angle between the edge in z axis and the corresponding diagonal of the face. The second, β, is the angle between the edge in z axis and the internal diagonal (see figure 5.1.b).

Although some foam materials display very complex mechanical behaviour, most common materials become thinner in cross section when the sample is stretched. Consequently, this last assumption is adopted for the description of the material deformations in the following sections.

5.1.1 QUALITATIVE STUDY OF THE BEHAVIOUR

A qualitative analysis of a single cube subject to uniaxial forces provides important information about the behaviour of cubical MSMs. The adopted approach focuses on analyzing separately the effect of each type of spring. That is, studying first the effect of edge springs and then the consequences of adding face and internal diagonal springs.

Performing a tensile test on a cube where the stiffness value k_e is positive and k_f and k_d are null produces an elongated prism whose cross-sectional faces do not change in size. However, the faces aligned with z axis deform enlarging L_z (see figure 5.2.a). Indeed, the edge springs aligned with x and y axes remain in resting state, whereas, the other four springs that are aligned with the applied loads (z axis) offer a linearly proportional resistance to the elongation. In other words, the force-displacement response along the z axis is linear (see figure 5.3).

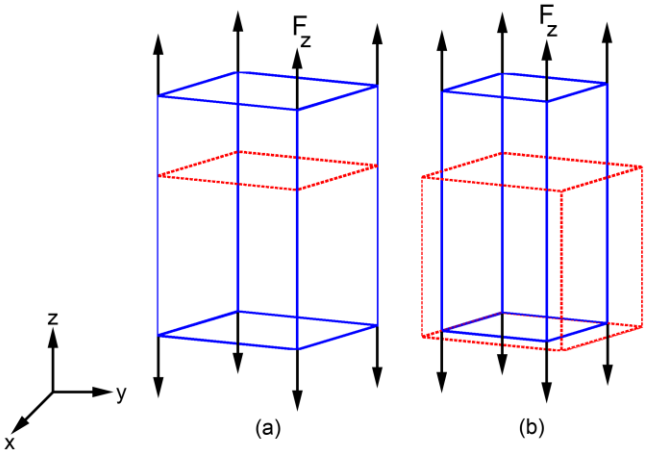

Figure 5.2. The appearance of the MSM subject to uniaxial tensile forces (a) when k_f and k_d are null and (b) when k_f or k_d are not null.

However, if k_f becomes non null, three new forces appear on each node of the MSM. Only two of them have a direct influence in the z direction since the third one is contained in the cross-sectional face. In this

configuration, the directions of the face diagonal springs that have z component change as the deformation rate is modified. That is, as L_z increases the angle α decreases (see figure 5.2.b). Additionally, under the assumptions made above, as the elongation in z axis grows the value of L_x and L_y becomes smaller, increasing the effect over α.

The direct consequence of increasing the applied force along the z axis in this situation is twofold. On the one hand, focusing the discussion on the spring between nodes 6 and node 3 for example, decreasing the value of the angle α increases the projection of the force of that spring over the z axis. On the other hand, the elongation of the cube increases the length of that spring. As the deformation grows these two characteristics add to the initial linear response of the edge springs an increasing influence of the face diagonal springs contained in axial faces. This induces a stiffening of the MSM with regards to the previous linear response. A similar analysis can be made with the internal diagonal springs.

The final effect of adding face diagonal and internal diagonal springs is that the initial linear force-elongation curve turns into a nonlinear relation at large deformations (see figure 5.3).

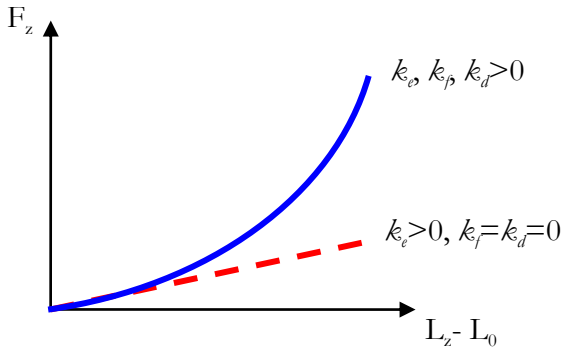

Figure 5.3. At large deformations, when kf or kd are non null, the influence of diagonal springs grows and the initial linear behaviour of the MSM turns into a nonlinear relation.

This nonlinear curve is similar to the response of living tissues presented in section 2.2 (see figure 2.3) except from the last phase where the rupture of the material occurs. As soft tissues are frequently characterized by using hyperelastic material models it is proposed to adjust the stiffness coefficients of the MSM so that they approximate the behaviour of such materials.

5.1.2 EQUILIBRIUM EQUATIONS FOR A TENSILE TEST

In an ideal uniaxial tensile test performed over a continuous medium, stress (σ) is uniformly distributed on the surface. However, when the model is made up of discrete elements as in MSMs, it is necessary to concentrate the stress in the point masses becoming punctual forces. Consequently, six spring forces and one external force ($\mathbf{F}_z$) that is equivalent to a quarter of the total theoretical force applied to a face in a continuous model act on each point mass of the cube.

Considering the symmetries of the cube and the applied forces, it is sufficient to study the equilibrium of a particular point mass as the remaining nodes are subject to identical forces. In this case, node 6 will be taken as example.

Considering equilibrium in point mass 6 and keeping in mind the existing symmetries, the resulting equation for either x axis or y axis (see equation 5.1) and the corresponding one to the z axis (see equation 5.2) can be written as follows:

$$0 = f_{(6,7)} + f_{(6,8)}\cos\frac{\pi}{4} + f_{(6,3)}\sin\alpha + f_{(6,4)}\sin\beta\cos\frac{\pi}{4} \qquad 5.1$$

$$F_z = f_{(6,2)} + f_{(6,1)}\cos\alpha + f_{(6,3)}\cos\alpha + f_{(6,4)}\cos\beta \qquad 5.2$$

Where $f_{(i,j)}$ is the module of the force made by the spring that connects nodes i with j. Taking into account the stiffness coefficients of the of the cubical MSM, these equations can be rewritten as follows:

$$\frac{L_x}{L_0} = \frac{k_e + \left(1+\sqrt{2}\sin\alpha\right)k_f + \left(\frac{\sqrt{6}\sin\beta}{2}\right)k_d}{k_e + 2k_f + k_d} \qquad 5.3$$

$$F_z = L_z\left(k_e + 2k_f + k_d\right) - L_0\left(k_e + 2\sqrt{2}k_f\cos\alpha + \sqrt{3}k_d\cos\beta\right) \qquad 5.4$$

These two equations describe the behaviour of the cubical MSM in the transversal as well as axial direction, using edge lengths and forces. However, material models used in soft-tissue simulation frequently are given by means of stress and strain magnitudes. Therefore, it is necessary to transform equations 5.3 and 5.4 in order to use these magnitudes.

Different definitions of stress and strain are used in solid mechanics. In contrast to the engineering stress and strain used in the previous chapter

(see section 4.2.1.1), here the Cauchy true stress and the logarithmic strain will be adopted. Although these magnitudes are defined for a continuum context, in a tensile test it is possible to define an equivalent relation in the discrete domain, assuming that the total applied load over a face is the sum of the external nodal forces. Consequently, the Cauchy true stress in z axis in the present tensile test may be defined as the relation between the applied load ($4F_z$) and the final cross-sectional area (L_xL_y):

$$\sigma_z = \frac{4F_z}{L_x L_y} \tag{5.5}$$

Likewise, the logarithmic strain along the i axis may be estimated as the logarithm of the relation between the final length and the original reference length:

$$\varepsilon_i = \ln \frac{L_i}{L_0} \tag{5.6}$$

The definition of the Poisson's ratio is the same as in the previous chapter (see equation 4.24).

Considering the definition of stress (see equation 5.5) and combining it with equation 5.4, the relation between the derived stress and the corresponding deformation for the particular case of a pure uniaxial tensile test results:

$$\sigma_z = \frac{4L_z}{L_x{}^2}\left(k_e + 2k_f + k_d\right) - \frac{4L_0}{L_x{}^2}\left(k_e + 2\sqrt{2}k_f \cos\alpha + \sqrt{3}k_d \cos\beta\right) \tag{5.7}$$

Finally, the logarithmic strains along the x and y axes for the pure uniaxial tensile test can be calculated by combining equations 5.3 and 5.6:

$$\varepsilon_x = \varepsilon_y = \ln\left[\frac{k_e + \left(1+\sqrt{2}\sin\alpha\right)k_f + \left(\frac{\sqrt{6}\sin\beta}{2}\right)k_d}{k_e + 2k_f + k_d}\right] \tag{5.8}$$

To define the stress-strain relation of a cubical MSM subject to tensile loads it is enough to use three of the previous relations: equations 5.6, 5.7 and 5.8. Note that this relation is clearly nonlinear and it cannot be explicitly expressed using a unique equation.

5.1.3 OBJECTIVE FUNCTION

In the previous sections it has been demonstrated that cubical MSMs have nonlinear behaviour when they are subject to tensile tests and work under large deformations. Using this kind of experiment is a common practice in the determination of the material properties of biological soft tissue and the derivation of the parameters of other models such as nonlinear FEM (Chui2004, Hu2004, Martins2006, Zhong2007, Kim2008, Ma2009).

Therefore, in this thesis it is proposed to design MSMs that approximate the behaviour of nonlinear material models focusing on uniaxial tensile tests and using the previously obtained analytical expressions of stress and strain.

Usually, material models of soft tissue are defined using constitutive equations that make it possible to obtain directly their behaviour under uniaxial tensile tests. These models provide the deformation in the axial direction caused by tensile loads and allow computing the corresponding transversal deformation through the Poisson's ratio. Similar data can be acquired performing specifically designed experiments.

This information defines two curves that describe the reference material model: stress-strain dependence in the axial direction and the transversal-axial strain relation. The proposed method is based on finding the MSM that better approximates these two reference curves. In particular, the stiffness coefficients will be obtained by adjusting the curves of the axial and transversal responses of the MSM to those reference curves. As it is expected that the curve fitting problem will hardly ever produce an exact solution a minimization strategy will be adopted to approximate it.

The stress-strain curve σ_z-ε_z of a cubical MSM subject to tensile loads can be computed using the equations 5.6, 5.7 and 5.8 presented in the previous section. The transversal-axial strain curve ε_x-ε_z, in turn, is calculated using the equations 5.6 and 5.8. Note that angles α and β relate the edge lengths of the cube.

Figure 5.4 displays the curves that the proposed method has to fit. Figure 5.4.a shows the stress-strain response of a generic MSM during a tensile test before the adjustment process and the corresponding reference data. Figure 5.4.b displays the relation between the axial and the transversal strain of the same generic MSM and the corresponding reference data. For

this example, the parameters of the generic MSM are k_e=k_f=k_d=50 N/m and L_0=1 mm.

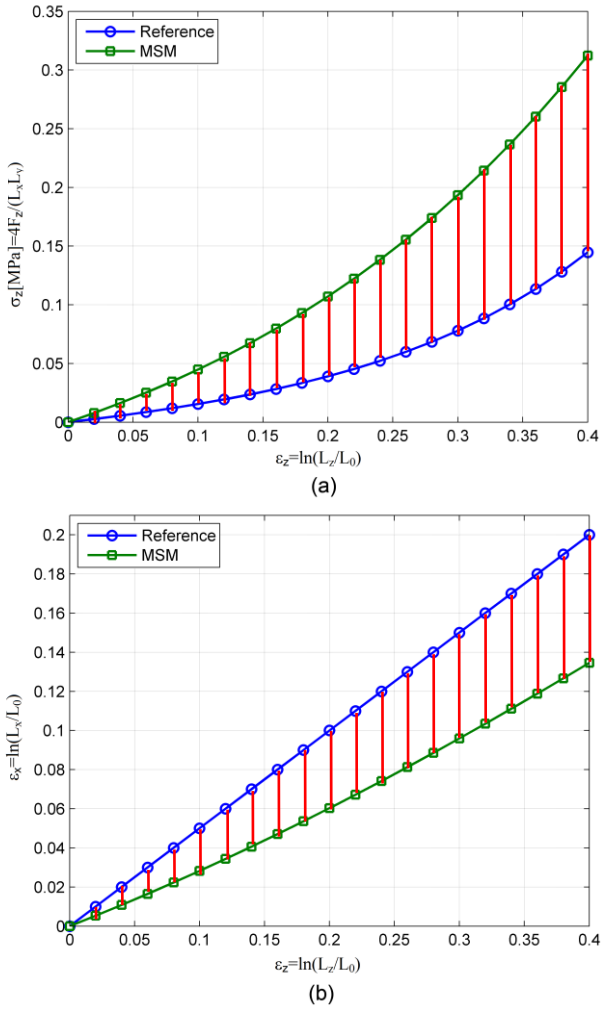

Figure 5.4. (a) The axial response of a generic MSM before the adjustment process in a tensile test and the corresponding reference data. (b) The relation between the axial and the transversal response of the same generic MSM and the corresponding reference data.

The adjustment of the stiffness coefficients of the cubical MSM is performed by minimizing an objective function ϕ that simultaneously considers the square root error of the difference between both reference curves, as described in equation 5.9.

$$\phi = \frac{\sum_{i=1}^{N}\left[\sigma_{zi}^{MSM}\left(\varepsilon_{zi},k_e,k_f,k_d\right)-\sigma_{zi}^{ref}\left(\varepsilon_{zi}\right)\right]^2}{\sum_{i=1}^{N}\left[\sigma_{zi}^{ref}\left(\varepsilon_{zi}\right)\right]^2} + \frac{\sum_{i=1}^{N}\left[\varepsilon_{xi}^{MSM}\left(\varepsilon_{zi},k_e,k_f,k_d\right)-\varepsilon_{xi}^{ref}\left(\varepsilon_{zi}\right)\right]^2}{\sum_{i=1}^{N}\left[\varepsilon_{xi}^{ref}\left(\varepsilon_{zi}\right)\right]^2} \qquad 5.9$$

The first term refers to the error associated to the stress that is required to produce a certain strain in the axial direction. The second one represents the error of the transversal strain in function of the axial strain. Both terms are normalized in order to avoid numeric problems and deal with the whole function as a dimensionless expression.

The objective function is evaluated for a set of N axial strain values, namely, ε_{zi}. The stress value and the transversal strain corresponding to these strain values are denoted by σ_{zi} and ε_{xi} respectively. The superscript *MSM* stands for Mass-Spring Model while *ref* stands for the reference model. The specific ε_{zi} values depend on the available reference data and the range in which the model is supposed to work.

The strategy proposed to obtain the stiffness parameters of the MSM is to minimize the objective function using a nonlinear least-squares technique. This minimization is made using the function *lsqnonlin* of the *Optimization Toolbox* of *Matlab*[1], a programme that allows performing computationally intensive tasks.

In this case the objective function uses only uniaxial tensile data. In the case of having information about shear and torsion tests this function could be extended with analogous terms that relate the corresponding strain and stress values.

5.2 RESULTS

The method for obtaining cubical MSMs from stress and strain reference data presented in this chapter can be applied to many different input data. As the method is going to be used for approximating living soft tissues, it is

[1] http://www.mathworks.com/products/matlab/

important to make first a general study of the potential of this model to represent such materials. In particular, if cubical MSMs are able to behave like nearly incompressible materials then it will be possible to approximate accurately the behaviour of living tissues.

5.2.1 CAPABILITY OF CUBICAL MSMS FOR MODELLING TISSUES

The qualitative study of section 5.1.1 has shown the nonlinear behaviour of cubical MSMs. However, it does not provide enough information to illustrate the capability that cubic MSMs have to describe different material models. Thus, it is necessary to analyze the capability that MSMs have to represent materials such as those in biological tissues.

As soft tissues frequently show quasi-incompressible behaviour, the following study will focus on defining the family of parameter sets that make a single cubical MSM behave in a nearly incompressible way. For this study, each spring parameter (k_e, k_f and k_d) is varied from 0 to 0.1 N/mm using increments of 0.02 N/mm. The error associated to the volume variation is described with a magnitude equivalent to the second term of the objective function ϕ (see equation 5.9) and its value is arbitrarily limited to 0.01. The behaviours of the MSMs obtained that fulfil this requirement are grouped into the family of curves displayed in figure 5.5.

Increasing the range of the stiffness values above 0.1 N/mm or decreasing the stiffness step just increases the number of curves that fulfil the condition of volume variation. Those curves would have different slope but they would maintain their nonlinear hyperelastic behaviour.

As it can be seen in figure 5.5b the slope of the transversal versus axial strain of the reference material model is 0.5 which is the value of the Poisson's ratio that corresponds to the behaviour of incompressible materials.

The numerous curves displayed in figure 5.5 demonstrate that there are many cubical MSMs that approximate quite accurately the transversal response in function of the axial one. In other words, they fulfil the condition of quasi-incompressibility and they can be appropriate to use in soft-tissue simulations.

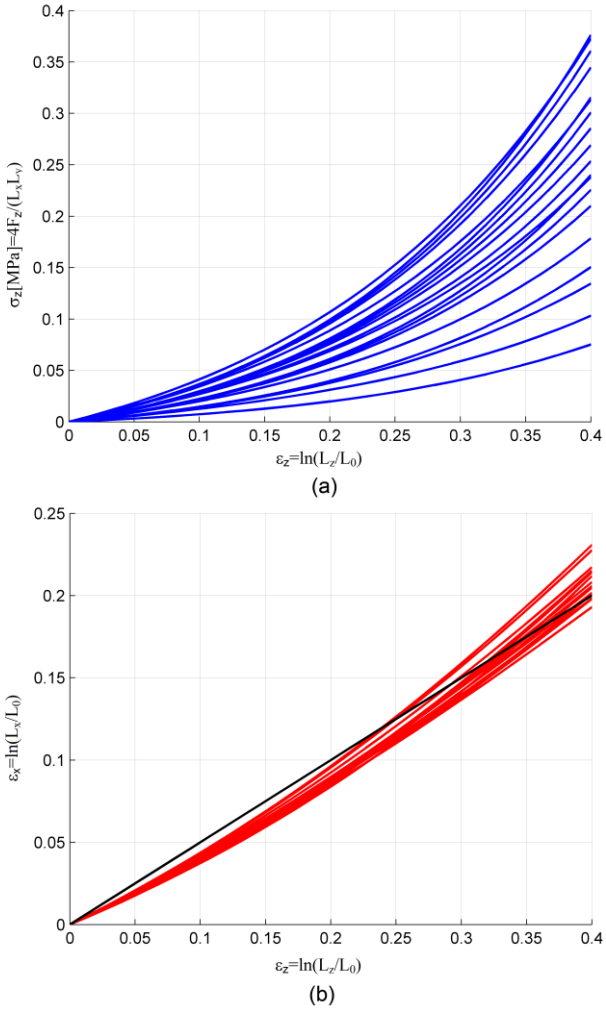

Figure 5.5. The behaviour of the parameter sets that make a MSM behave in a nearly incompressible way. The potential candidates have been evaluated from 0 to 0.1 N/mm stiffness constant using increments of 0.02 N/mm. (a) stress-strain relation and (b) the transversal against the axial response.

5.2.2 EXAMPLES OF MSM PARAMETER DERIVATIONS

As it has been shown in the previous section, many cubical MSMs with a single element can behave in a quasi-incompressible way under uniaxial deformations. Now, the objective is to find the stiffness parameters that

simultaneously fit this requirement and approximate the stress-strain response of a certain material model.

5.2.2.1 Incompressible hyperelastic material model

Martins et al. (Martins2006) studied the nonlinear mechanical behaviour of biological soft tissues under uniaxial loads and they obtained the coefficients for seven different hyperelastic material models. Among others, they studied Neo-Hookean, Mooney-Rivlin, Yeoh, and Ogden models which are some of the most frequent constitutive equations adopted in soft-tissue simulation.

In order to make an example of the method proposed to obtain cubical MSMs, the Ogden type material model is taken as reference using the particular constants values obtained by Martins et al. (Martins2006) for soft tissues (see equation 5.10).

$$\sigma_{Ogden} = \sum_{i=1}^{3} c_{2i-1}\left(\lambda^{c_{2i}} - \lambda^{-c_{2i}/2}\right) \qquad 5.10$$

where σ denotes the Cauchy true stress, λ the axial stretch, and c_i the constant coefficients with the following values: $c_1 = c_3 = c_5 = 0.005044$ and $c_2 = c_4 = c_6 = 5.7255$. As stated in their assumptions (Martins2006), this model is obtained considering a homogeneous, isotropic, and incompressible sample of soft tissue.

The constitutive equation and the property of incompressibility are not enough for the minimization process that calculates the MSM that approximates the desired hyperelastic behaviour. It is also necessary to define the range of strain values in which the material model is valid.

In the work of Martins et al. (Martins2006), the range of valid strain values is not specified. From the figures included, it can be assumed that their model behaves accurately, at least, for stretch values between 1 and 1.5. Considering the relation between stretch and true strain (see equation 5.11), this Ogden material model is valid, at least, for strain values between 0 and 0.4.

$$\varepsilon = \ln \lambda \qquad 5.11$$

In order to compute the objective function of the minimization process (see equation 5.9), the range of strain values has been divided into 20 values of ε_{zi}. These strain values allow obtaining L_z using equation 5.6.

Then, L_x can be calculated with equation 5.8. Note that the angles α and β are related with L_x and L_z. With all these values the stress magnitude is determined by equation 5.7 and both curves can be obtained.

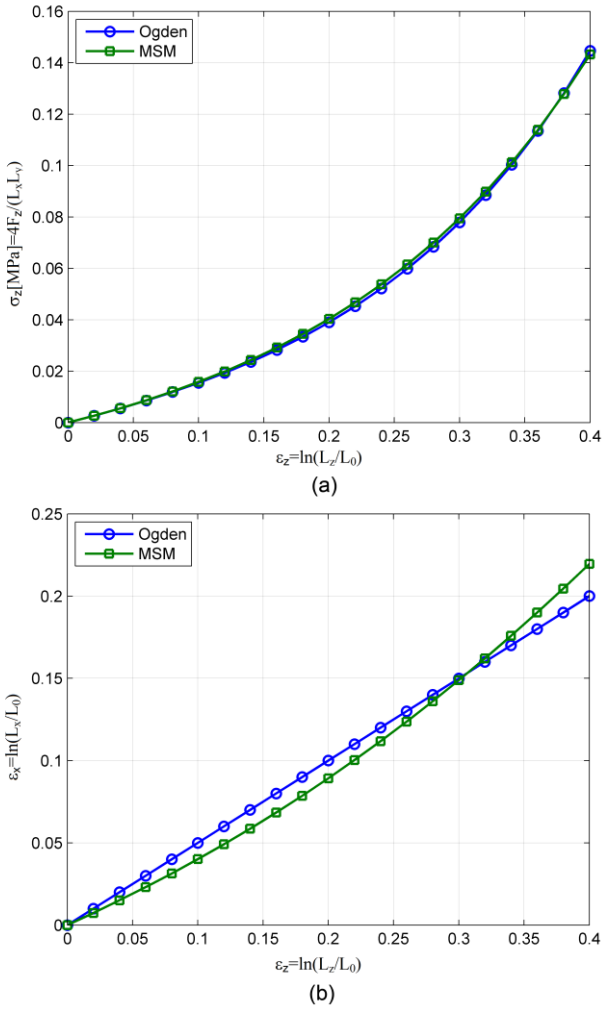

Figure 5.6. Example of curve fitting method using as reference the Ogden model proposed by Martins et al. (Martins2006). (a) Stress-strain curves and (b) the strain relation between axial and transversal direction.

The curve fitting method based on fixing a set of strain values gives the following stiffness values (in N/mm) for the case of a cube with edges 1 mm long:

$$k_e = 14\ N/m$$
$$k_f = 17\ N/m \quad (5.12)$$
$$k_d = 63\ N/m$$

The curves of stress-strain and axial strain against transversal strain of the obtained MSM and the corresponding reference data are shown in figure 5.6. As it can be seen in figure 5.6.b the slope of the transversal versus axial strain of the reference material model is 0.5 which is the value of Poisson's ratio that corresponds to incompressibility.

5.2.2.2 Incompressible linear elastic material model

In addition to the hyperelastic case, and even though MSMs have been shown to behave in a nonlinear way when subject to large tensile deformations, it is also possible to find MSMs equivalent to linear elastic materials working under small deformations. The procedure is the same, except for the fact that the reference data in this case has to be linear. As an example, a MSM equivalent to a linear elastic material model with E=0.3MPa has been calculated. In this case, the stress-strain relation is defined as:

$$\sigma_z = E\varepsilon_z \quad (5.13)$$

Additionally, the condition of incompressibility of the reference data has been defined by giving a value of 0.5 to the Poisson's ratio. That is, the slope of the curve that represents the relation between the transversal and axial strains is 0.5 (see figure 5.7.b).

The curve fitting method gives the following stiffness values (in N/mm) for the case of a cube with edges 1 mm long:

$$k_e = 23\ N/m$$
$$k_f = 43\ N/m \quad (5.14)$$
$$k_d = 509\ N/m$$

In contrast to the previous example, there is not a specific range of strain values in which the reference material model is valid. As the linear elastic behaviour is suitable for small deformations in this case the maximum strain is limited to a value of 0.1. The resulting curves of stress-strain and axial strain against transversal strain of the obtained MSM and the corresponding reference data are shown in figure 5.7.

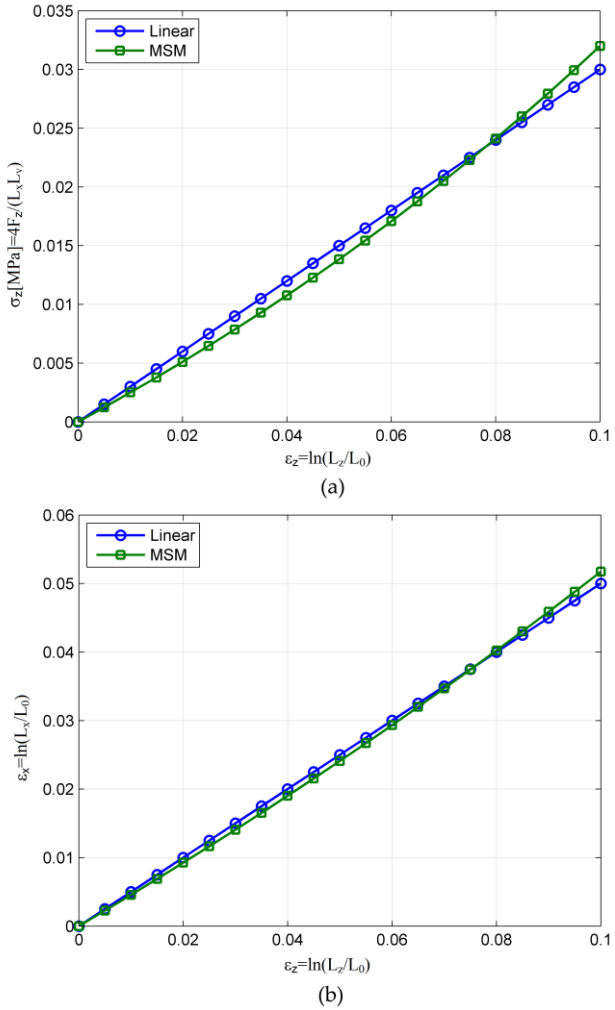

Figure 5.7. (a) The stress-strain curve and (b) the strain relation between axial and transversal direction using as reference a linear elastic material model with Young modulus 300 KPa and Poisson's ratio 0.5.

5.2.2.3 Contribution of each stiffness coefficient

In the case of the linear material model the internal diagonal springs have a much larger stiffness value than the other spring types. Particularly, k_d is one order of magnitude larger than k_e and k_f. These values might lead to the false conclusion that k_d determines the behaviour of the MSM. Or in other

words, that the contribution of k_e and k_f is small and that they can be neglected.

The first point to consider is that in the cube there are only four internal diagonal springs, three times less than edge and face diagonal springs. Secondly, the strain induced in a test affects each spring in a different way. That is, given some particular strain ε_z the elongation of each spring is different due to their original orientations (α and β).

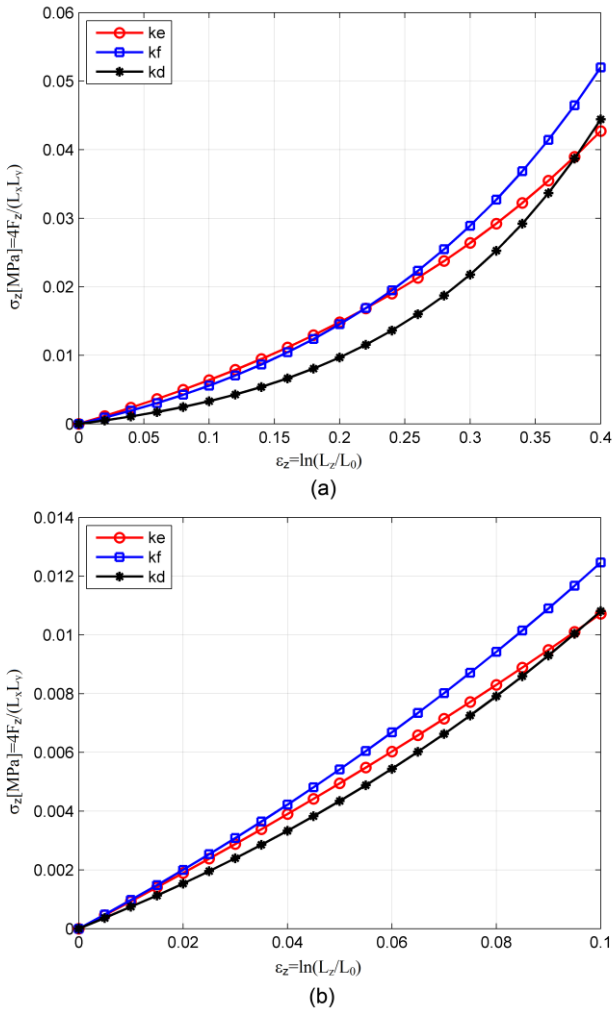

Figure 5.8. Contribution made to the total stress by each type of spring. (a) Nonlinear material model and (b) Linear material model.

Figure 5.8 shows the contribution of each type of spring to the total stress in function of the strain. Figure 5.8.a shows the results obtained for the nonlinear material model case while figure 5.8.b for the example of the linear case.

According to figure 5.8, being k_d much larger does not mean that the influence of diagonal springs is bigger and that the other springs contribute less to the behaviour of the model. Conversely, these curves show that the proposed method obtains stiffness values whose contribution is balanced.

5.3 EXPERIMENTS

In the previous section two parameter derivation examples have been presented, the first from a hyperelastic material model and the second from a linear elastic one. As the range of deformations for the linear elastic model is small, the following experiments will be focused only on the hyperelastic model.

The proposed derivation method takes into account uniaxial tensile tests and single elements. In order to study the performance of the MSM in other situations, it is necessary to make some experiments using multi-element models working under different loading types. In this way, the accuracy of the behaviour of the obtained models will be studied and the assessment of the strategy proposed to obtain the stiffness coefficients will be completed.

The experimental analysis is divided into three sections. The first one studies the behaviour of a multi-element cube subject to uniaxial tensile, shear and torsion forces. The second one is focused on the influence of the mesh resolution in the accuracy of the results. To this end, a bar deflexion experiments is proposed. Finally, as the two methods addressed in the previous and present chapters are able to derive MSMs from linear elastic FEM, a comparison between both approaches will be made to see which of them is more suitable.

5.3.1 MULTI-ELEMENT CUBE

The comparison of the behaviour of a MSM and a FEM subject to large deformations is performed using the same geometrical model as in the previous chapter (see section 4.3.1). That is, both models share the same cubical geometry: a multi-element model with cubical form composed by 10x10x10 elements (1 mm^3 each).

According to the reference material model, in this study the Ogden material proposed by Martins et al. (Martins2006) is adopted. The derivation of the MSM corresponding to this material model is presented in section 5.2.2.1 and the stiffness coefficients are the values given in equation 5.12.

On the other hand, the deformable body modelled using nonlinear FEM will be simulated using the same commercial software as in the previous chapter, namely, *Abaqus*. Because of the specific way of defining the Ogden material model in *Abaqus*, the values of the constants of the characteristic equation (see equation 5.10) have to be transformed in the following way:

$$\begin{aligned} \mu_i^{Abaqus} &= \frac{\mu_i \alpha_i}{2} = \frac{0.005044 * 5.7255}{2} = 0.01444 \\ \alpha_i^{Abaqus} &= \alpha_i = 5.7255 \\ D_i^{Abaqus} &= 0 \end{aligned} \qquad 5.15$$

The experiments are performed in the same way to those made to the MSM derived from linear elastic FEM in chapter 4. That is, the behaviour of the MSM and the FEM is studied under the same uniaxial tensile, shear and torsion forces for small and large deformations described in section 4.3.2.

5.3.1.1 Simulations

In order to better compare the results of the simulations of the six tests, the corresponding final deformed states of the MSM and the FEM are shown in superimposed images in figure 5.9.

The visual comparison of the simulations of the MSM and the FEM shows that the axial behaviour has been accurately approximated. However, when the models are subject to shear and torsion loads the MSM deforms less than the reference model. In other words, the obtained MSM can be seen as a model that is stiffer than the reference one. This characteristic is present in both small and large deformations.

Note that, the objective function proposed in section 5.1.3 only uses information related to uniaxial tensile tests. This can be the reason for obtaining shear and torsion simulations less accurate than the ones corresponding to the *linear method*, which uses the stiffness matrix that characterizes the whole behaviour of the model (see section 4.3.3).

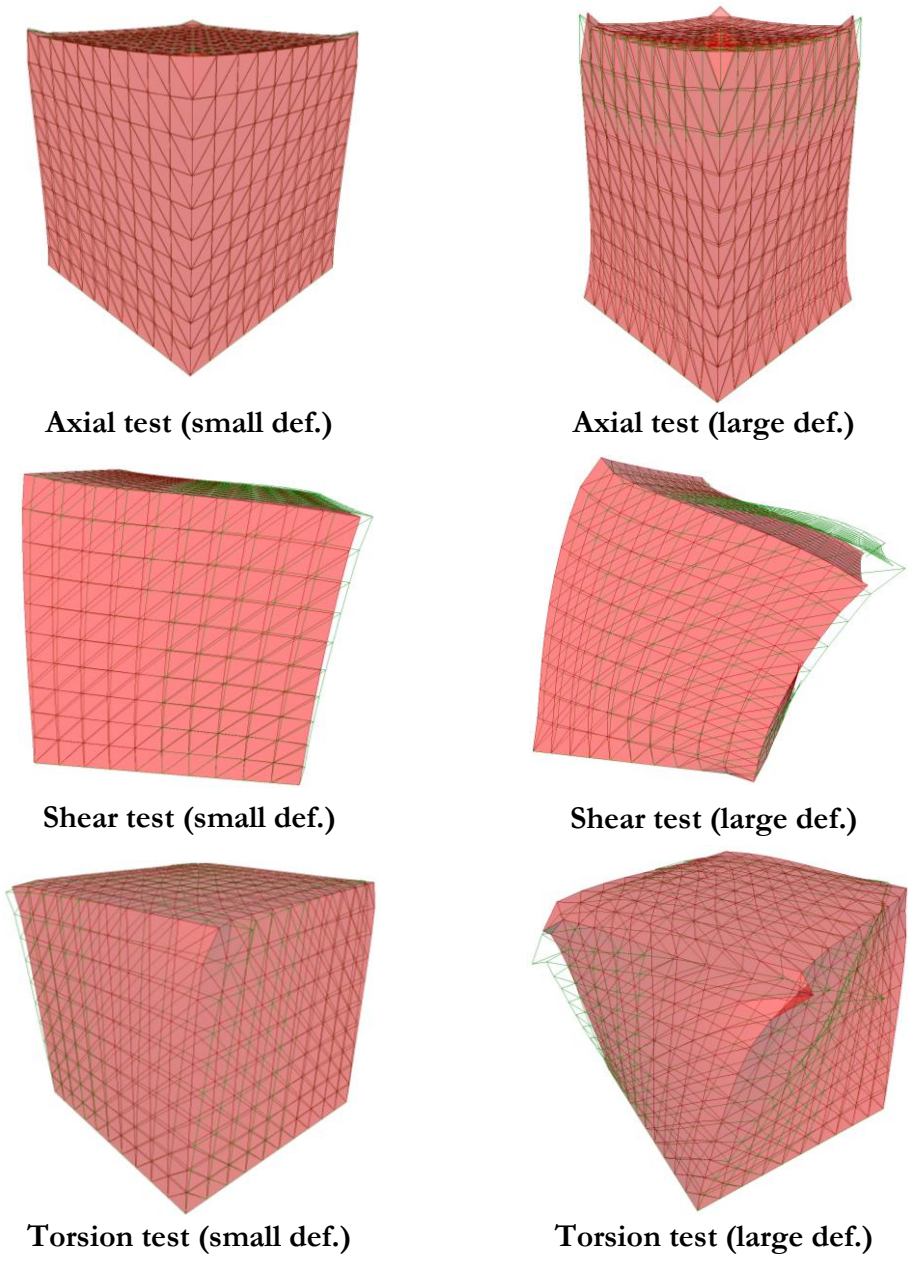

Figure 5.9. Simulation of the deformable bodies using MSM (red mesh) and FEM (green wire-frame). Left column corresponds to small deformations and right column large deformations. From top to bottom: axial, shear and torsion tests.

5.3.1.2 Accuracy of the MSM

The visual comparison of the results of the MSM with the simulations of the FEM gives a qualitative idea of the accuracy of the obtained deformations. This information can be completed with the measurement of some magnitudes of the deformed models in order to give quantitative data about the accuracy of the MSMs. The proposed magnitudes are the same to the ones presented in section 4.3.4.

Table 5.1 shows the errors obtained in the three tests, both for small and large deformations. The adopted relative error was defined in section 4.3.4 (see equation 4.27).

	Small deformations	**Large deformations**
L_1 (axial)	0.40%	1.37%
L_2 (axial)	-0.49%	0.52%
α_1 (shear)	-23.64%	-7.26%
α_2 (shear)	-25.46%	-12.23%
β_1 (torsion)	-3.72%	-11.54%
β_2 (torsion)	-46.88%	-33.36%

Table 5.1. Errors of the MSM with respect to incompressible hyperelastic FEM for different experiments.

These values indicate that the performance of the MSM obtained with the proposed method behaves very accurately when the model is subject to uniaxial tensile loads. The measured magnitudes show that the error is below 1.4% even for large deformations.

However, in the case of shear deformations the results are less accurate. The error is around 25% under small deformations while under large deformations is below 13%.

The worst approximation corresponds to torsion loads. In this case the error reaches 47% for the measurements made to the vertex of the top face. However, the nodes that are located in the middle of the edge of the top face are more accurate with an error below 12%.

5.3.1.3 Volume preservation analysis

Another magnitude that is important for the analysis of the quality of the simulation is the final volume of the MSM. As the reference material model is incompressible, the obtained MSM should also maintain the initial volume (1000 mm^3).

The final volume of the whole model in the three tests performed under small and large deformations is detailed in table 5.2.

	Small deformations			**Large deformations**		
	Test 1	Test 2	Test 3	Test 1	Test 2	Test 3
Volume [mm^3]	1025	999	1000	1046	974	994
Error [%]	2.5	-0.1	0	4.6	-2.6	-0.6

Table 5.2. Errors of the MSM obtained from ν=0.35 with respect to incompressible FEM.

The study of the total volume of the simulated model gives an idea of its general behaviour. However, it is also necessary to analyze the volume of each cubic element to see whether the volume preservation is achieved locally or not. With this aim, for each test, the box plot of all the elements is shown in figure 5.10.

In this table, for each test, the blue box shows the range between the lower and upper quartile of the volumes of the elements. The red horizontal line corresponds to the median value. Black whiskers extend from each end of the box to the adjacent values in the data, being the most extreme values within 1.5 times the interquartile range from the ends of the box. Red + signs are outliers, that is, data with values beyond the ends of the whiskers.

The data corresponding to each element of the model show that the volume varies locally more than what the global volume suggests since the volume variation of the elements is larger than the total one. That is, the excess and defect on the final volume of the elements compensated each

others making the model nearly incompressible. Under small deformations, for the three tests, this error is below 4.8% if the outliers are not taken into account. This value reaches 17% in the case of large deformations.

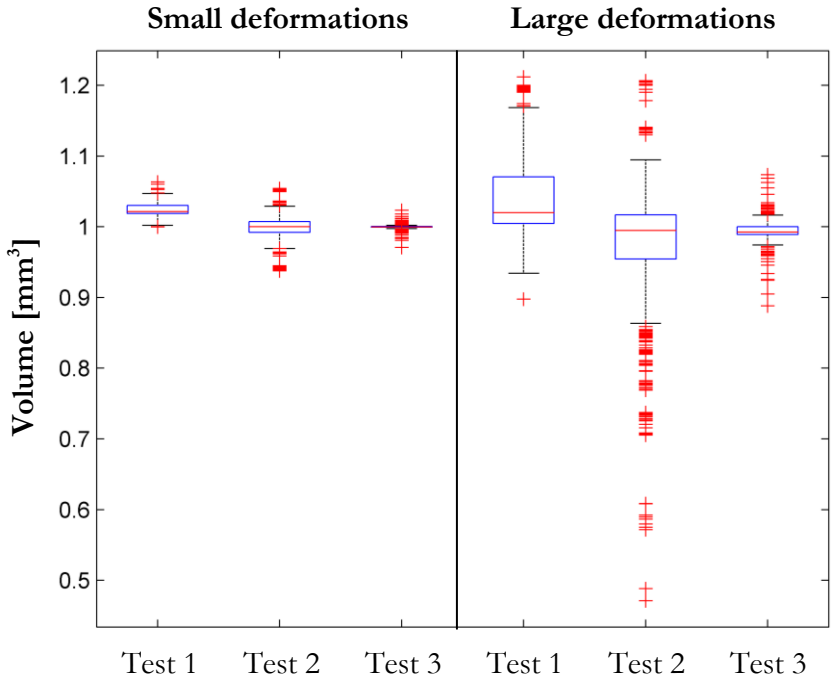

Figure 5.10. Final volume of each element of the simulated MSM depending on the test.

Most of the outliers identified in figure 5.10 correspond to the elements where there is a high stress concentration. In the case of test 2 under large deformations, for example, the highest volume variations are located in the right lower edge where the compression forces are maximal. The reason for this is that the parameters of the MSM have been adjusted in a specific range of the axial strain. When the working load causes deformations out of this range the MSM behaves less accurately.

5.3.1.4 Discussion and conclusions

The method presented in this chapter obtains the stiffness coefficients of cubical MSMs considering only a single element subject to uniaxial tensile loads. When a multi-element model is built with those coefficients, the simulation of the uniaxial tensile test keeps being very accurate, even under large deformations. However, the results obtained in the shear and torsion

tests are less accurate. As the proposed method does not take into account these experiments in the minimization strategy, the resulting MSM is not able to provide such good results in shear and torsion tests.

In the case of the torsion test, it can be seen that the error corresponding to β_1 is much smaller than for β_2 (see table 5.1). The reason for this difference probably falls on the stress concentration that exists in the vertices of the top face. Note that these nodes are subject to the double of the force of the rest of the top edge nodes. The same reason can lay behind the error measured in α_2 when the model is subject to large shear deformations, because the right face is the one that supports more compression in its bottom edge elements.

According to the property of incompressibility, the total volume variation of the MSM is small in all the experiments even under large deformations. In the case of making a local analysis, most of the elements change their volume below 10%. However, some elements can reach up to 50% of volume reduction. Again, the worst results are measured in the elements with higher compression stress values.

An important conclusion of the volume study is that, although the local variations can be high, the global behaviour of the model is quasi-incompressible, even if no specific volume preserving forces or constraint based strategies have been used.

5.3.2 DESIGNING LINEAR ELASTIC MODELS

Two different methods have been proposed in this thesis to obtain deformable models that approximate the behaviour of living soft tissues: the *linear method* and the *nonlinear method*. Although they are different approaches, both methods are able to derive MSMs from linear elastic material models.

In this section, the *linear* and *nonlinear methods* will be used to obtain cubical MSMs, in order to evaluate which of them produces more accurate models. With this aim two linear elastic material models are taken as reference: a compressible model with E=300 KPa and ν=0.35 and an incompressible model with E=300 KPa and ν=0.5. Regarding the model geometry, as in the previous section, the body is formed by 10x10x10 cubical elements whose total volume at rest state is 1000 mm^3.

5.3.2.1 Compressible linear elastic model

To build the compressible model using the *linear method* the parameters of the MSM are calculated using equation 4.21 and table 4.1. The resulting stiffness coefficients are:

$$\begin{aligned} k_e &= 31\,N/m \\ k_f &= 47\,N/m \\ k_d &= 33\,N/m \end{aligned} \qquad 5.16$$

To build the model corresponding to the *nonlinear method* a minimization strategy equivalent to that made in section 5.2.2.2 is required. The only difference is that instead of having a slope of 0.5 in figure 5.7.b this value changes to 0.35 since this is the value of ν for this material model. The resulting stiffness values are the following:

$$\begin{aligned} k_e &= 47\,N/m \\ k_f &= 5\,N/m \\ k_d &= 132\,N/m \end{aligned} \qquad 5.17$$

Both models are subject to the same experiments presented in section 4.3.2 but only considering small deformations. These tests are described in figure 4.14 and table 4.4. Using the relative error definition proposed in section 4.3.4 the resulting errors are detailed in table 5.3.

	Linear method	**Nonlinear method**
L_1 (axial)	**0.05%**	-0.26%
L_2 (axial)	-0.57%	**-0.28%**
α_1 (shear)	**-4.91%**	-11.03%
α_2 (shear)	**-6.67%**	-12.94%
β_1 (torsion)	-1.54%	**-0.77%**
β_2 (torsion)	**-22.28%**	-23.70%

Table 5.3. Errors of the tests under small deformations of the *linear* and *nonlinear methods*.

Analyzing the errors corresponding to the compressible models obtained using both methods (see table 5.3), it can be concluded that the *linear method* provides better results. Even though in the case of the uniaxial and torsion tests both models perform similarly, in the shear experiment the model obtained with the *nonlinear method* is less accurate.

5.3.2.2 Incompressible linear elastic model

In section 4.3.7 it was concluded that the best way of approximating incompressible materials with the *linear method* is by building a cubical MSM from a reference model whose Poisson's ratio is 0.35. Thus, the same coefficients adopted in the previous section are used (see equation 5.16). Regarding the model designed with the *nonlinear method*, the stiffness constants are those detailed in equation 5.14.

The relative errors obtained with these two models are shown in table 5.4.

	Linear method	**Nonlinear method**
L_1 (axial)	0.18%	**-0.11%**
L_2 (axial)	**-0.44%**	-1.05%
α_1 (shear)	**-2.93%**	-41.79%
α_2 (shear)	**-5.57%**	-44.68%
β_1 (torsion)	**-1.89%**	-3.00%
β_2 (torsion)	**-28.65%**	-65.67%

Table 5.4. Errors under small deformations of the *linear* and *nonlinear methods* for different experiments.

Analyzing the errors corresponding to the incompressible models obtained using both methods (see table 5.4), it can concluded that the *linear method* provides better results. The greatest differences are observed in the shear and torsion tests where the errors are much higher in the simulations performed with the MSM derived using the *nonlinear method*.

5.3.2.3 Conclusions

In this section a study of linear elastic material modelling has been done, in order to compare the two methods proposed in this thesis. The main conclusion of this analysis is that the *linear method* provides more accurate models than the *nonlinear method* both, for compressible and incompressible linear elastic materials working under small deformations.

This result is reasonable for two reasons. The first one is that the *linear method* takes into account the whole behaviour of the cubical MSM while the *nonlinear method* makes the design considering only uniaxial tensile tests. The second one is that the *nonlinear method* needs to define a range of deformations in which the model is going to work. These bounds are chosen previous to the simulations and the deformations obtained finally may differ from the initial estimation.

5.3.3 MULTI-ELEMENT BAR MODEL

Apart from the previously studied tensile, shear and torsion experiments, another test widely known in continuum mechanics is the bar deflection test. This experiment consists in subjecting a beam fixed at one end to distributed or punctual loads to study its behaviour. Some authors (Marchal2008, Baudet2009) propose using this kind of analysis to validate deformable models such as MSMs. Furthermore, Baudet et al. (Baudet2009) studied simultaneously the accuracy of the MSM and the dependence of the results with the size of the elements. Following this idea, in this section a bar deflection experiment is performed to analyze the influence of the mesh resolution on the behaviour of the model. In particular, the size of the beam is 4x4x16 mm^3 and its material model is the one described in section 5.2.2.1.

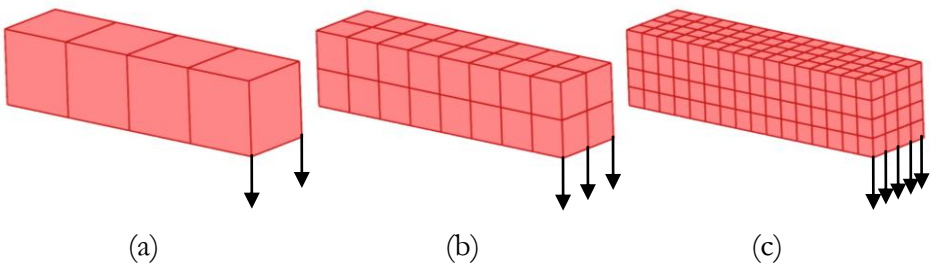

Figure 5.11. Forces applied in the bar deflection test, using different element sizes: (a) 1x1x4, (b) 2x2x8 and (c) 4x4x16.

The test is performed using a MSM with three different levels of resolution: (a) 1x1x4 elements, (b) 2x2x8 and (c) 4x4x16. In all the cases, at the lower edge of the free end of the beam a total force of $\mathbf{F}$=0.05 N is applied. That is, the force applied at each node is $\mathbf{F}_a$=F/2, $\mathbf{F}_b$=F/3 or $\mathbf{F}_c$=F/5 depending on the resolution (see figure 5.11).

The deformation of these three bar models that use cubical MSMs are compared with the deformation of a bar of 4x4x16 elements modelled with the FEM, using the nonlinear Ogden material presented in section 5.2.2.1. The corresponding results are displayed in figure 5.12.

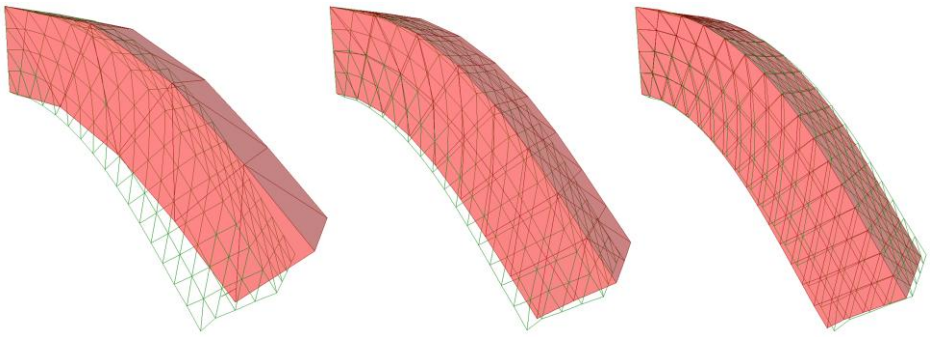

Figure 5.12. A deflection test performed to a bar with different element sizes. In green wire-frame the bar with 4x4x16 elements simulated using nonlinear FEM. In red the same test but using a MSM with different resolutions: (a) 1x1x4, (b) 2x2x8 and (c) 4x4x16.

In this study one of the most representative results is the displacement of any of the two bottom vertices of the free end. In the case of the FEM this displacement is around 11 mm, which is a large value compared with the size of the bar (16 mm). The simulation of the MSM with the highest resolution (see figure 5.12.c) demonstrates that these models can approximate accurately the behaviour of nonlinear FEM in deflection tests, even though the resulting displacements are large.

Using the relative error definition proposed in chapter 4 (see equation 4.27), the errors corresponding to the three tests ordered in increasing resolution are -20.21 %, -8.03 % and -0.70 %. The difference between the MSM and the FEM decreases as the size of the elements converges.

5.4 CONCLUSIONS

In this chapter a new method to derive cubical MSMs from nonlinear elastic models has been proposed. The main characteristics of this method are:

- The response of cubical MSMs working under uniaxial tensile loads is nonlinear and they become stiffer as the deformations grow, as show qualitative and quantitative analyses of their behaviour.

- This nonlinear behaviour is similar to the response of living tissues except in the last phase, where the rupture of the material occurs.

- The method proposed to obtain the stiffness coefficients of the MSM is able to adjust simultaneously the axial as well as the transversal response of the model. This makes it possible to consider the incompressibility characteristic in the derivation process.

- Using the right parameters allows cubical MSMs fulfilling the condition of quasi-incompressibility making them appropriate for simulating soft tissues.

- The *nonlinear method* allows deriving MSMs from nonlinear as well as linear reference data. However, experiments show that in the case of linear material models the MSMs obtained using the *linear method* behave more accurately.

- The obtained stiffness coefficients have similar contribution to the stress magnitude in the uniaxial tensile tests, although there is even a difference of one order of magnitude between the values of k_e, k_f and k_d.

- Experiments performed using multi-element cubical models show that the response of the MSM is accurate under uniaxial tensile loads where the error is below 1.5%. The quality of the approximation decreases in the case of studying shear and torsion tests. Under large deformations, the corresponding errors are below 13% and 34% respectively.

- The global incompressible behaviour shown by many soft tissues is accurately approximated when using the proposed MSM, although locally some elements vary their volume.

- Bar deflection tests using multi-element models show that the response of the MSM is accurate when the size of cubes is the same

to the size of the elements of the nonlinear model. As the size of the cubes of the MSM increases its behaviour gets less accurate.

- When designing MSM that approximate the behaviour of compressible and incompressible linear elastic materials working under small deformations, the *linear method* provides more accurate results than the *nonlinear method*.

The main conclusion reached in this chapter is that discrete nonlinear models such as cubical MSMs are able to approximate accurately the behaviour of incompressible hyperelastic materials working under axial forces. However, when the model is subject to shear or torsion loads the approximation is less accurate.

CHAPTER 6

APPLICATIONS

Two different methods have been proposed in this thesis to obtain MSMs that approximate the behaviour of living soft tissues. The *linear method* assumes that deformations are small and derives the stiffness coefficients of the MSM from linear elastic FEM. The *nonlinear method* is valid for small as well as large deformations and its design is based on the fitting of nonlinear mechanical curves. As it was shown in the previous chapter the latter model is also able to describe linear elastic materials but it is less accurate than the former.

The objective of this chapter is to present real applications developed using both approaches. In particular, the MSM obtained using the *linear method* will be used to simulate maxillofacial surgery and the MSM designed using the nonlinear strategy will be adopted to construct a platform that allows interacting with a brain model.

6.1 MAXIPLAN: MAXILLOFACIAL SURGERY SIMULATOR

Medical imaging techniques have been used to better understand anatomical structures in diagnostic and visualization processes. In the last decades, computer science has given a new dimension to all this information, enabling the prediction and simulation of surgical treatments. In the case of maxillofacial surgery, for example, surgical simulation is becoming a very powerful tool to plan and simulate different procedures (Zachow2006, Mollemans2007) because of its reduced cost (Xia2006).

In this thesis a maxillofacial surgery simulation software named *Maxiplan* has been developed to predict the new facial appearance of the

patient that undergoes an operation before performing the surgery. This allows the surgeon to check the aesthetic results caused by the planed intervention and make the corresponding changes if needed.

The surgery types that are considered in this thesis are focused on the bones belonging to the maxilla and mandible. First, the bone is cut into one or multiple pieces and then each part is moved to the desired position. The objective of the simulation is to predict the change in the skin caused by these bone relocations.

The following sections are divided into five main topics. First, the modular structure of *Maxiplan* and some details about the simulation strategy are presented. Then, detailed information regarding the MSM design. In third place, the soft-tissue area which is in contact with the bone that is going to be cut during surgery is studied. This area suffers the highest modifications and wrong assumptions can lead to unrealistic simulations. After that, a real case of maxillofacial surgery is performed and the post-surgery results are compared with simulated prediction. To end this section some conclusions are addressed.

6.1.1 MODULES OF *MAXIPLAN*

Software oriented to medical simulation is usually divided into different modules depending on the specific interventions that are going to be studied and the tools that the surgeons request. In particular, *Maxiplan* is divided into five modules:

- Graphical interface: it lets the user interact with programme.
- Segmentation: it processes the medical images to identify soft tissue and bone.
- Surgery planning: it allows defining the cuts and movements of the maxilla and mandible as it is planned in the real intervention.
- Surgery simulation: it simulates the effects that the surgery plan has over the face.
- Visualization: it shows the medical data and the results of the different steps of the surgery planning and simulation.

In this thesis three of these modules have been designed and implemented: segmentation, surgery planning and surgery simulation

modules. The graphical interface and the visualization tools are out of the scope of this thesis.

6.1.1.1 Segmentation

Segmentation is the process of partitioning a digital image into multiple regions to locate objects and boundaries. In this case, the segmentation module reconstructs the medical images taken with a computer tomography (CT) scanner and converts it into hard and soft-tissue objects (see figure 6.1).

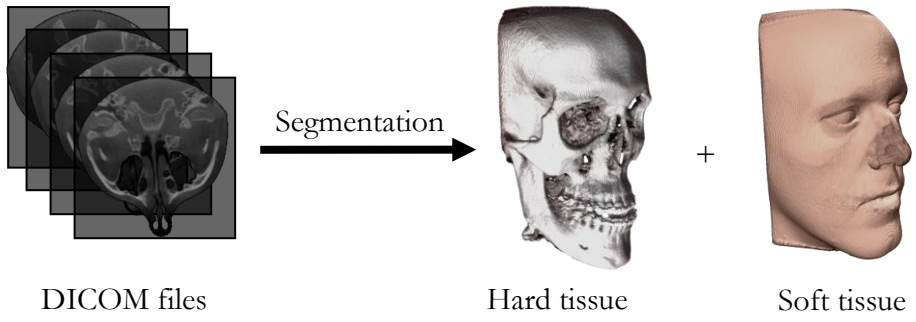

Figure 6.1. Segmentation of the medical data to extract hard and soft-tissue boundaries.

Frequently, medical images contain noise and artefacts which are misrepresentations of tissue structures. They may be caused by a variety of phenomena such as patient movement, presence of metallic objects or lack of precision. To avoid this kind of wrong data, in the segmentation module of *Maxiplan* an image filtering algorithm based on region growing techniques has been implemented.

6.1.1.2 Surgery planning

The surgery planning consists in defining the different bone cuts that the surgeon is going to make and assigning to them the corresponding translation and rotation movements. In *Maxiplan* this planning is build upon the previously segmented images using reference planes specified by the user (see figure 6.2) and provides the simulation module with all the necessary information to start simulating a procedure.

The developed software does not indentify automatically the maxilla and the mandible. Instead, the user defines the planes displayed in figure 6.2

to determine their location. In addition, these references help establishing the cutting area and the relative movements of the bone pieces.

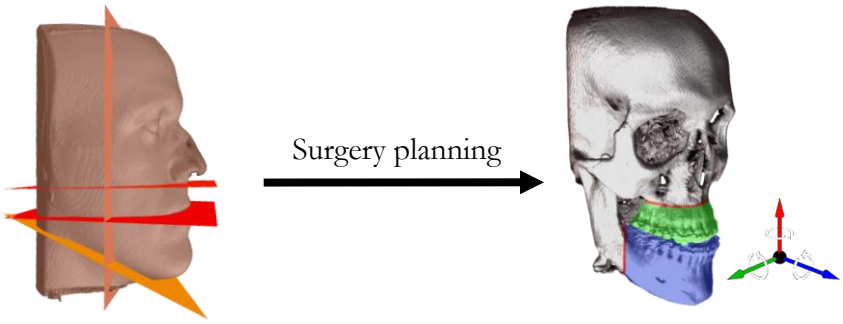

Figure 6.2. Identification of the maxilla and mandible to plan and simulate the surgery.

6.1.1.3 Surgery simulation

The objective of *Maxiplan* is to calculate the appearance of the patient after the surgery, which means that only the computation of the final deformed state is needed. There are two ways of determining these deformations: directly and gradually. The direct one makes all the required bone displacements simultaneously and simulates afterwards the soft-tissue behaviour. In turn, the gradual method determines the bone movements in several steps, computing the soft-tissue equilibrium in each step.

When the displacements are large compared with the size of the elements of the MSM the direct method can lead to simulation problems, such as instabilities caused by large forces and overlapping of the springs. These problems can be avoided doing the simulation gradually, since it allows limiting the maximal movement of the bone in each time step. In *Maxiplan* the gradual strategy has been adopted because it makes the simulation more stable and avoids implementing restrictions to control mesh overlapping.

The gradual method can be seen as a dynamic simulation in which in each time step some parts of bone are displaced. The simulation ends when all these parts achieve the final desired position. Figure 6.3 displays the process of calculating the results of a maxillofacial surgery by moving gradually the affected bones.

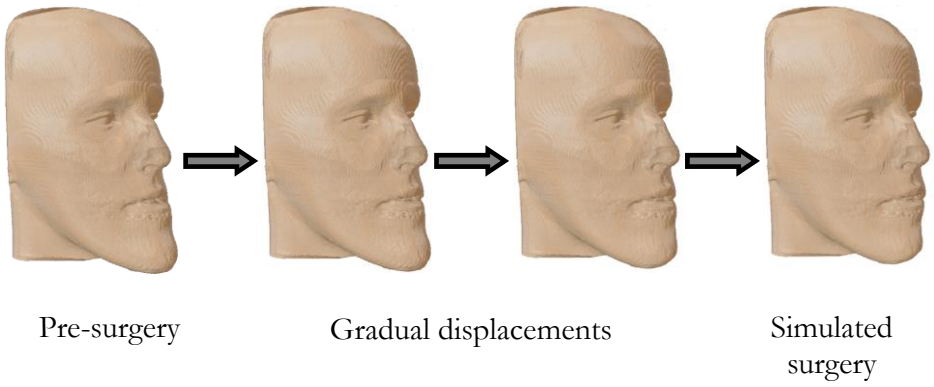

Figure 6.3. Calculating the results of a maxillofacial surgery by gradual approximations.

Frequently, the computation of each time step is made using time integration methods based on finite differences (Haile1992) like Euler, Runge-Kutta, Verlet, and Gear's predictive-corrective methods. In this case, as the objective of the simulation is to calculate the final appearance of the patient, the intermediate deformed positions do not need to be accurately computed. Therefore, the force scaling method proposed by Brown et al. (Brown2001) and detailed in section 2.5.1 is used. The main advantages of this method is that it reaches equilibrium faster than other strategies and it only needs to keep one set of positions, which makes it computationally efficient.

6.1.2 DEFORMABLE MODEL DESIGN

6.1.2.1 Material model

As it was discussed in section 2.2, living tissues have non-uniform, anisotropic, nonlinear, visco-elastic behaviour and these properties depend on the history of applied loads (Fung1993). However, in order to obtain fast results most simulators simplify this complex behaviour using linear elastic (Cotin2000, Maciel2003, Chabanas2004, Zachow2004, Mollemans2005, Westermark2005, Zachow2006, Mollemans2007), geometrically nonlinear (Picinbono2003, Nesme2005, Mollemans2007) or hyperelastic material models (Chabanas2004, Martins2006, Wang2009).

Westermark et al. (Westermark2005) studied the effect of considering non-homogeneous tissue models in the prediction of osteotomies in cranio-maxillofacial surgery. They differentiated between fat and muscle tissue and

assigned for each tissue type different values to E and ν. They concluded that the net improvement obtained by using such non-homogeneous tissue models did not significantly influence the prediction quality.

Chabanas et al. (Chabanas2004) compared the performance of linear and hyperelastic material models in the simulation of the post-operative facial appearance. In the cases they studied the linear FEM provided accurate results, even better than using nonlinear FEM. Probably, the reason for this is that the properties of the face are not uniform and it is difficult to define the properties that best describe the global behaviour.

There is little information about the range of deformations in which the linear model is valid. According to Chabanas et al. (Chabanas2004) the use of linear material models is appropriate for maxillofacial soft-tissue simulations that undergo deformations bellow 20%. On the other hand, Gladilin et al. (Gladilin2003) suggested that the limit of the maximum distraction allowed using linear material models is about 1 cm.

Taking into account these studies, it seams acceptable to use homogeneous linear elastic material models to make fast simulations of maxillofacial procedures where the deformations are small; particularly when a fast response is required. Therefore, the surgery simulation tool will be developed using cubical MSMs obtained from linear elastic FEM which involves calculating the stiffness coefficients with the method presented in chapter 4.

6.1.2.2 Material properties

Although linear elastic material models are very common in maxillofacial surgery simulation, there are great discrepancies when settling the mechanical properties. The main reason is that it is difficult to assign an elasticity modulus and a Poisson's ratio to the grey levels of the images provided by medical imaging techniques such as CT and MRI. Unfortunately, there is no unique relationship between Hounsfield Units (gray levels) and mechanical properties, and the determination of suitable values for different tissue types is still the subject of ongoing research in biomechanics and elastography (Zachow2006).

In the maxillofacial simulations performed by researchers like Zachow et al. (Zachow2004, Zachow2006), Chabanas et al. (Chabanas2004) or Mollemans et al. (Mollemans2005, Mollemans2007) the optimum

Young's modulus varies from 3 kPa to 300 kPa while the Poisson's ratio is recommend to be between 0.3 and 0.5.

The method proposed in chapter 4 to design MSMs provides more accurate results when ν=0.35 (see section 4.3). Consequently, this will be the value used since it is in the range of valid ν when approximating the behaviour of soft tissues involved in maxillofacial surgery simulation. Regarding Young's modulus, E=50 kPa is adopted because it is an intermediate value.

6.1.3 NEW METHODS FOR BONE REMODELLING

The maxillofacial surgeries simulated in *Maxiplan* involve bone cuts and displacements. If the objective of the intervention is to shorten the mandible or the maxilla, it is necessary to remove certain portion of bone which is typically known as bone *setback* operation. On the contrary, if the objective is to make it larger then it is called *advancement*. In this case, the gap caused by the relocation of the bone is filled again.

In interventions that involve bone relocation it is important to study the soft-tissue area which is in contact with the bone that is going to be cut and displaced during surgery. This area suffers the highest modifications and wrong assumptions can lead to unrealistic simulations.

Biological mechanisms such as tissue regeneration and bone growth are very complex and describing them is usually computationally expensive, if not directly impossible with current knowledge. Thus, it is necessary to analyse the way that geometrical assumptions can help representing more realistically physical and physiological characteristics. This section is focused on the study of the soft-tissue bounding conditions, that is, in the boundary layer in contact with the bone.

In this thesis two possible methods for performing bone setback and advancement are proposed: Scaled Displacement Method (SDM) and Removing Method (RM). Note that these approaches are applicable both to MSM and FEM.

The SDM represents a bone cut and displacement by scaling certain area of the affected bone. In this way, the bone modifies its length according to the desired osteotomy. The soft tissue that is in direct contact with the bone also suffers a similar compression of its surface. This method modifies the geometry of the model but it does not remove any element of

the mesh. On the other hand, the RM removes a piece of bone exactly like in the actual surgery, which involves eliminating the soft tissue in direct contact with the removed bone. Therefore, this method requires restructuring the affected elements and removing some elements of the MSM in contact with the bone.

In order to illustrate how these methods work, a practical example of a mandibular setback is studied (see figure 6.4).

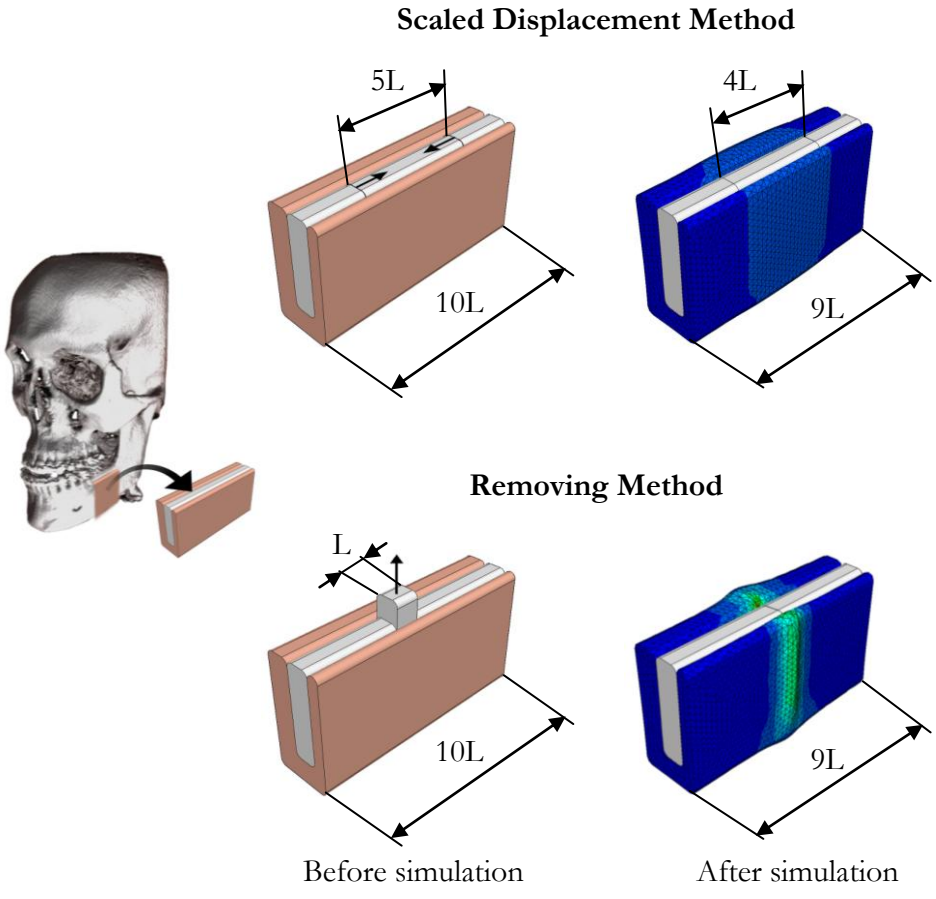

Figure 6.4. An example of the application of the SDM and the RM in a mandibular setback.

In particular, the length of the mandible is reduced certain amount L and an area equivalent to ten times the setback length is analyzed. As it can be seen, the SDM scales the central part of the sample while the RM extracts a portion equivalent to the setback amount. In particular, the size

of the area selected for scaling in the SDM is five times bigger than the setback size in order to distribute the effect of the osteotomy in a wide area.

In figure 6.4 can be seen that the SDM distributes stress and strain uniformly along the area close to the cut. The RM, in turn, shows a bending effect in this area caused by a stress concentration located near to the surface that connects the two bone pieces. Concerning real surgeries, after a recovery period, soft tissue relaxes losing any stress concentration caused during the operation. Therefore, from this point of view, the prediction made by the SDM is more realistic.

Another advantage of the SDM is that it avoids remeshing and removing elements like the RM does. Therefore, it maintains the initial mesh of the model. As a consequence the mathematical formulation is simplified and the computation time is improved.

6.1.4 PRACTICAL APPLICATION

In this section a real case of maxillofacial surgery is presented, where facial asymmetry and long face pathology are treated: asymmetric mandibular setback (3 mm left, 5 mm right), maxillary impaction (2 mm), maxillary advancement (3 mm) and arch widening (0.5 mm) (see figure 6.5). Note that this case involves the most common osteotomies in maxillofacial surgery.

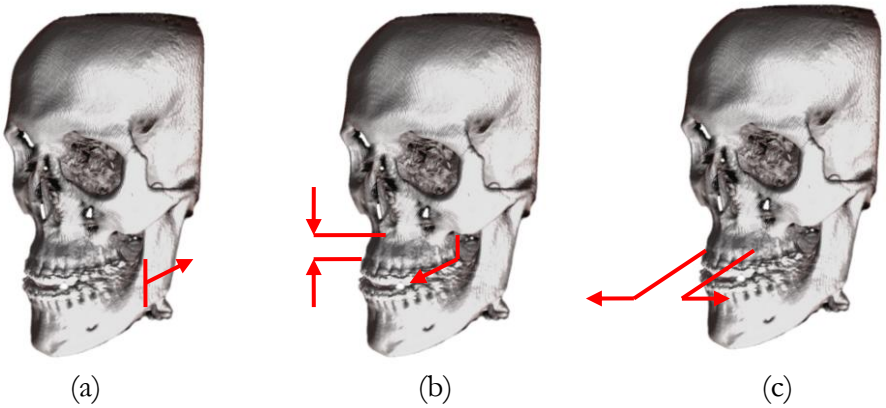

Figure 6.5. Surgical bone movements performed: (a) mandibular setback, (b) maxillary advancement and impaction, and (c) maxillary arch widening.

6.1.4.1 MSM design

The medical images are taken with an i-Cat scanner[1] that generates regular voxels with edges 0.4 mm long. This size is too small for simulation because it leads to a large amount of elements. Therefore, each axis is simplified by 4 resulting in a model that is 64 times smaller than the original one. In this case, the model has 303178 equal sized voxels with edges 1.6 mm long. Larger simplifications are also possible but they do not result in a mesh fine enough for the surface reconstruction process and important details can be lost.

The MSM is derived from a homogeneous linear elastic material model following the indications of previous research works mentioned above (see section 6.1.2.1). To build the deformable model it is necessary to calculate the parameters of the MSM using equation 4.21 and table 4.1. The stiffness coefficients corresponding to L=1.6 mm, E=50 kPa and ν=0.35 are the following:

$$\begin{aligned} k_e &= 8\ N/m \\ k_f &= 12\ N/m \\ k_d &= 9\ N/m \end{aligned} \qquad 6.1$$

6.1.4.2 Simulation

The simulation module needs to guarantee a stable and accurate performance. For this reason, the strategy proposed to compute the final appearance of the patient is divided in two parts. The first one is focused on computing a fast but rough approximation of the final outcome and the second one is concerned with the refinement of the results.

To avoid stability and overlapping problems *Maxiplan* uses the SDM in the first phase. In particular, the scaling of the bone areas involved in the operation is made gradually in 10 steps. In each of them the soft tissue is simulated in a rough way in order to give intermediate quasi-static results. These successive approximations that take place each time the bone is reconfigured are driven in 30 steps using the force scaling method (see section 6.1.1.3). Consequently, the first phase calculates 300 times the deformations of the MSM.

[1] Imaging Sciences International, Inc. (www.imagingsciences.com)

The second part of the simulation begins with the bone in its final configuration and the soft tissue in a roughly approximated state. The refinement of the results is performed using the force scaling method and is designed to compute 2000 steps.

The results of the simulation corresponding to the surgery studied in this section are displayed in figure 6.6. Three data reconstructions for the same patient are shown: (a) before surgery, (b) simulated model and (c) after surgery.

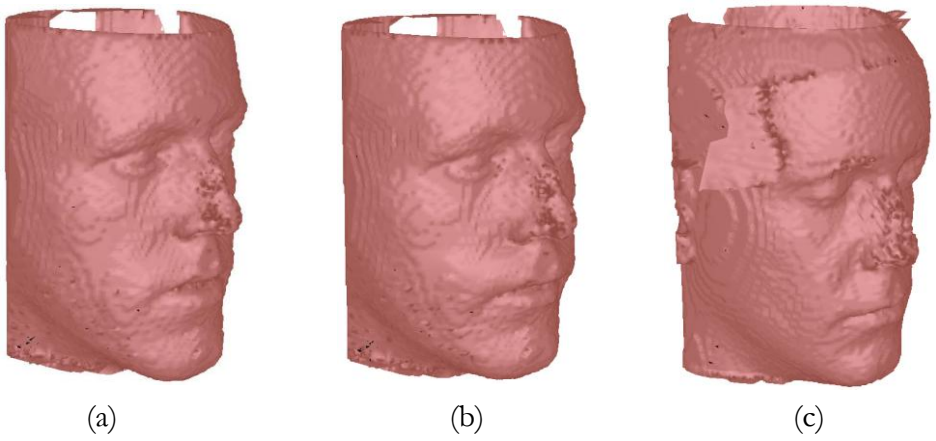

Figure 6.6. Patient data reconstruction: (a) patient before surgery, (b) simulated result after surgery and (c) actual surgery results.

The simulation module of *Maxiplan* took 4.5 minutes to simulate the outcome of the surgery procedure using an Intel® Core ™ 2 Quad 2.4 GHz with 3.25 GB of RAM. No precomputed data has been used apart from the stiffness calculations.

6.1.4.3 Error computation

The scanner images of the patient before and after surgery have been taken in different days and in different postures, which makes the comparison process more complex. Thus, before measuring the error of the simulation, both models have to be oriented in the same direction. The simplest way to reorient correctly the model is to match regions that surgery has not modified (the forehead, for example) and calculate the translation and rotation matrices. In this case, six points that do not displace during surgery

are taken and then the transformation that minimizes the sum of the distances between the equivalent points in the two models is computed.

The evaluation of the difference between the simulated model and the actual surgery can be accomplished in many ways. In the particular case of the face, there are some representative points that have to be especially considered when analyzing simulation results, namely, soft-tissue landmarks of the face. In this field, Swennen et al. (Swennen2006) made a detailed 3D cephalometric study to identify the most meaningful points of the face.

Following their work, in *Maxiplan*, the landmarks belonging to the mandible, maxilla and cheekbone selected to measure the error of the simulation are: (1) right soft-tissue cheekbone, (2) pronasale, (3) subnasale, (4) *labiale superius*, (5) *labiale inferius*, (6) soft-tissue pogonion, (7) subspinale and (8) left soft-tissue cheekbone. Their location is detailed in figure 6.7.

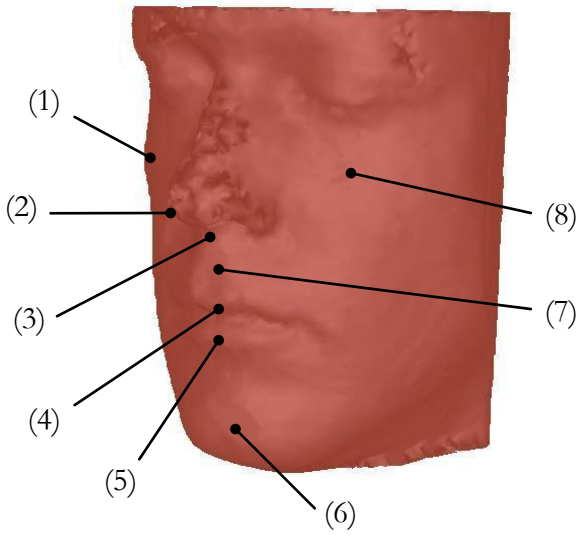

Figure 6.7. Soft-tissue landmarks that allow evaluating the error in representative regions.

The error at these points is measured by using ray tracing techniques. First, a set of triangles of the simulated mesh in the area of the landmark is selected. Then, from each triangle, a ray is traced perpendicular to its barycentre. The error is the distance covered by the ray between the simulated model and the actual surgery model (see figure 6.8).

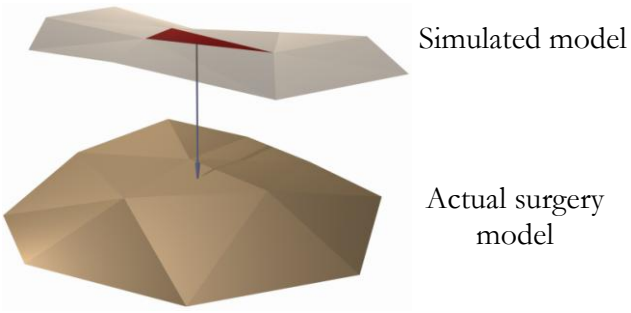

Figure 6.8. The distance between two triangular meshes is calculated measuring the distance covered by a perpendicular ray from the barycentre of each triangle of the simulated mesh to the actual surgery mesh.

The value of this error varies significantly with the selected triangle. Thus, to give a statistical idea of this deviation, for each landmark the five nearest triangle barycentres are measured and the average and standard deviation for their errors are calculated. These results are shown in table 6.1.

	Average error [mm]	**Standard deviation**
(1) Soft-tissue cheekbone (right)	1.43	0.90
(2) Pronasale	1.72	0.99
(3) Subnasale	1.51	0.98
(4) *Labiale superius*	4.44	0.24
(5) *Labiale inferius*	2.01	1.81
(6) Soft-tissue pogonion	0.68	0.38
(7) Subspinale	1.82	0.85
(8) Soft-tissue cheekbone (left)	0.37	0.25

Table 6.1. Error measured at the landmarks.

Note that the surgery simulation has been performed taking into account the pre-surgery planning and not the real surgery. During the operation the procedure may change due to unexpected bone characteristics, deficient medical images or teeth malocclusion. In *Maxiplan*, these changes are not considered during the simulation. Conversely, Marchetti et al. (Marchetti2010), for instance, adapt the virtual plan to match post-operative bone situation. In this way, they avoid the error associated to the planning process. However, it is preferable to comply with the initial plan in order to reproduce fairly the way in which the doctor is going to work. For these reasons, errors shown in table 6.1 have to be considered carefully.

6.1.5 DISCUSSION

When analysing the simulation error it is important to consider the impossibility of having CT images after surgery with exactly the same posture and facial expression of the ones previous to it. Furthermore, the distance measured perpendicularly from the barycentre, in general, is not the smallest distance between one triangle and the other mesh because the relative angles can make this distance larger.

In spite of these sources of error, in the landmarks the average error is between 0.37 and 2.01 mm, that is, less than the internal diagonal length of a cube except for *labiale superius* whose error is 4.44 mm. Concerning the standard deviation, the worst value corresponds to *labiale inferius* due to the curvature of this region. Taking into account that the cube size is 1.6 mm, these error values are reasonable and similar to those obtained by other researchers that use linear FEM (Zachow2006, Mollemans2007).

Although there is no significant effect on the error in the proposed landmarks when using the scaled displacement method and the removing method, it has been observed that the error corresponding to the region where the cut is performed is bigger for the latter, reaching in some cases 1.5 times the error of the scaled displacement method. This issue supports the theoretical reasons mentioned above.

6.1.6 CONCLUSIONS

In this section a tool to simulate maxillofacial surgical procedures is presented. The patient specific MSM is generated using the method proposed in chapter 4. The main conclusions reached in this implementation are the following:

- The new MSM proposed in chapter 4 has been applied to a surgery simulation tool and it has been tested using real surgery procedures information.

- The addressed case report shows that the new model provides accurate results, which are comparable to those obtained by other authors that use linear FEM.

- A new method to emulate cuts is proposed, namely, SDM. This method is applicable both to MSM and FEM, and it allows translating realistically the effects of a bone cut and the following movement to a geometrical scope.

- The SDM describes more reliably the effects of the surgery than the RM, as it is shown in a comparative test made in a small sample using both methods.

- The implementation of the SDM in the *Maxiplan* simulation tool proves that it does not give unrealistic results like wrinkles in the cutting area.

The main conclusion reached in this section is that the MSM design proposed in chapter 4 combined with the SDM makes it possible to develop accurate medical simulators such as those used to predict facial appearance of patients after maxillofacial surgery.

6.2 I-BRAIN: INTERACTIVE BRAIN SIMULATOR

Neurosurgery is concerned with the prevention, diagnosis, treatment and rehabilitation of disorders that affect the entire nervous system including the brain, spinal column, spinal cord, peripheral nerves and extra-cranial cerebrovascular system.

Brain surgery, in particular, is suffering a great evolution due to new neuronavigation techniques. During image guided navigation, pre-operatively acquired image data of different modalities such as CT or MRI are registered to the anatomy of the patient. Rigid registration (see section 1.3.1) is relatively straightforward; however, deformations of the brain tissue reduce its usefulness, especially in the case of large skull openings. These deformations may occur due to physical phenomena (e.g. dura opening, intra-operative position of the patient, loss of cerebrospinal fluid, surgical manipulation, characteristics of the tissue, etc.) and to physiological phenomena (e.g. swelling due to osmotic drugs, anaesthetics).

Studies have reported a continuous dynamic shift of the brain tissue evolving differently in distinct brain regions, with a surface shift up to 24 mm that occurs throughout surgery and with a subsurface shift exceeding 3 mm for the deep tumour margin that mainly occurs during resection (Nabavi2001, Hastreiter2004). As a consequence of this phenomenon the images acquired before surgery are no longer valid representations of the brain of the patient. Therefore, intraoperative changes in brain morphology significantly deteriorate the accuracy of any neuronavigation system during the surgery.

For these reasons, biomechanical models that simulate brain deformations under loading and boundary conditions typically found in this kind of surgeries are gaining attention. The main objective of these simulation tools is to help in computer assisted and image-guided neurosurgery by providing reliable models that deform like actual brains. In a similar way, simulators focused on training programs have to provide models that behave realistically in order to transfer the trainees the skills required to tackle with real surgeries.

In this section, a deformable brain model developed for neurosurgery training purposes, called *I-Brain*, is presented. In contrast to *Maxiplan*, *I-Brain* does not use patient specific data. In turn, the geometric information is provided by a brain atlas whose weight has been set to 1.3 Kg. (Kewitz1980).

There is a lack of *in vivo* actual medical image data of a whole brain working under different loading conditions. This is a remarkable limitation when trying to validate the deformable models used in neurosurgery simulators. Therefore, the development of *I-Brain* is a proof-of-concept to see the suitability of MSM to be used in this kind of tools.

6.2.1 DEFORMABLE MODEL DESIGN AND SIMULATION

6.2.1.1 Material model

Experimental results show that the mechanical response of brain tissue to external loading is very complex because the stress-strain as well as the stress-strain rate relationship are nonlinear (Miller2010). Miller et al. (Miller2010) adopted an Ogden-based hyper-viscoelastic constitutive model and assumed that the brain is incompressible and isotropic. Schiavone et al.

(Schiavone2009) proposed a Mooney-Rivlin model with ν=0.45 to describe the hyperelastic nearly incompressible behaviour.

Both researches (Schiavone2009, Miller2010) insist on the hyperelastic and quasi-incompressible behaviour of the brain. Therefore, the surgery simulation tool will be developed using cubical MSMs obtained from hyperelastic material models. This requires calculating the stiffness coefficients with the method presented in chapter 5.

6.2.1.2 Material properties

There are two reasons that make it difficult to select the material properties of the model of human brain. The first one is that many authors provide the characteristics of porcine brains (Miller2002, Zhang2010) because obtaining them has less ethical consequences. The second ones is that the material models calculated using post-mortem samples vary dramatically depending on the preservation conditions, particularly on the preservation temperature (Zhang2010).

Recently, Schiavone et al. (Schiavone2009) provided for the first time *in vivo* data on human brain elasticity. They extracted a constitutive law of the human brain measuring pre-operatively on the patient, just before the resection of the brain parenchyma. However, as they point out, the main aim of their work was not to describe a universal constitutive law for the brain elasticity, but to propose a new procedure to obtain reliable data.

The hyperelastic incompressible material model used to obtain the MSM in section 5.2.2.1 is compared with the data provided by Zhang et al. (Zhang2010). As it can be seen in figure 6.9 the proposed model behaves like the set of brains they call *group A*. Note that behaviour data has been transformed into engineering stress and strain in order to use the same magnitudes as Zhang et al. (Zhang2010).

In Zhang's work, *group A* refers to the set of the brain tissues stored at low temperatures above freezing point and warmed to a temperature of 37ºC in saline bath prior to testing. That is, the group whose behaviour has been obtained following the procedure the authors recommend. Therefore, the Ogden constitutive equation described in equation 5.10 has been selected for brain modelling in *I-Brain*.

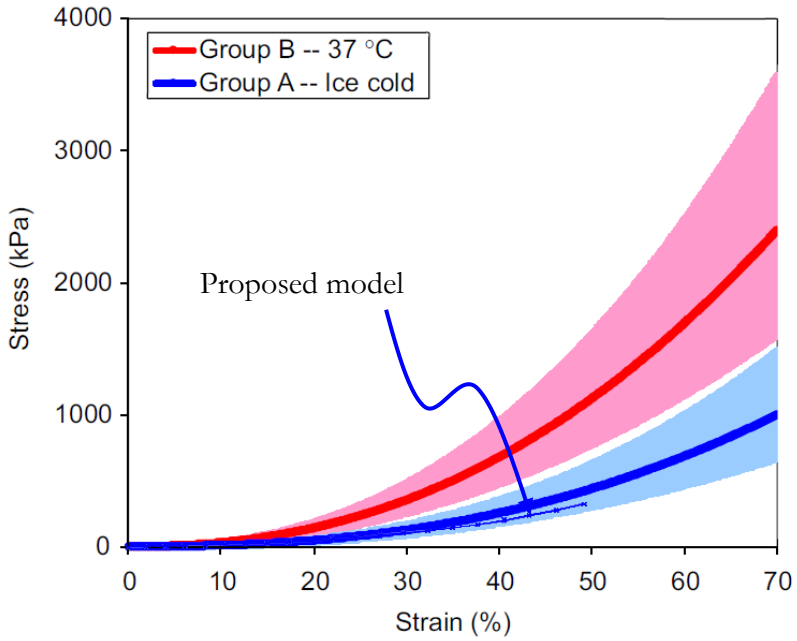

Figure 6.9. Mean engineering stress-strain curves for porcine brain tissue preserved in ice cold (*group A*) and37 ºC (*group B*) saline solution with the 95% confidence bands plotted in 0-70% (Zhang2010) and the material model proposed in this thesis (see section 5.2.2.1).

6.2.1.3 Simulation

The objective of *I-Brain* is to provide a proof-of-concept tool to interact with a brain model in real time. The main difference with respect to the maxillofacial surgery simulator is that, in this case, there is a continuous interaction between the model and the user. Therefore, in contrast to *Maxiplan*, this simulator requires computing the actual deformation in each time step, not only in the final deformed configuration. This involves detecting the collisions between the brain and the medical instruments and computing the effect that they have over the deformable model.

The whole mass of the brain is distributed uniformly in the collection of point masses that forms the MSM. At each point a set of springs is connected and when their length changes they apply a force on the masses they connect, making them accelerate according to equation 2.10. The new position of the nodes of the model can be evaluated using different types of integration schemes. In *I-Brain* an Euler Implicit integration has been

chosen, in order to make fast simulations and fulfil the requirement of real-time performance.

6.2.2 IMPLEMENTATION AND TESTING

In order to implement *I-Brain* in a flexible manner the *Simulation Open Framework Architecture* (*SOFA*[1]) has been used. *SOFA* is an open-source, C++ library for physical simulation, primarily targeted to medical simulation. The data structure that uses to model the scene is similar to hierarchical scene graphs commonly used in graphics libraries.

As it is usual in this kind of applications, several models have been combined to build the deformable object of *I-Brain*: a visual model, a deformable model and a collision model. In this section only the key information related to these models will be addressed.

6.2.2.1 Visual model

The purpose of this simulator is to help with training tasks. Therefore, it is not necessary to use patient specific data and the geometric information can be obtained from brain atlases. In particular, a free human brain atlas[2] is used as the brain visual model. This model contains a detailed triangle mesh with 36758 elements (see figure 6.10).

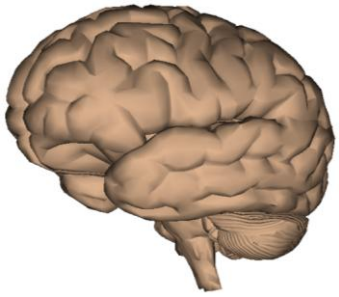

Figure 6.10. The visual model of the brain contains 36758 triangles.

6.2.2.2 Mechanical model

A cubical MSM has been implemented in *SOFA* with the aim of modelling the mechanical response of the brain. Following the discussion about the

[1] http://www.sofa-framework.org

[2] http://artist-3d.com/free_3d_models/dnm/model_disp.php?uid=568

generic behaviour of the brain (see sections 6.2.1.1 and 6.2.1.2) the Ogden model proposed by Martins et al. (Martins2006) has been used as a reference. Given the nonlinear nature of the material model and taking into account that the deformations can be large, the brain has been modelled using the method proposed in chapter 5 (see section 5.2.2.1).

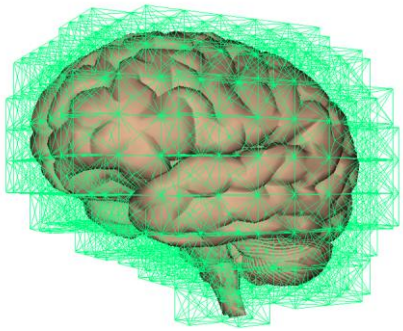

Figure 6.11. Cubical MSM that describes the nonlinear behaviour of the brain.

Taking the edge length 2 cm, the resulting MSM is composed of 706 point masses and 6951 springs (see figure 6.11) and the corresponding parameters are shown in equation 6.2.

$$\begin{aligned} k_e &= 199\ N/m \\ k_f &= 487\ N/m \\ k_d &= 1081\ N/m \end{aligned} \qquad 6.2$$

In *SOFA*, by default, the method that automatically constructs regular MSMs uses a unique stiffness coefficient. In order to be able to use three different stiffness values, the implementation of this model has required modifying the source code of the module of *SOFA* involved in MSM generation.

As the detail level of the mechanical model is much smaller than the one of the visual model a barycentric mapping between both models is performed. In this way, it is possible to display detailed results even though the deformation is computed using a coarser physical model. This technique is widely used in computer graphics because it allows making computationally efficient simulations with high resolution visualizations (Mosegaard2005, Nesme2009).

6.2.2.3 Collision model

Among the different types of collision models that *SOFA* allows defining, in *I-Brain* the sphere collision model has been used. This model is integrated into the collision detection and response pipeline, and when contact or mouse interaction forces are applied to the set of spheres, the forces are propagated to the mechanical model by mapping them. Then, these contact forces are incorporated in the dynamics equations producing the corresponding deformations. In particular, the proposed collision model is composed of 271 spheres (see figure 6.12).

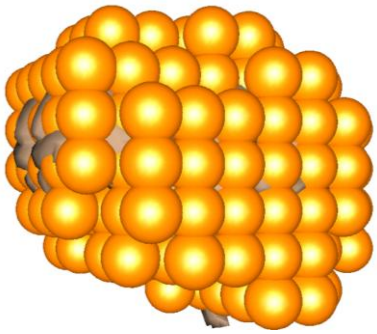

Figure 6.12. Collision model composed of a collection of spheres.

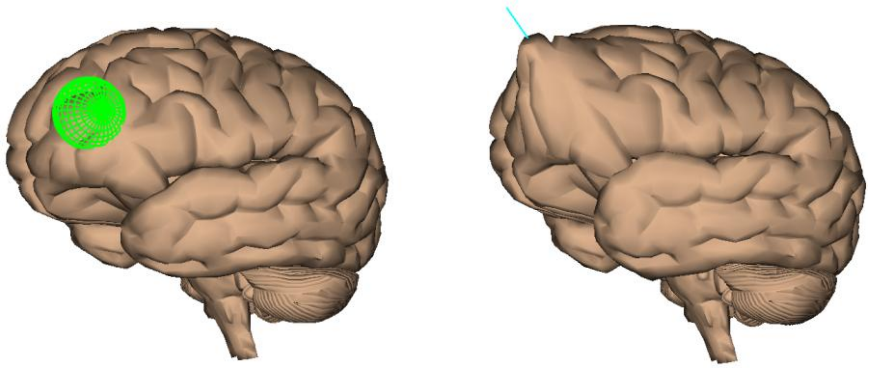

(a) (b)

Figure 6.13. (a) The green sphere is the one intersected by the ray casted from the mouse. (b) The deformations caused by the spring created during the mouse interaction.

6.2.2.4 Interaction mode

The user interacts with the collision models using rays casted from the mouse pointer and hitting collection of spheres. If any ray intersects one of the spheres that form the collision model of the scene (see figure 6.13.a) then, a spring is created between the model and the mouse pointer (see figure 6.13.b). Moving the mouse allows pulling on some elements of the mechanical model and deforming it.

6.2.2.5 Simulation performance

The computation of the deformation suffered by the brain due to user interactions takes about 5 ms. These simulations have been performed using a time step of 20 ms and an Euler Implicit Integrator. The corresponding results have been obtained with a CPU-based implementation using a computer with an Intel Dual Core Pentium D processor at 3.2 GHz and 2 GB of RAM.

Some frames of a deformation sequence taken when interacting with the model are displayed in figure 6.14.

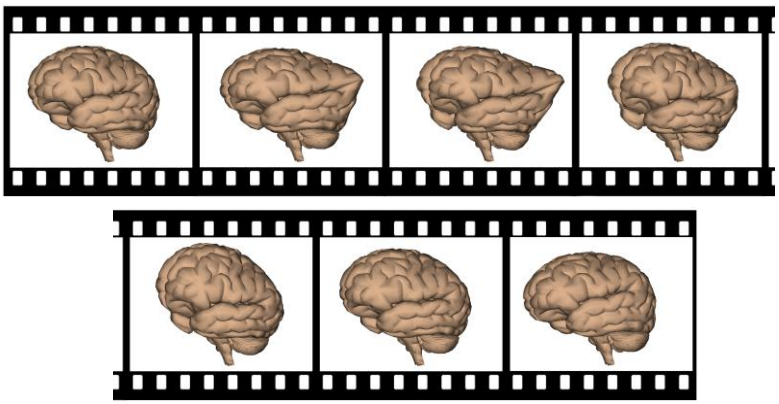

Figure 6.14. Some frames of a deformation sequence taken when interacting with *I-Brain*.

Taking these results into account, this implementation shows the suitability of MSMs designed with the proposed approach to describe nonlinear material behaviour in real-time interactive applications. The present implementation has been focused on palpation-like interactions but it can be include in other kind of medical applications such as procedures planning or surgery simulation.

Moreover, the proposed model can be an interesting alternative to nonlinear FEM, since computationally efficient GPU based implementations such as the one proposed by Rasmusson et al. (Rasmusson2008) show that MSMs are, in general, faster than nonlinear FEM implementations such as the one published by Comas et al. (Comas2008) (see discussion in section 2.6.3).

6.2.3 CONCLUSIONS

In this section a proof-of-concept tool to physically interact with nonlinear elastic deformable models is presented. The model is generated using the method proposed in chapter 5. The main conclusions reached in this implementation are the following:

- Although *SOFA* is focused on physical simulation and primarily targeted to medical simulation it still does not include nonlinear material models. The proposed approach has allowed developing models that behave like hyperelastic materials adopting cubical MSMs and avoiding the implementation of nonlinear FEM.

- The simulation of the interactions using bodies whose behaviour is nonlinear has been achieved at real-time rates. In particular, the computation of the deformation of a detailed brain model has been carried out in 5 ms.

The lack of actual medical image data of a whole brain working under different loading conditions has been a limitation when trying to validate the MSM implemented in *I-Brain*. However, the performed simulations show that MSMs are an interesting choice for medical simulators that need nonlinear deformable models whose behaviour has to be computed in real time.

CHAPTER 7

CONCLUSIONS AND FUTURE WORK

This thesis presents new methods for obtaining soft-tissue mechanical models typically used in medical simulators. These models are valid either for surgeon training, surgery planning or surgical simulation. The main contributions of this work are focused on the field of MSM design, in particular, on the computation of the stiffness coefficients of cubical MSMs.

Two new methods to design cubical MSMs are proposed. The first one, called *linear method*, obtains the stiffness parameters of the MSM from linear elastic FEM and is focused on modelling soft tissues for the simulation of small deformations. The second one, namely *nonlinear method*, obtains the MSM from the behaviour of nonlinear material models and is able to work accurately under large deformations.

The general conclusions and characteristics of these two methods are:

- The proposed approaches allow simulating fast and with enough accuracy for interactive training, the behaviour of the most frequent soft tissues present in surgical procedures.

- Both methods are based on the study of the behaviour of a single cubical element. Even if they are based on a single element, the behaviour of the corresponding multi-element model is also accurate.

- The analytical study of the behaviour of a single element makes these methods independent from the global shape of the body. In addition, they are based only on the constitutive model of the body,

without requiring a set of experiments to obtain the MSM. These two characteristics are clear advantages with respect to data-driven methods used by other authors.

- Even though the formulation of MSMs does not permit defining directly properties such as incompressibility, the experiments simulated in this thesis show that the proposed models achieve quasi-incompressible behaviour without using constraint based methods.

- Both methods allow defining different compressibility ratios. This is an advantage with respect to the energy-based approaches which usually focus on volume preservation constraints, thus limiting their usability to only incompressible materials.

- The complexity of the evaluation of nonlinear FEM is greater than linear FEM. In contrast, the simulation of the MSMs presented in this thesis has always the same computational cost, in spite of the fact that some of them are suitable for nonlinear behaviour modelling, while others are specifically designed for modelling linear elastic materials.

- Both MSM design approaches proposed in this thesis have been integrated into medical simulator prototypes, one of them in a real-time interactive environment. This proves the suitability of these approaches for surgery training, planning and simulation.

7.1 LINEAR METHOD FOR CUBICAL MSM DESIGN

A new analytical approach has been proposed to design MSMs from linear elastic FEM by linearizing the equilibrium equations of the MSMs and equating the stiffness matrices of both models. The main contributions in this topic are:

- A new method for obtaining analytically cubical MSMs from linear elastic FEM is proposed in this thesis. The method is based on the study of the eigenvectors and eigenvalues of the stiffness matrices of the linear FEM and the linearized MSM. The linearized model is only used to obtain the stiffness coefficients of the MSM. The computation of the real deformation is performed using the nonlinear model.

- As the eigenvectors and eigenvalues of both stiffness matrices can rarely be the same, the spring coefficients of the MSM are computed

using a minimization method that takes into account the results of both eigenproblems simultaneously.

- The *linear method* is specifically developed for small deformations because of the linearization involved in the MSM design and the linear elastic assumption.

- In this thesis three complementary methods are proposed to evaluate the quality of the obtained MSM: (a) the axial and transversal behaviour of the model working under uniaxial tensile loads, (b) the residual error of the minimization and (c) a new metric that quantifies the similarity between the eigenspaces of the stiffness matrices of the linearized MSM and the FEM. These methods allow identifying the range of Poisson's ratios in which the approximation is accurate.

- In contrast to previous works, the proposed method can handle any value of Poisson's ratio in the range of 0 to 0.5. However, it approximates better the behaviour of the reference FEM when the value of this parameter is around 0.35. Below this value, the obtained MSM behaves softer than the reference model and stiffer above it.

- As Poisson's ratio ν gets further from 0.35, the minimization error increases, reaching high error values for ν =0.49. Therefore, it is preferable to use the MSM obtained from ν =0.35 to represent incompressible materials. Numerical experiments show that this solution provides accurate simulations and a quasi-incompressible behaviour.

- In this thesis it has been shown that cubical MSMs are able to approximate quite accurately the behaviour of linear elastic materials and can be used in medical applications. In particular, its implementation in *Maxiplan* shows that this approach can be used to predict facial appearance of patients after maxillofacial surgery.

- The use of MSMs obtained from linear elastic FEM is recommended when the real-time requirement is more important than the accuracy. It can be an interesting alternative solution to linear FEM when preprocessing techniques are not useful, for instance, when topological changes are involved in the simulation.

7.2 NONLINEAR METHOD FOR CUBICAL MSM DESIGN

A new analytical approach to design MSMs from nonlinear elastic material models by adjusting their behaviour under uniaxial tensile loads has been proposed. The main contributions in this topic are:

- A new analytical method for designing cubical MSMs that behave like nonlinear materials is presented in this thesis. This method is based on the nonlinear behaviour study of cubical MSMs working under uniaxial tensile tests and it is especially suitable for medical simulators that use hyperelastic models.

- The study of the behaviour of a single element explains the characteristic stiffening of the response of MSMs as the deformations grow. This behaviour reproduces with enough accuracy the main properties of many biological soft tissues.

- The *nonlinear method* developed in this thesis is able to adjust, simultaneously, the axial and the transversal behaviour of the model. This makes possible to work with compressible or incompressible reference material models, as the derivation process can use different values of Poisson's ratios.

- Even under large deformations the MSMs is able to approximate complex characteristics such as the nonlinear incompressible behaviour found in living tissues. This is achieved adopting just linear springs and cubical topology.

- This method also allows designing MSMs from linear elastic material models. However, they behave less accurately than the MSMs obtained with the linearization approach also presented in this thesis.

- The use of MSMs obtained from nonlinear elastic material models is an interesting alternative solution when nonlinear FEM cannot meet the real-time requirement in interactive applications, since they are computationally very efficient.

7.3 FUTURE WORK

The MSM is an interesting alternative to the FEM especially for real-time interactive applications. In the present work a new approach to define the parameters of a MSM is proposed based on a comparison to linear elastic FEM for small deformations and another method based on the constitutive

law of a material working under large deformations. In the first case, a good approximation of the behaviour of linear FEM is obtained. In the second case, it has been shown that a simple approach such as approximating the behaviour in simple uniaxial tensile tests allows the definition of MSMs with mechanical behaviour similar to nonlinear material models, but with a significantly reduced computational cost. However, several possible research lines are open to continue with this work:

- Validate the performance of the MSMs proposed in this thesis using real experimental data instead of considering only the results obtained using the FEM.

- Extend or modify the objective function used in the *nonlinear method* with the aim of considering the behaviour of a cubical element under additional types of loads. This could improve in some cases the accuracy of the MSM designed using this method, specially when stretching is not the dominant load.

- Study cubical MSMs with more than the three stiffness coefficients used in this thesis. For instance, making the edge springs aligned with the axial direction and the transversal ones have different stiffness values might help modelling tissues such as muscle, whose behaviour in the fibre direction generally differs from the behaviour in the transversal one.

- Design of MSMs with additional types of springs, such as nonlinear and torsion springs. This provides the MSMs with additional parameters that may improve the quality of the approximation.

- Take dynamic properties into consideration in the process of the MSM design. This could involve analyzing issues such as inertia and damping.

- Develop friendlier soft-tissue simulating environments. The existing software development tools focused on medical applications are not easy to modify and test, or do not provide properly documented code.

APPENDIX A: EIGENSPACES

In section 4.2.2 the projections of each eigenvector of the linearized MSM onto each eigenvector of the linear FEM are studied, in order to evaluate the quality of the MSM obtained using the *linear method*. In this appendix the dot diagrams corresponding to the set of Poisson's values $\nu=\{0, 0.05, 0.10, 0.15, 0.20, 0.25, 0.30, 0.35, 0.40, 0.45$ and $0.49\}$ are displayed. Note that, in some cases, the resulting figures are the same for different Poisson's ratios.

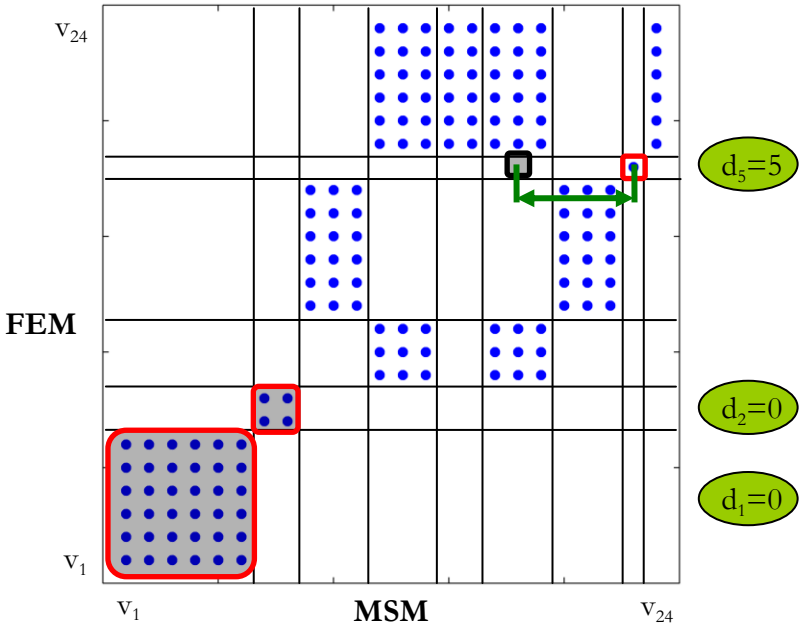

Figure A.1. Projections of the eigenvectors of $\mathbf{K}^{FEM}$ and $\mathbf{K}^{MSM}$ for $\nu=0$.

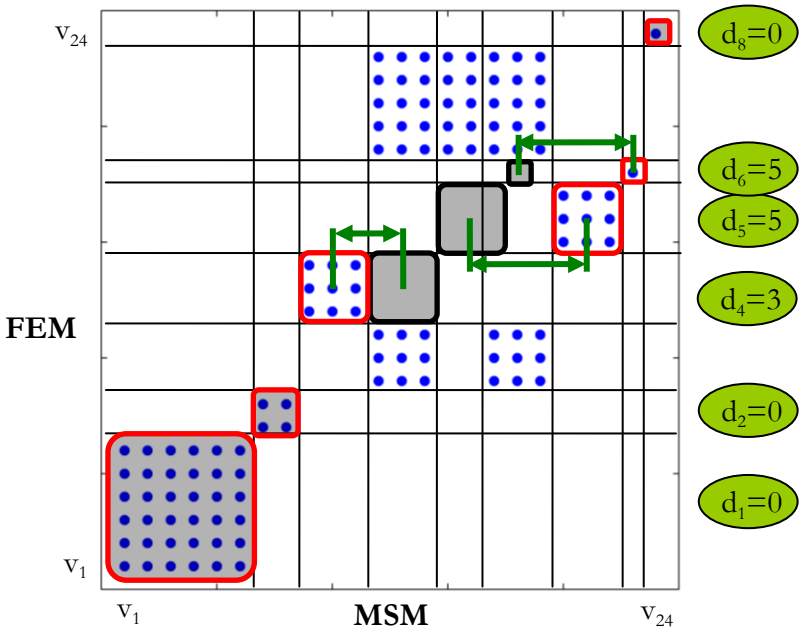

Figure A.2. Projections of the eigenvectors of $\mathbf{K}^{FEM}$ and $\mathbf{K}^{MSM}$ for ν=0.05, 0.10 and 0.15.

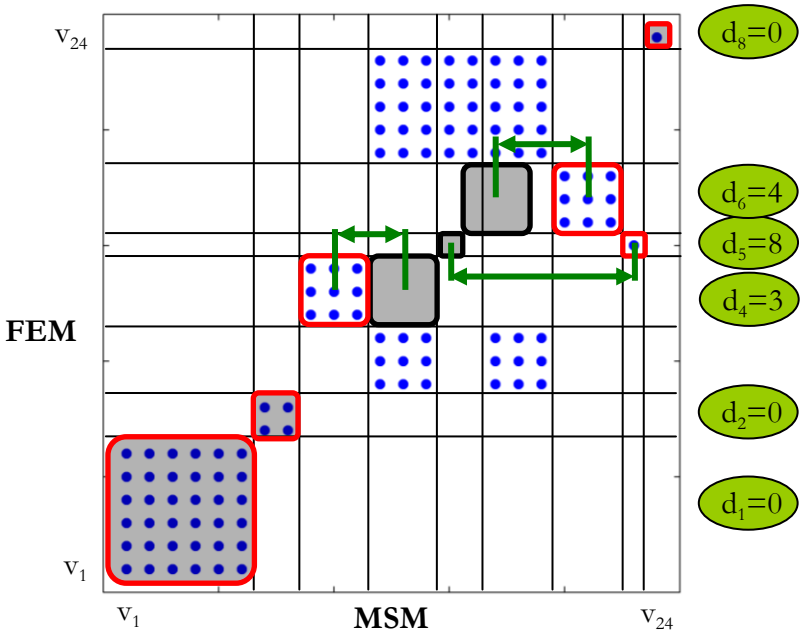

Figure A.3. Projections of the eigenvectors of $\mathbf{K}^{FEM}$ and $\mathbf{K}^{MSM}$ for ν=0.20 and 0.25.

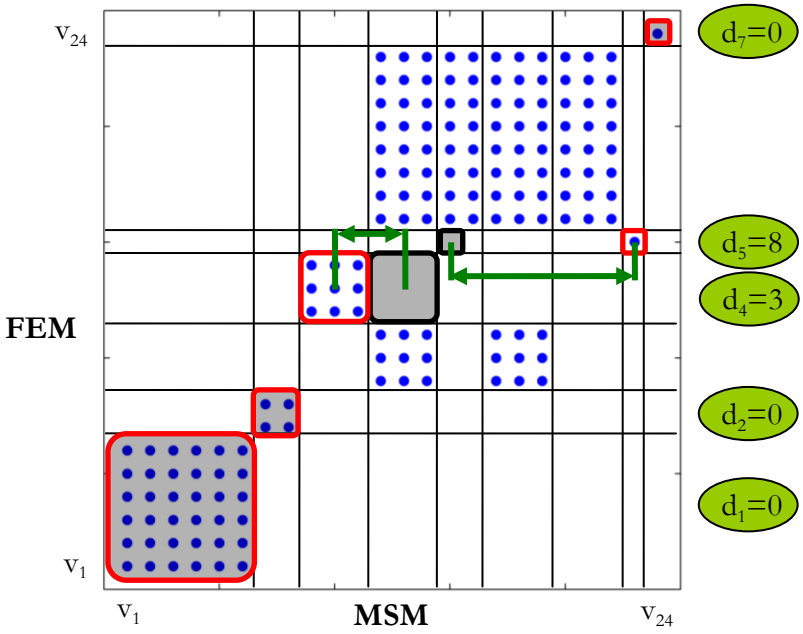

Figure A.4. Projections of the eigenvectors of $\mathbf{K}^{FEM}$ and $\mathbf{K}^{MSM}$ for ν=0.30.

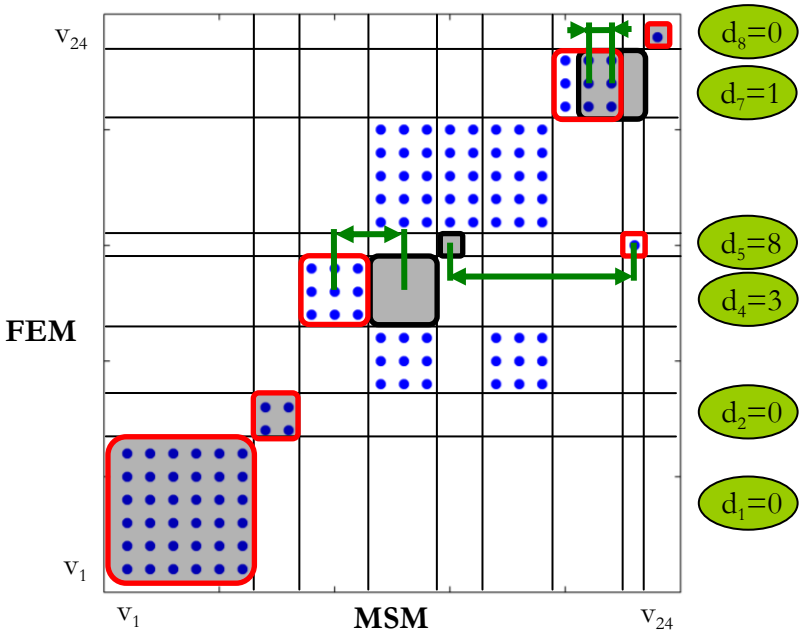

Figure A.5. Projections of the eigenvectors of $\mathbf{K}^{FEM}$ and $\mathbf{K}^{MSM}$ for ν=0.35.

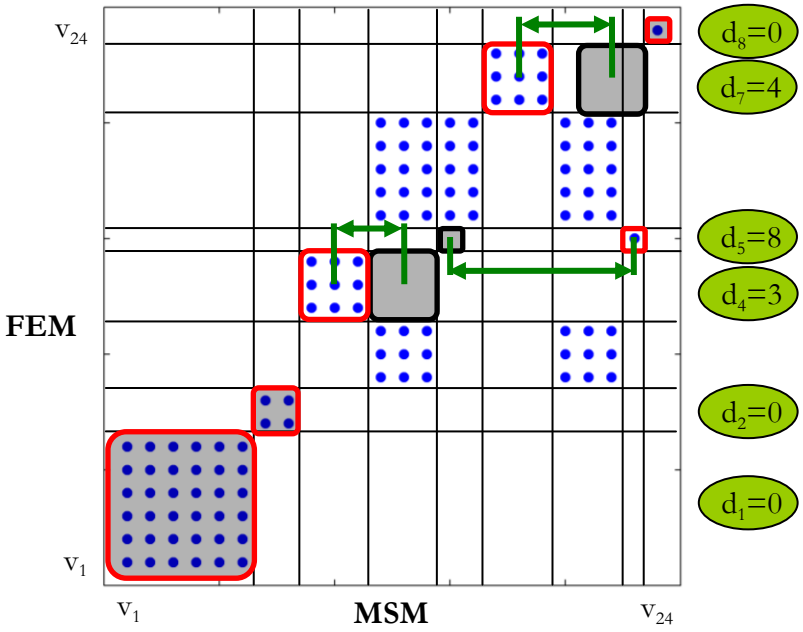

Figure A.6. Projections of the eigenvectors of $\mathbf{K}^{FEM}$ and $\mathbf{K}^{MSM}$ for ν=0.40.

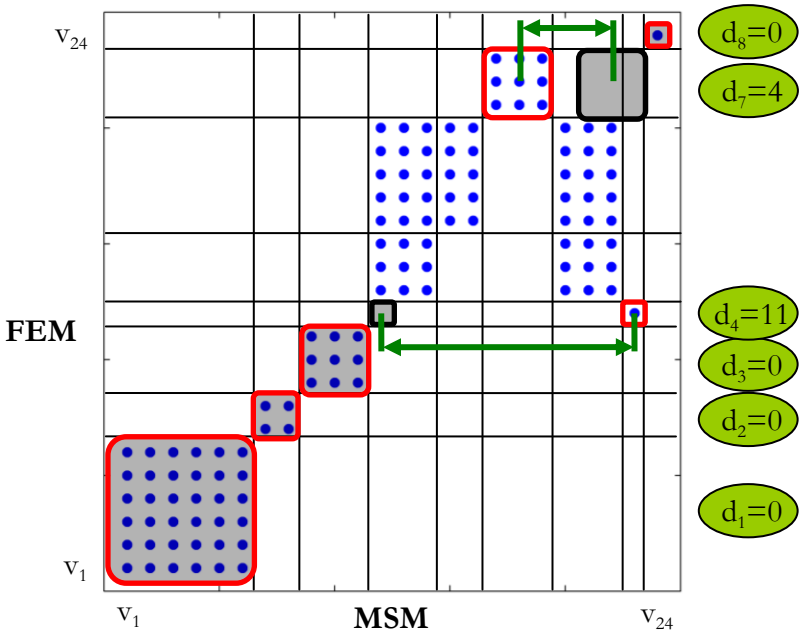

Figure A.7. Projections of the eigenvectors of $\mathbf{K}^{FEM}$ and $\mathbf{K}^{MSM}$ for ν=0.45.

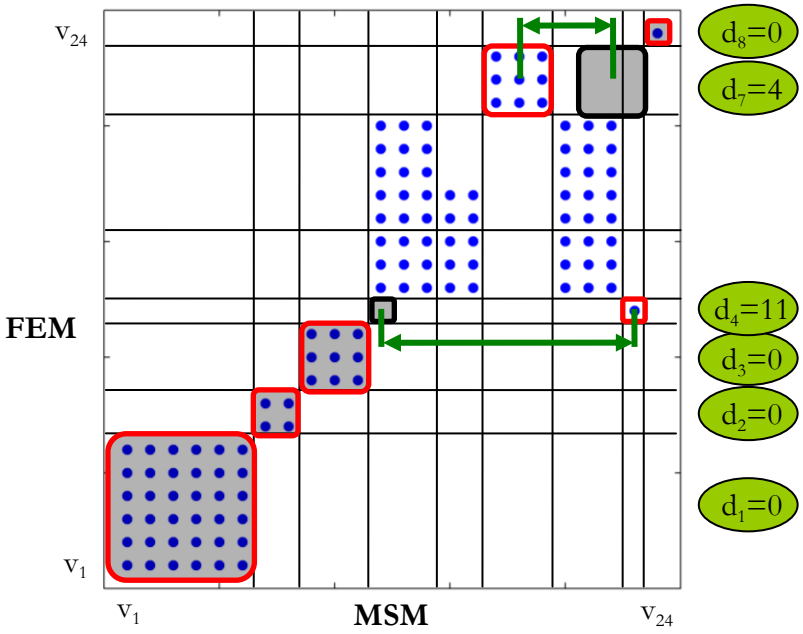

Figure A.8. Projections of the eigenvectors of $\mathbf{K}^{FEM}$ and $\mathbf{K}^{MSM}$ for ν=0.49.

APPENDIX B: PUBLICATIONS

San-Vicente, G.; Buchart, C.; Borro, D. & Celigüeta, J. T., 'Cubical Mass-Spring Model design based on a tensile deformation test and nonlinear material model', *IEEE Transactions on Visualization and Computer Graphics*, accepted for publication, in Press.

Buchart, C.; San-Vicente, G.; Amundarain, A. & Borro, D. (2009), Hybrid visualization for maxillofacial surgery planning and simulation, *in* '13th International Conference on Information Visualisation (IV'09)', IEEE Computer Society, Barcelona, pp. 266-273. DOI: 10.1109/IV.2009.98

San-Vicente, G.; Buchart, C.; Borro, D. & Celigüeta, J. T. (2009), 'Maxillofacial surgery simulation using a mass-spring model derived from continuum and the scaled displacement method', *International Journal of Computer Assisted Radiology and Surgery* **4**(1), 89-98. DOI: 10.1007/s11548-008-0271-0

San-Vicente, G.; Buchart, C.; Borro, D. & Celigüeta, J. T. (2008), Maxillofacial surgery simulation using a mass-spring model derived from continuum and the scaled displacement method, *in* '12th Annual Conference of the International Society for Computer Aided Surgery (ISCAS'08) - Poster Session', Springer, Barcelona, pp. S296-S297. DOI: 10.1007/s11548-008-0203-z

REFERENCES

Alcañiz, M.; Monserrat, C.; Meier, U.; Juan, M.; Grau, V. & Gil, J. (2003), GeRTiSS: Generic real time surgery simulation, *in* 'Medicine Meets Virtual Reality (MMVR11)', IOS Press, Amsterdam, pp. 16-18.

Baraff, D. & Witkin, A. (1998), Large steps in cloth simulation, *in* 'SIGGRAPH '98: Proceedings of the 25th annual conference on Computer graphics and interactive techniques', ACM, New York, NY, USA, pp. 43-54.

Basafa, E.; Farahmand, F. & Vossoughi, G. (2008), A non-linear mass-spring model for more realistic and efficient simulation of soft tissues surgery, *in* 'Medicine Meets Virtual Reality 16 (MMVR16)', IOS Press, Long Beach, pp. 23-25.

Baudet, V.; Beuve, M.; Jaillet, F.; Shariat, B. & Zara, F. (2009), Integrating tensile parameters in hexahedral mass-spring system for simulation, *in* '17th International Conference on Computer Graphics, Visualization and Computer Vision (WSCG'2009)', pp. 145-152.

Berkley, J.; Turkiyyah, G.; Berg, D.; Ganter, M. & Weghorst, S. (2004), 'Real-time finite element modeling for surgery simulation: An application to virtual suturing', *IEEE Transactions on Visualization and Computer Graphics* **10**(3), 314-325.

Bhasin, Y. & Liu, A. (2006), Bounds for damping that guarantee stability in mass-spring systems, *in* 'Medicine Meets Virtual Reality 14 (MMVR14)', IOS Press, Long Beach, pp. 55-60.

Bianchi, G.; Harders, M. & Székely, G. (2003), Mesh topology identification for mass-spring models, *in* Springer Berlin / Heidelberg, ed., 'Medical Image Computing and Computer-Assisted Intervention - MICCAI 2003', pp. 50-58.

Bianchi, G.; Solenthaler, B.; Székely, G. & Harders, M. (2004), Simultaneous topology and stiffness identification for mass-spring models based on FEM reference deformations, *in* Springer Berlin / Heidelberg, ed.,

'7th Medical Image Computing and Computer-Assisted Intervention - MICCAI 2004', pp. 293-301.

Bourguignon, D. & Cani, M.-P. (2000), Controlling anisotropy in mass-spring systems, *in* 'Eurographics Workshop on Computer Animation and Simulation (EGCAS)', Springer-Verlag, Interlaken, pp. 113-123.

Breen, D. E.; House, D. H. & Wozny, M. J. (1994), Predicting the drape of woven cloth using interacting particles, *in* 'SIGGRAPH '94: Proceedings of the 21st annual conference on Computer graphics and interactive techniques', ACM, New York, NY, USA, pp. 365-372.

Bro-Nielsen, M. (1998), 'Finite element modeling in surgery simulation', *Proceedings of the IEEE* **86**(3), 490-503.

Brown, J.; Sorkin, S.; Bruyns, C.; Latombe, J.-C.; Montgomery, K. & Stephanides, M. (2001), Real-time simulation of deformable objects: tools and application, *in* 'Computer Animation, 2001. The Fourteenth Conference on Computer Animation. Proceedings', pp. 228-258.

Brunon, A.; Bruyère-Garnier, K. & Coret, M. (2010), 'Mechanical characterization of liver capsule through uniaxial quasi-static tensile tests until failure', *Journal of Biomechanics* **43**(11), 2221-2227.

Chabanas, M.; Payan, Y.; Marecaux, C.; Swider, P. & Boutault, F. (2004), 'Comparison of linear and non-linear soft tissue models with post-operative CT scan in maxillofacial surgery', *Lecture Notes in Computer Science* **3078**, 19-27.

Chadwick, J. E.; Haumann, D. R. & Parent, R. E. (1989), Layered construction for deformable animated characters, *in* 'SIGGRAPH '89: Proceedings of the 16th annual conference on Computer graphics and interactive techniques', ACM, New York, NY, USA, pp. 243-252.

Chen, F.; Gu, L.; Huang, P.; Zhang, J. & Xu, J. (2007), Soft tissue modeling using nonlinear mass spring and simplified medial representation, *in* 'Engineering in Medicine and Biology Society, 2007. EMBS 2007. 29th Annual International Conference of the IEEE', pp. 5083-5086.

Choi, K.-S.; Sun, H. & Heng, P.-A. (2004), 'An efficient and scalable deformable model for virtual reality-based medical applications', *Artificial Intelligence in Medicine* **32**(1), 51-69.

Chui, C.; Kobayashi, E.; Chen, X.; Hisada, T. & Sakuma, I. (2004), 'Combined compression and elongation experiments and non-linear modelling of liver tissue for surgical simulation', *Medical and Biological Engineering and Computing* **42**(6), 787-798.

Clatz, O.; Delingette, H.; Talos, I.-F.; Golby, A. J.; Kikinis, R.; Jolesz, F. A.; Ayache, N. & Warfield, S. K. (2005), 'Robust nonrigid registration to capture brain shift from intraoperative MRI', *IEEE Transactions on Medical Imaging* **24**(11), 1417-1427.

Comas, O.; Taylor, Z. A.; Allard, J.; Ourselin, S.; Cotin, S. & Passenger, J. (2008), Efficient nonlinear FEM for soft tissue modelling and its GPU implementation within the open source framework SOFA, *in* 'Proceedings of the 4th International Symposium on Computational Models for Biomedical Simulation (ISBMS), 2008', Springer-Verlag, Berlin, Heidelberg, pp. 28-39.

Cooper, L. & Maddock, S. (1997), Preventing collapse within mass-spring-damper models of deformable objects, *in* 'The Fifth International Conference in Central Europe on Computer Graphics and Visualization (WSCG'97)', pp. 70-78.

Cotin, S.; Delingette, H. & Ayache, N. (2000), 'A hybrid elastic model allowing real-time cutting, deformations and force-feedback for surgery training and simulation', *The Visual Computer* **16**(8), 437-452.

Cui, T.; Song, A. & Wu, J. (2009), 'Simulation of a mass-spring model for global deformation', *Frontiers of Electrical and Electronic Engineering in China* **4**(1), 78-82.

Darzi, A. & Mackay, S. (2001), 'Assessment of surgical competence', *Quality in Health Care* **10**(suppl 2), ii64-ii69.

Delingette, H. (2008), 'Triangular springs for modeling nonlinear membranes', *IEEE Transactions on Visualization and Computer Graphics* **14**(2), 329-341.

Delingette, H. & Ayache, N. (2004), *Handbook of numerical analysis*, Elsevier, chapter Soft tissue modeling for surgery simulation, pp. 453-550.

Desbrun, M.; Schröder, P. & Barr, A. (1999), Interactive animation of structured deformable objects, *in* 'Proceedings of the 1999 conference on Graphics interface '99', Morgan Kaufmann Publishers Inc., San Francisco, CA, USA, pp. 1-8.

Deussen, O.; Kobbelt, L. & Tücke, P. (1995), Using simulated annealing to obtain good nodal approximations of deformable objects, *in* '6th Eurographics Workshop on Simulation and Animation (EGCAS)', Springer, Maastricht, pp. 30-43.

DiMaio, S. P. (2003), 'Modelling, simulation and planning of needle motion in soft tissues', PhD thesis, The University of British Columbia.

Etzmuss, O.; Gross, J. & Strasser, W. (2003), 'Deriving a particle system from continuum mechanics for the animation of deformable objects', *IEEE Transactions on Visualization and Computer Graphics* **9**(4), 538-550.

Fung, Y.-C. (1993), *Biomechanics: mechanical properties of living tissues*, Springer-Verlag, New York.

Galoppo, N.; Otaduy, M. A.; Mecklenburg, P.; Gross, M. & Lin, M. C. (2006), Fast simulation of deformable models in contact using dynamic deformation textures, *in* 'Eurographics/ ACM SIGGRAPH Symposium on Computer Animation (2006)'.

Gao, Z.; Lister, K. & Desai, J. P. (2010), 'Constitutive modeling of liver tissue: experiment and theory', *Annals of Biomedical Engineering* **38**(2), 505-516.

García, M.; Gómez, M.; Óscar Ruiz & Boulanger, P. (2007), 'Spring-particle model for hyperelastic cloth', *DYNA* **74**(151), 137-145.

Gayle, R.; Lin, M. C. & Manocha, D. (2005), 'Constraint-based motion planning of deformable robots', *Robotics and Automation, 2005. ICRA 2005. Proceedings of the 2005 IEEE International Conference on* **-**, 1046-1053.

Gelder, A. V. (1998), 'Approximate simulation of elastic membranes by triangulated spring meshes', *Journal of Graphics Tools* **3**(2), 21-42.

Georgii, J.; Echtler, F. & Westermann, R. (2005), Interactive simulation of deformable bodies on GPUs, *in* 'Proceedings of Simulation and Visualisation 2005', pp. 247-258.

Georgii, J. & Westermann, R. (2005a), 'Mass-spring systems on the GPU', *Simulation Modelling Practice and Theory* **13**(8), 693-702.

Georgii, J. & Westermann, R. (2008), Corotated finite elements made fast and stable, *in* 'Proceedings of the 5th Workshop On Virtual Reality Interaction and Physical Simulation'.

Gladilin, E.; Zachow, S.; Deuflhard, P. & Hege, H.-C. (2003), 'On constitutive modeling of soft tissue for the long-term prediction of cranio-maxillofacial surgery outcome', *International Congress Series* **1256**, 343-348.

Haile, J. (1992), *Molecular dynamics simulation: elementary methods*, Wiley-Interscience, New York.

Harders, M.; Hutter, R.; Rutz, A.; Niederer, P. & Székely, G. (2003), Comparing a simplified FEM approach with the mass-spring model for surgery simulation, *in* 'Medicine Meets Virtual Reality (MMVR11)', IOS Press, Amsterdam, pp. 103-109.

Hastreiter, P.; Rezk-Salama, C.; Soza, G.; Bauer, M.; Greiner, G.; Fahlbusch, R.; Ganslandt, O. & Nimsky, C. (2004), 'Strategies for brain shift evaluation', *Medical Image Analysis* **8**(4), 447-464.

Hauth, M. & Strasser, W. (2004), Corotational simulation of deformable solids, *in* 'Proc. 12th Int. Conf. Computer Graphics, Visualization and Computer Vision (WSCG'04)', UNION Agency - Science Press, Plzen, Czech Republic, pp. 137-145.

Hirota, G.; Fisher, S.; State, A.; Lee, C. & Fuchs, H. (2001), An implicit finite element method for elastic solids in contact, *in* 'Computer Animation, 2001. The Fourteenth Conference on Computer Animation. Proceedings', pp. 136-146.

Holzapfel, G. A. (2000), *Nonlinear solid mechanics: a continuum approach for engineering*, Wiley.

Hong, M.; Jung, S.; Choi, M.-H. & Welch, S. W. J. (2006), 'Fast volume preservation for a mass-spring system', *IEEE Computer Graphics and Applications* **26**(5), 83-91.

Hu, T. & Desai, J. P. (2004), Characterization of soft-tissue material properties: large deformation analysis, *in* Springer Berlin - Heidelberg, ed., 'Medical Simulation', pp. 28-37.

Iglesias-García, J. J.; Noia, J. L.; Álvarez Castro, A.; Cigarrán, B. & Muñoz, J. E. D. (2009), 'Second-generation endoscopic ultrasound elastography in the differential diagnosis of solid pancreatic masses: Pancreatic cancer vs. inflammatory mass in chronic pancreatitis', *Revista Española de Enfermedades Digestivas* **101**(10), 723-727.

James, D. L. & Pai, D. K. (2003), 'Multiresolution Green's function methods for interactive simulation of large-scale elastostatic objects', *ACM Transactions on Graphics* **22**, 47-82.

Jeřábková, L. & Kuhlen, T. (2009), 'Stable cutting of deformable objects in virtual environments using XFEM', *IEEE Computer Graphics and Applications* **29**(2), 61-71.

Johnson, R. G. (2005), 'The history of surgery', Saint Louis University.

Joldes, G. R.; Wittek, A. & Miller, K. (2009), 'Suite of finite element algorithms for accurate computation of soft tissue deformation for surgical simulation', *Medical Image Analysis* **13**(6), 912 - 919.

Kähler, K. (2003), 'A head model with anatomical structure for facial modeling and animation', PhD thesis, Universität des Saarlandes.

Kaldor, J.; James, D. L. & Marschner, S. (2008), Simulating knitted cloth at the yarn level, *in* 'ACM SIGGRAPH 2008 computer animation festival (SIGGRAPH '08)', ACM, New York, NY, USA, pp. 100-100.

Keeve, E.; Girod, S.; Kikinis, R. & Girod, B. (1998), 'Deformable modeling of facial tissue for craniofacial surgery simulation', *Computer Aided Surgery* **3**(5), 228-238.

Kewitz, H.; Hanke, T. & Hillebrand, J. (1980), 'Human brain weight and acetylcholinesterase in relation to aging', *Neurochemistry International* **2**, 209-213.

Kim, J.; Ahn, B.; De, S. & Srinivasan, M. A. (2008), 'An efficient soft tissue characterization algorithm from in vivo indentation experiments for medical simulation', *The International Journal of Medical Robotics and Computer Assisted Surgery* **4**(3), 277-285.

Krummel, T. M. (2006), 'What is surgery?', *Seminars in Pediatric Surgery* **15**(4), 237-241.

Kyriacou, S. K.; Davatzikos, C.; Zinreich, S. J. & Bryan, R. N. (1999), 'Nonlinear elastic registration of brain images with tumor pathology using a biomechanical model', *IEEE Transactions on Medical Imaging* **18**(7), 580-592.

Lafleur, B.; Thalmann, N. M. & Thalmann, D. (1991), Cloth animation with self-collision detection, *in* 'IFIP, Modeling in Computer Graphics'.

Lee, B.; Popescu, D. C.; Joshi, B. & Ourselin, S. (2006), Efficient topology modification and deformation for finite element models using condensation, *in* 'Medicine Meets Virtual Reality 14 (MMVR14)', IOS Press, Long Beach, pp. 299-304.

Lloyd, B. A.; Szekely, G. & Harders, M. (2007), 'Identification of spring parameters for deformable object simulation', *Visualization and Computer Graphics, IEEE Transactions on* **13**(5), 1081-1094.

Lorensen, W. E. & Cline, H. E. (1987), 'Marching cubes: A high resolution 3D surface construction algorithm', *ACM SIGGRAPH Computer Graphics* **21**(4), 163-169.

Louchet, J.; Provot, X. & Crochemore, D. (1995), Evolutionary identification of cloth animation models, *in* Dimitri Terzopoulos & Daniel Thalmann, ed., 'Computer Animation and Simulation '95', pp. 44-54.

Ma, J.; Wittek, A.; Singh, S.; Joldes, G.; Washio, T.; Chinzei, K. & Miller, K. (2009), Accuracy of non-linear FE modelling for surgical simulation study using soft tissue phantom, *in* 'Computational Biomechanics for Medicine IV (CBM2009)', London, pp. 29-40.

Maciel, A.; Boulic, R. & Thalmann, D. (2003), Deformable tissue parameterized by properties of real biological tissue, *in* Springer Berlin / Heidelberg, ed., 'Surgery Simulation and Soft Tissue Modeling', pp. 74-87.

Marchal, M.; Allard, J.; Duriez, C. & Cotin, S. (2008), Towards a framework for assessing deformable models in medical simulation, *in* '4th International Symposium on Biomedical Simulation (ISBMS)', pp. 176-184.

Marchetti, C.; Bianchi, A.; Muyldermans, L.; Martino, M. D.; Lancellotti, L. & Sarti, A. (2010), 'Validation of new soft tissue software in orthognathic surgery planning', *International Journal of Oral and Maxillofacial Surgery* **In Press, Corrected Proof**, -.

Martins, P. A. L. S.; Jorge, R. M. N. & Ferreira, A. J. M. (2006), 'A comparative study of several material models for prediction of hyperelastic properties: application to silicone-rubber and soft tissues', *Strain* **42**(3), 135-147.

Maurel, W.; Wu, Y.; Thalmann, N. M. & Thalmann, D. (1998), *Biomechanical models for soft tissue simulation*, Springer-Verlag, Berlin.

Mazza, E.; Bauer, M.; Bajka, M. & Holzapfel, G. A. (2007), Characterizing the mechanical response of soft human tissue for medical applications, *in* E. Oñate & D. R. J. Owen, ed., 'IX International Conference on Computational Plasticity (COMPLAS IX)'.

Meseure, P. & Chaillou, C. (2000), 'A deformable body model for surgical simulation', *The Journal of Visualization and Computer Animation* **11**(4), 197-208.

Miller, G. S. P. (1988), The motion dynamics of snakes and worms, *in* 'SIGGRAPH '88: Proceedings of the 15th annual conference on Computer graphics and interactive techniques', ACM, New York, NY, USA, pp. 169-173.

Miller, K. & Chinzei, K. (2002), 'Mechanical properties of brain tissue in tension', *Journal of Biomechanics* **35**(4), 483-490.

Miller, K.; Chinzei, K.; Orssengo, G. & Bednarz, P. (2000), 'Mechanical properties of brain tissue in-vivo: experiment and computer simulation', *Journal of Biomechanics* **33**(11), 1369-1376.

Miller, K.; Joldes, G.; Lance, D. & Wittek, A. (2007), 'Total Lagrangian explicit dynamics finite element algorithm for computing soft tissue deformation', *Communications in Numerical Methods in Engineering* **23**(2), 121-134.

Miller, K.; Wittek, A. & Joldes, G. (2010), 'Biomechanics of the brain for computer-integrated surgery', *Biomechanics of the brain for computer-integrated surgery* **12**(2), 25-37.

Mollemans, W.; Schutyser, F.; Nadjmi, N.; Maes, F. & Suetens, P. (2007), 'Predicting soft tissue deformations for a maxillofacial surgery planning system: From computational strategies to a complete clinical validation', *Medical Image Analysis* **11**(3), 282-301.

Mollemans, W.; Schutyser, F.; Nadjmi, N. & Suetens, P. (2005), 'Very fast soft tissue predictions with mass tensor model for maxillofacial surgery planning systems', *International Congress Series* **1281**, 491-496.

Morris, D. & Salisbury, K. (2008), 'Automatic preparation, calibration, and simulation of deformable objects', *Computer Methods in Biomechanics and Biomedical Engineering* **11**(3), 263-279.

Mosegaard, J. & Sorensen, T. S. (2005), Real-time deformation of detailed geometry based on mappings to a less detailed physical simulation on the GPU, *in* Erik Kjems & Roland Blach, ed., 'Proceedings of Eurographics Workshop on Virtual Environment', Eurographics Association, Aalborg, Denmark, pp. 105-111.

Müller, M.; Dorsey, J.; McMillan, L.; Jagnow, R. & Cutler, B. (2002), Stable real-time deformations, *in* 'SCA '02: Proceedings of the 2002 ACM SIGGRAPH/Eurographics symposium on Computer animation', ACM, New York, NY, USA, pp. 49-54.

Nabavi, A.; Black, P. M.; Gering, D. T.; Westin, C.-F.; Mehta, V.; Richard S. Pergolizzi, J.; Ferrant, M.; Warfield, S. K.; Hata, N.; Schwartz, R. B.; III, W. M. W.; Kikinis, R. & Jolesz, F. A. (2001), 'Serial intraoperative

magnetic resonance imaging of brain shift', *Neurosurgery* **48**(4), 787-798.

Nava, A.; Mazza, E.; Furrer, M.; Villiger, P. & Reinhart, W. (2008), 'In vivo mechanical characterization of human liver', *Medical Image Analysis* **12**(2), 203-216.

Nedel, L. P. & Thalmann, D. (1998), Modeling and deformation of the human body using an anatomically-based approach, *in* 'Proceedings of Computer Animation 98', pp. 34-40.

Nesme, M.; Kry, P. G.; Jeřábková, L. & Faure, F. (2009), Preserving topology and elasticity for embedded deformable models, *in* 'ACM Transactions on Graphics (Proc. of SIGGRAPH)'.

Nesme, M.; Marchal, M.; Promayon, E.; Chabanas, M.; Payan, Y. & Faure, F. (2005), 'Physically realistic interactive simulation for biological soft tissues', *Recent Research Developments in Biomechanics* **2** , 1-22.

Nogami, R.; Noborio, H.; Ujibe, F. & Fujii, H. (2004), Precise deformation of rheologic object under MSD models with many voxels and calibrating parameters, *in* 'Proceedings of the IEEE International Conference on Robotics and Automation - ICRA '04', pp. 1919-1926.

Oezkaya, N. & Nordin, M., Leger, D. L., ed. (1999), *Fundamentals of biomechanics*, Springer, Berlin.

Palmeri, M.; Wang, M.; Dahl, J.; Frinkley, K. & Nightingale, K. (2008), 'Quantifying hepatic shear modulus in vivo using acoustic radiation force', *Ultrasound in Medicine & Biology* **34**(4), 546-558.

Picinbono, G.; Delingette, H. & Ayache, N. (2003), 'Non-linear anisotropic elasticity for real-time surgery simulation', *Graphical Models* **65**(5), 305 - 321.

Platt, S. M. & Badler, N. I. (1981), 'Animating facial expressions', *SIGGRAPH Comput. Graph.* **15**(3), 245-252.

Provot, X. (1995), Deformation constraints in a mass-spring model to describe rigid cloth behavior, *in* Wayne A. Davis & Przemyslaw Prusinkiewicz,

ed., 'Graphics Interface '95', Canadian Human-Computer Communications Society, Quebec, pp. 147-154.

Rasmusson, A.; Mosegaard, J. & Sørensen, T. S. (2008), Exploring parallel algorithms for volumetric mass-spring-damper models in CUDA, *in* Springer Berlin / Heidelberg, ed., 'Biomedical Simulation', pp. 49-58.

Reznick, R. K. & MacRae, H. (2006), 'Teaching surgical skills - Changes in the wind', *The New England Journal of Medicine* **355**(25), 2664-2669.

Samur, E.; Sedef, M.; Basdogan, C.; Avtan, L. & Duzgun, O. (2007), 'A robotic indenter for minimally invasive measurement and characterization of soft tissue response', *Medical Image Analysis* **11**(4), 361-373.

Satava, R. M. (1994), Medicine 2001: The King is dead, *in* 'Virtual Reality Conference'.

Schiavone, P.; Chassat, F.; Boudou, T.; Promayon, E.; Valdivia, F. & Payan, Y. (2009), 'In vivo measurement of human brain elasticity using a light aspiration device', *Medical Image Analysis* **13**(4), 673-678.

Skrinjar, O.; Nabavi, A. & Duncan, J. (2002), 'Model-driven brain shift compensation', *Medical Image Analysis* **6**(4), 361-373.

Steinemann, D.; Harders, M.; Gross, M. & Szekely, G. (2006), Hybrid cutting of deformable solids, *in* 'Virtual Reality Conference, 2006', pp. 35-42.

Sundaraj, K. (2004), 'Real-time dynamic simulation and 3D interaction of biological tissue: application to medical simulators', PhD thesis, Institut National Polytechnique de Grenoble - INPG.

Swennen, G. R.; Schutyser, F. & Hausamen, J.-E., Schröder, G., ed. (2006), *Three-dimensional cephalometry*, Springer-Verlag Berlin Heidelberg.

Taylor, Z. A.; Cheng, M. & Ourselin, S. (2007), Real-time nonlinear finite element analysis for surgical simulation using graphics processing units, *in* Springer Berlin / Heidelberg, ed., 'Medical Image Computing and Computer-Assisted Intervention – MICCAI 2007', pp. 701-708.

Taylor, Z. A.; Comas, O.; Cheng, M.; Passenger, J.; Hawkes, D.; Atkinson, D. & Ourselin, S. (2009), 'On modelling of anisotropic viscoelasticity for

soft tissue simulation: Numerical solution and GPU execution', *Medical Image Analysis* **13**(2), 234-244.

Tejada, E. & Ertl, T. (2005), 'Large steps in GPU-based deformable bodies simulation', *Simulation Modelling Practice and Theory* **13**(8), 703 - 715.

Terzopoulos, D. & Fleischer, K. (1988), Modeling inelastic deformation: viscolelasticity, plasticity, fracture, *in* 'SIGGRAPH '88: Proceedings of the 15th annual conference on Computer graphics and interactive techniques', ACM, New York, NY, USA, pp. 269-278.

Terzopoulos, D. & Waters, K. (1990), 'Physically-based facial modeling, analysis, and animation', *Journal of Visualization and Computer Animation* **1**(2), 73-80.

Teschner, M.; Girod, S. & Girod, B. (2000), Direct computation of nonlinear soft-tissue deformation, *in* '5th Vision Modeling and Visualization (VMV'00)', pp. 383-390.

Teschner, M.; Heidelberger, B.; Muller, M. & Gross, M. (2004), A versatile and robust model for geometrically complex deformable solids, *in* 'CGI '04: Proceedings of the Computer Graphics International', IEEE Computer Society, Washington, DC, USA, pp. 312-319.

Treloar, L. R. G. (2005), *The physics of rubber elasticity*, Oxford University Press.

Tu, X. & Terzopoulos, D. (1994), Artificial fishes: physics, locomotion, perception, behavior, *in* 'Proc. of ACM SIGGRAPH'94', pp. 43-50.

Vafai, N. M. & Payandeh, S. (2010), 'Toward the development of interactive virtual dissection with haptic feedback', *Virtual Reality* **14**(2), 85-103.

Völlinger, U.; Stier, H.; Priesnitz, J. & Krause, F.-L. (2009), 'Evolutionary optimization of mass-spring models', *CIRP Journal of Manufacturing Science and Technology* **1**(3), 137-141.

Volino, P.; Magnenat-Thalmann, N. & Faure, F. (2009), 'A simple approach to nonlinear tensile stiffness for accurate cloth simulation', *ACM Transactions on Graphics (TOG)* **28**(4), 105.

Wang, S. & Yang, J. (2009), 'An improved finite element model for craniofacial surgery simulation', *International Journal of Computer Assisted Radiology and Surgery* **4**(6), 579-587.

Wang, W.; Yan, X.; Xie, Y.; Qin, J.; Pang, W.-M. & Heng, P.-A. (2009a), A physically-based modeling and simulation framework for facial animation, *in* 'Fifth International Conference on Image and Graphics (ICIG'09)', pp. 521-526.

Wang, X. & Devarajan, V. (2005), '1D and 2D structured mass-spring models with preload', *The Visual Computer* **21**(7), 429-448.

Waters, K. (1987), A muscle model for animation three-dimensional facial expression, *in* 'SIGGRAPH '87: Proceedings of the 14th annual conference on Computer graphics and interactive techniques', ACM, New York, NY, USA, pp. 17-24.

Weiser, T. G.; Regenbogen, S. E.; Thompson, K. D.; Haynes, A. B.; Lipsitz, S. R.; Berry, W. R. & Gawande, A. A. (2008), 'An estimation of the global volume of surgery: a modelling strategy based on available data', *The Lancet* **372**(9633), 139-144.

Westermark, A.; Zachow, S. & Eppley, B. L. (2005), 'Three-dimensional osteotomy planning in maxillofacial surgery including soft tissue prediction', *Journal of Craniofacial Surgery* **16**(1), 100-104.

Wu, W. & Heng, P. A. (2004), 'A hybrid condensed finite element model with GPU acceleration for interactive 3D soft tissue cutting', *Computer Animation and Virtual Worlds* **15**(3-4), 219-227.

Wu, X.; Downes, M. S.; Goktekin, T. & Tendick, F. (2001), Adaptive nonlinear finite elements for deformable body simulation using dynamic progressive meshes, *in* 'Computer Graphics Forum', pp. 349-358.

Xu, S.; Liu, X. P.; Zhang, H. & Hu, L. (2010), An improved realistic mass-spring model for surgery simulation, *in* 'IEEE International Symposium on Haptic Audio-Visual Environments and Games (HAVE)', Phoenix, USA, pp. 1-6.

Xia, J. J.; Phillips, C. V.; Gateno, J.; Teichgraeber, J. F.; Christensen, A. M.; Gliddon, M. J.; Lemoine, J. J. & Liebschner, M. A. (2006), 'Cost-

effectiveness analysis for computer-aided surgical simulation in complex cranio-maxillofacial surgery', *Journal of oral and maxillofacial surgery* **64**(12), 1780-1784.

Zachow, S.; Hege, H.-C. & Deuflhard, P. (2006), 'Computer assisted planning in cranio-maxillofacial surgery.', *Journal of Computing and Information Technology* **14**(1), 53-64.

Zachow, S.; Hierl, T. & Erdmann, B. (2004), 'On the predictability of tissue changes for osteotomy planning in maxillofacial surgery: a comparison with postoperative results', *International Congress Series* **1268**, 648-653.

Zerbato, D.; Galvan, S. & Fiorini, P. (2007), Calibration of mass spring models for organ simulations, *in* 'Intelligent Robots and Systems, 2007. IROS 2007. IEEE/RSJ International Conference on', pp. 370-375.

Zhang, J.; Yoganandan, N.; Pintar, F. A.; Guan, Y.; Shender, B.; Paskoff, G. & Laud, P. (2010), 'Effects of tissue preservation temperature on high strain-rate material properties of brain', *Journal of Biomechanics* **In Press, Corrected Proof**, -.

Zhong, H. & Peters, T. (2007), 'A real time hyperelastic tissue model', *Computer Methods in Biomechanics and Biomedical Engineering* **10**(3), 185-193.

Zhou, X.; Zhang, N.; Sha, D.; Shen, Y.; Tamma, K. K. & Sweet, R. (2009), A discrete mechanics framework for real time virtual surgical simulations with application to virtual laparoscopic nephrectomy, *in* 'Medicine Meets Virtual Reality 17 (MMVR17)', IOS Press, Long Beach, pp. 459-464.

Zhuang, Y. & Canny, J. (1999), Real-time simulation of physically realistic global deformation, *in* 'IEEE Visualization Conference 1999'.

Zienkiewicz, O. C.; Taylor, R. L. & Zhu, J. Z. (2005), *The finite element method: Its basis and fundamentals*, Butterworth-Heinemann.